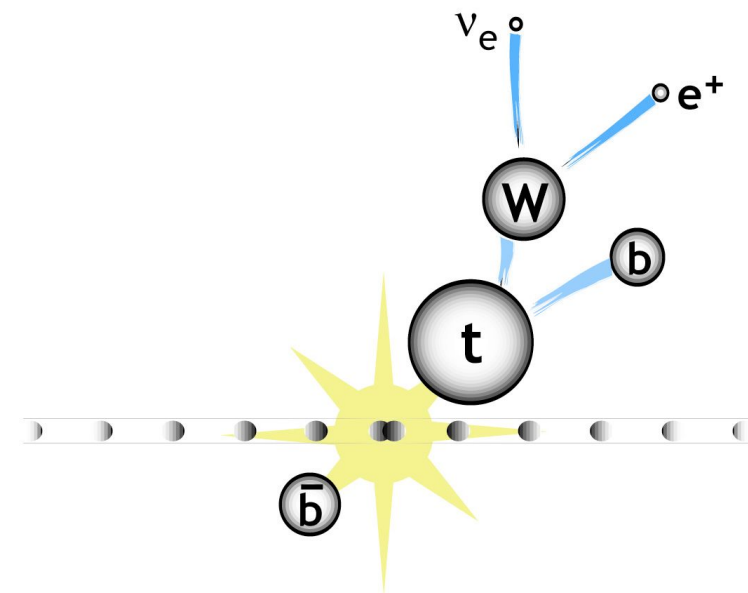


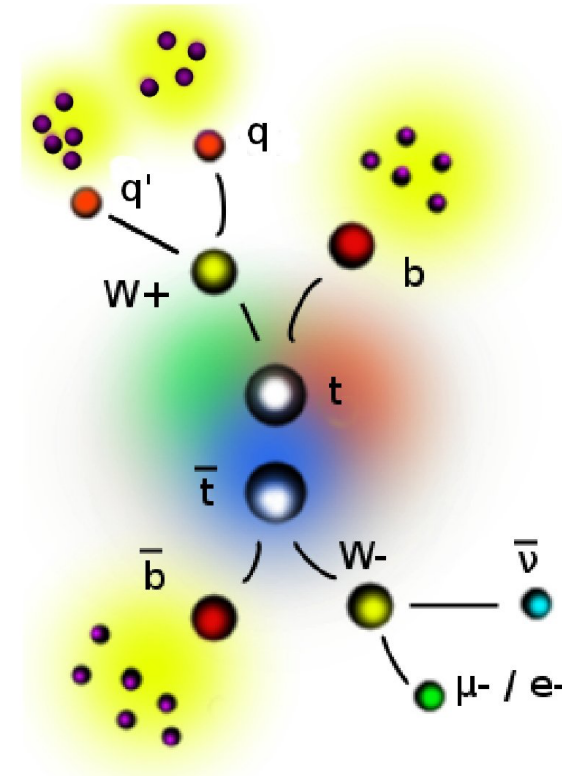
Challenging the Standard Model with top quarks

Wolfgang Wagner
Bergische Universität Wuppertal, Germany
and
ATLAS Collaboration

Seminar at Shandong University, Jinan
28 September 2019



- 1) The top-quark in the Standard Model (SM)
- 2) The Large Hadron Collider and the ATLAS detector
- 3) Direct searches for new particles
- 4) Indirect searches / searches for anomalous couplings
- 5) Precision measurements of top-quark properties



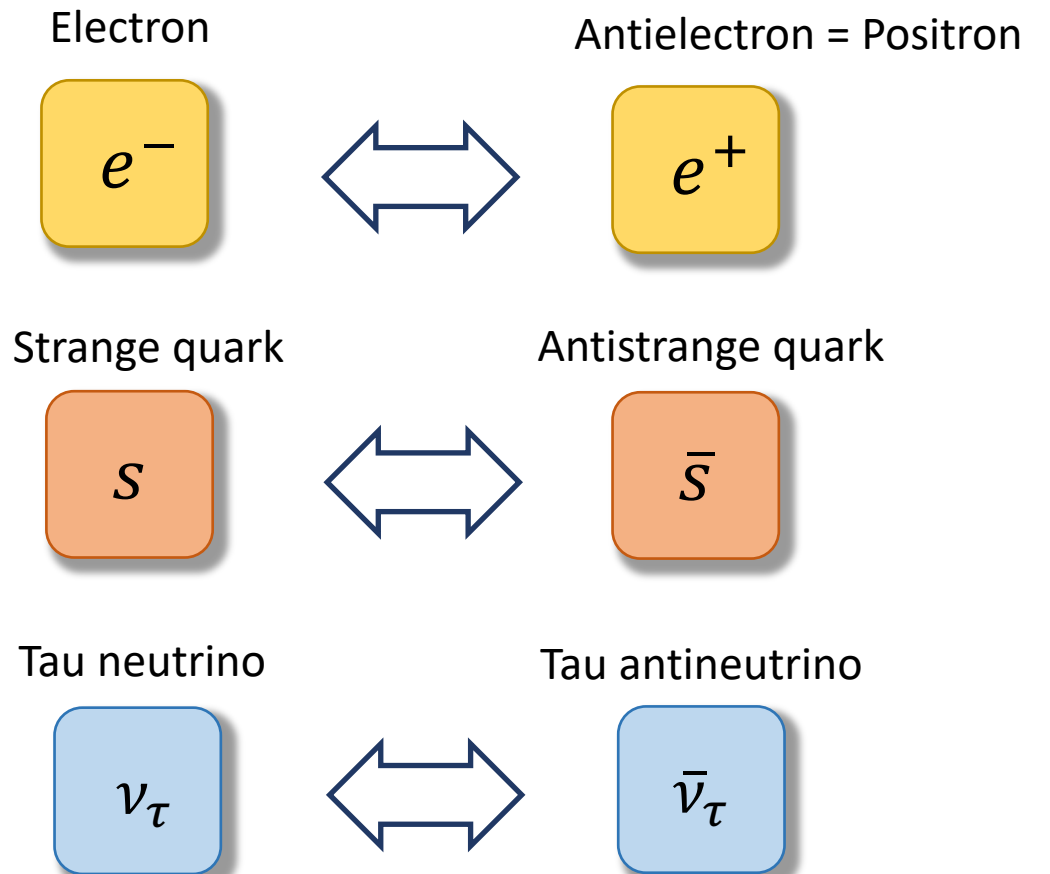
Quarks and leptons

Q_{em} $= +\frac{2}{3}e$	Up	Charm	Top
$= -\frac{1}{3}e$	Down	Strange	Bottom
$= 0$	ν_e	ν_μ	ν_τ
$= -e$	Elektron	Myon	Tauon

- Structureless, point-like.
- Fermions, carry spin $\frac{1}{2}$
- Quarks carry electric, weak and colour charge.
- „Matter fields“

Antiparticles

- Every quark species and every lepton species have a partner, their antiparticles.
- Particles and antiparticles have exactly the same mass.
- They have opposite charges (mirror charges).



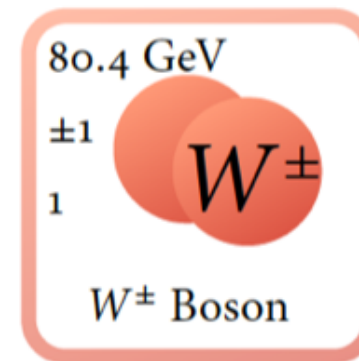
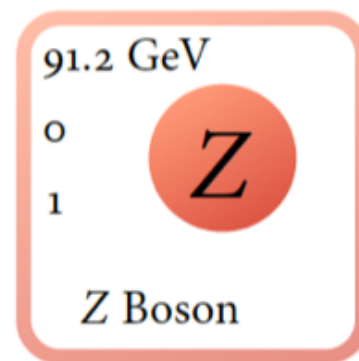
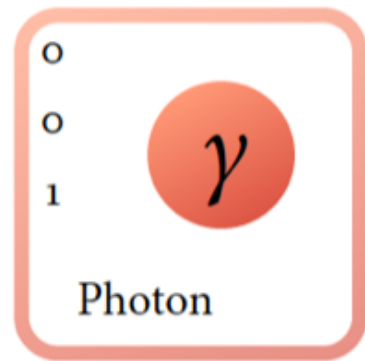
The Standard Model: a theory of interactions

Most remarkable feature of the SM:

Interactions are **predicted / derived** as a consequence of local gauge symmetry!







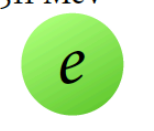
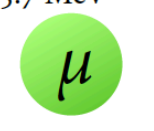
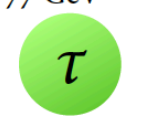
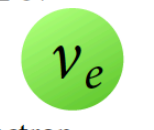
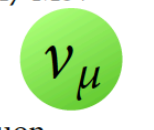
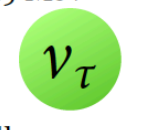
$$\psi \rightarrow \exp(i \vec{\theta}(x_\mu) \cdot \vec{a}) \psi \quad \lambda_1 = \begin{pmatrix} 0 & 1 & 0 \\ 1 & 0 & 0 \\ 0 & 0 & 0 \end{pmatrix} \quad \lambda_2 = \begin{pmatrix} 0 & -i & 0 \\ i & 0 & 0 \\ 0 & 0 & 0 \end{pmatrix} \quad \lambda_3 = \begin{pmatrix} 1 & 0 & 0 \\ 0 & -1 & 0 \\ 0 & 0 & 0 \end{pmatrix} \quad \dots$$

Gauge symmetry: $SU(3)_C \times SU(2)_L \times U(1)_Y$



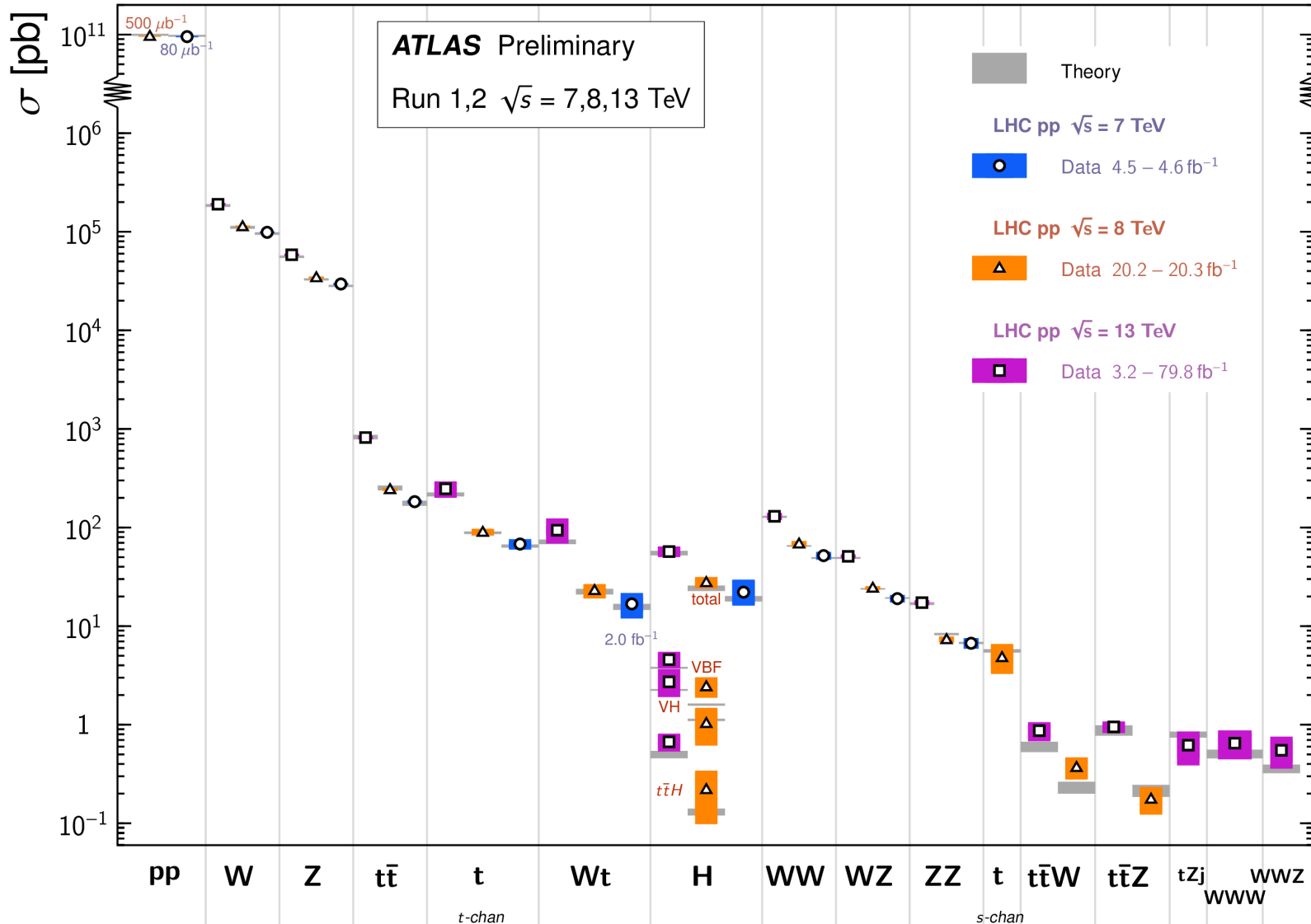
Gauge bosons
mediate
interactions

Particles of the Standard Model

	mass →	charge →	spin →				
Quarks	$\approx 2.3 \text{ MeV}$	$2/3$	$1/2$		Up Quark	Gauge Bosons	0
	$\approx 1.275 \text{ GeV}$	$2/3$	$1/2$		Charm Quark		0
	$\approx 173.2 \text{ GeV}$	$2/3$	$1/2$		Top Quark		1
	$\approx 4.8 \text{ MeV}$	$-1/3$	$1/2$		Down Quark		0
	$\approx 95 \text{ MeV}$	$-1/3$	$1/2$		Strange Quark		0
	$\approx 4.78 \text{ GeV}$	$-1/3$	$1/2$		Bottom Quark		1
Leptons	$\approx 0.511 \text{ MeV}$	-1	$1/2$		Electron	Gauge Bosons	0
	$\approx 105.7 \text{ MeV}$	-1	$1/2$		Muon		0
	$\approx 1.777 \text{ GeV}$	-1	$1/2$		Tau		1
	$< 2.2 \text{ eV}$	0	$1/2$		Electron Neutrino		0
	$< 0.17 \text{ MeV}$	0	$1/2$		Muon Neutrino		0
	$< 15.5 \text{ MeV}$	0	$1/2$		Tau Neutrino		1
							91.2 GeV
							0
							1
							80.4 GeV
							± 1
							1
							W^\pm Boson

Success of the Standard Model

Standard Model Total Production Cross Section Measurements *Status: July 2019*



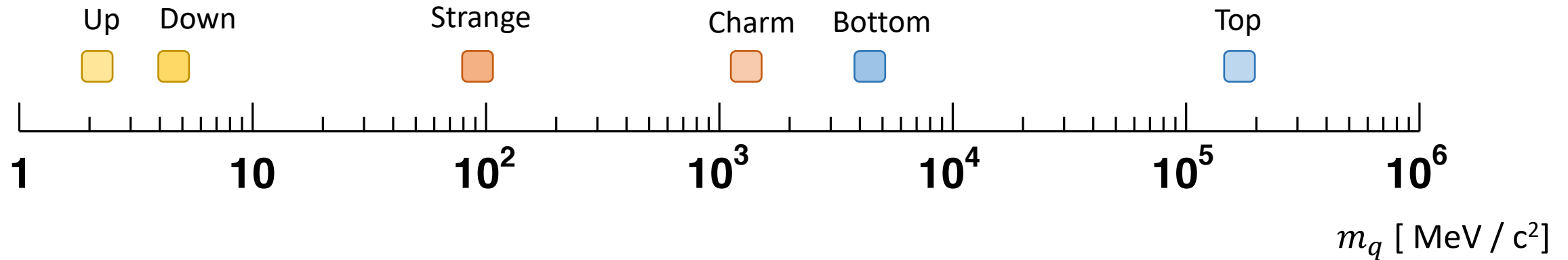
The SM describes all known particle physics phenomena with high precision.

A great success of 20th century science!

(Neutrino oscillations are an exception to some extent)

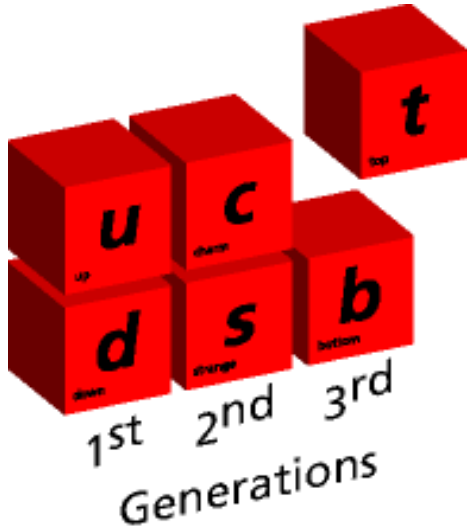
The astounding mass hierarchy quarks

- Quark masses exhibit a very pronounced mass hierarchy.
- Reason is unknown.
- Warning: Quark masses are a complex concept, since quarks are no free particles.



Reference:

<http://pdg.lbl.gov/2017/tables/rpp2017-sum-quarks.pdf>



- Weak-isospin partner of the b-quark.
- Charge: $+2/3 e$
- Spin: $1/2$
- The by far heaviest elementary particle: $m_t = 172.7 \pm 0.5 \text{ GeV}/c^2$
0,3% precision!
→ large loop corrections
- Coupling to the Higgs boson: $y_t \approx 1$

- No bound states:

$$\tau_{\text{top}} \propto \left(\frac{M_W}{M_{\text{top}}} \right)^3$$

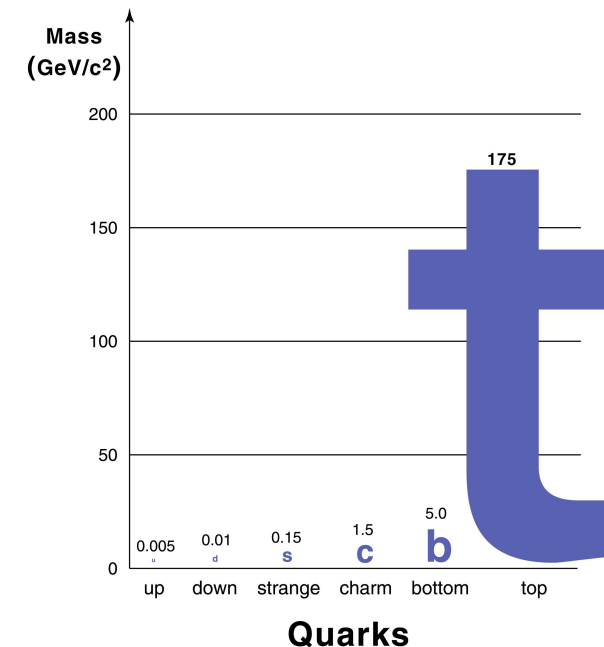
$$\tau_{\text{top}} \approx 4.7 \cdot 10^{-25} \text{ s}$$

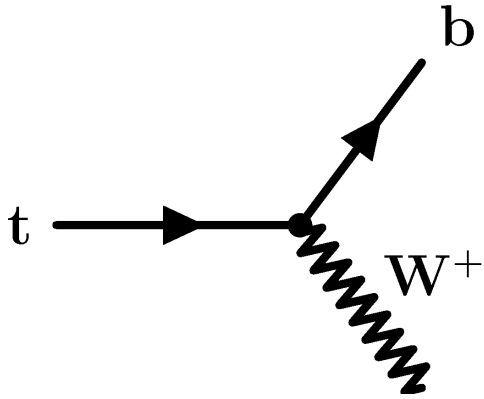
⇒ Top quark decays as a quasi free particle

⇒ Spin information and polarisation are accessible

(Spin decorrelation time: 10^{-21} s for hadrons)

QUARK MASSES





- Via the weak interaction
- Involves left-handed chiral fermion fields

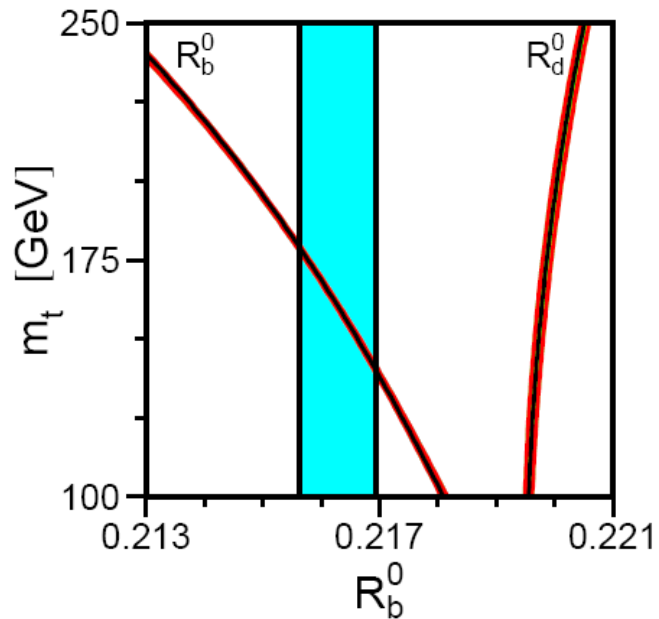
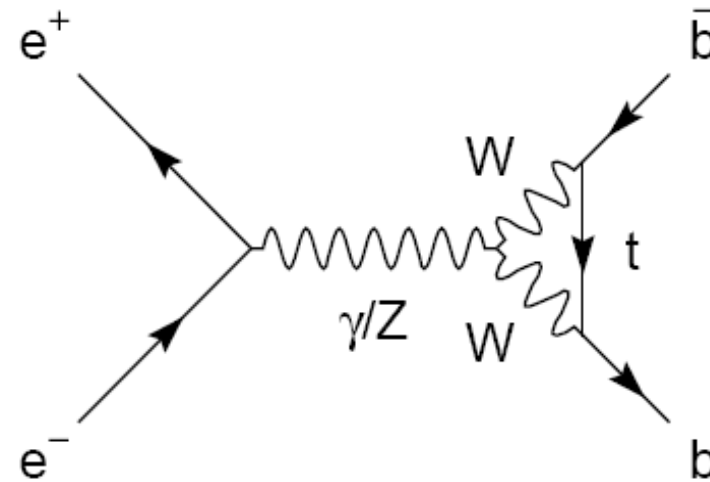
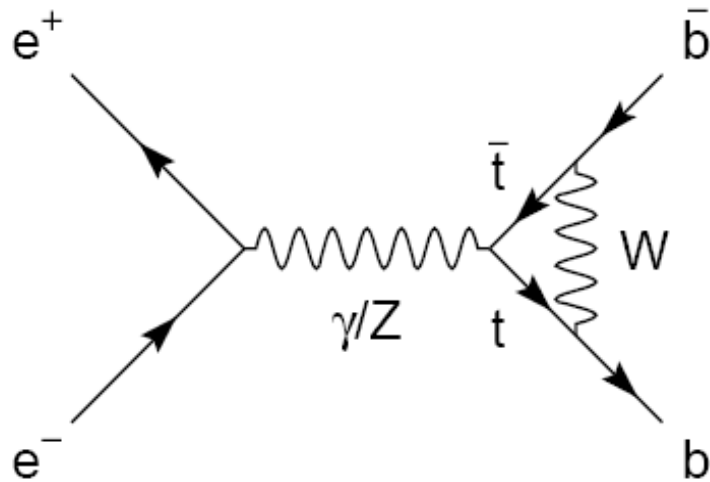
$$\psi_L = \frac{1}{2} (1 - \gamma_5) \psi$$

- Since $|V_{tb}| \approx 1$, $\mathcal{B}(t \rightarrow Wb) \approx 1$

$$\langle |\mathcal{M}|^2 \rangle = \frac{g_w^2}{16} \text{trace} [\gamma^\mu (1 - \gamma^5) (p_1^\mu \gamma_\mu + m_1 c) \gamma^\nu (1 - \gamma^5) (p_2^\mu \gamma_\mu + m_2 c)] (-g_{\mu\nu} + \frac{p_{3\mu} p_{3\nu}}{(m_w c)^2})$$

$$\langle |\mathcal{M}|^2 \rangle = \frac{g_w^2 c^2}{4 m_w^2} (m_t^2 - m_w^2) (m_t^2 + 2m_w^2)$$

Top-quarks in loops: Corrections to $Z \rightarrow b\bar{b}$



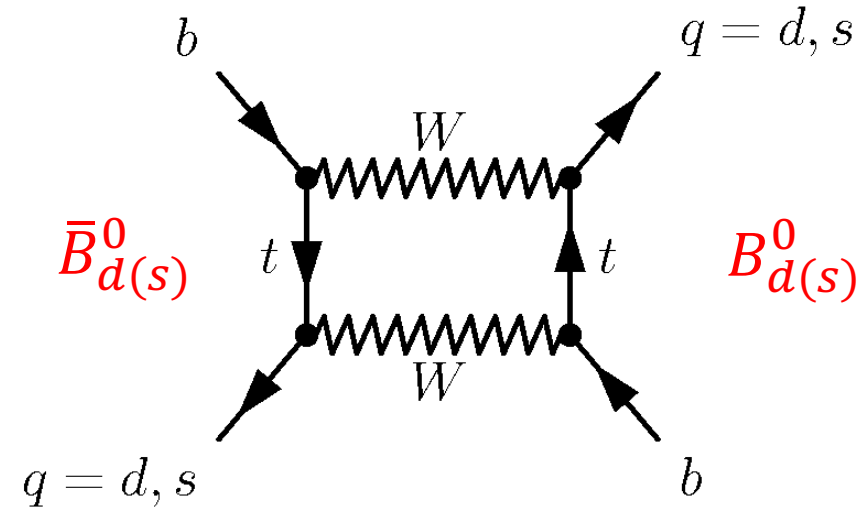
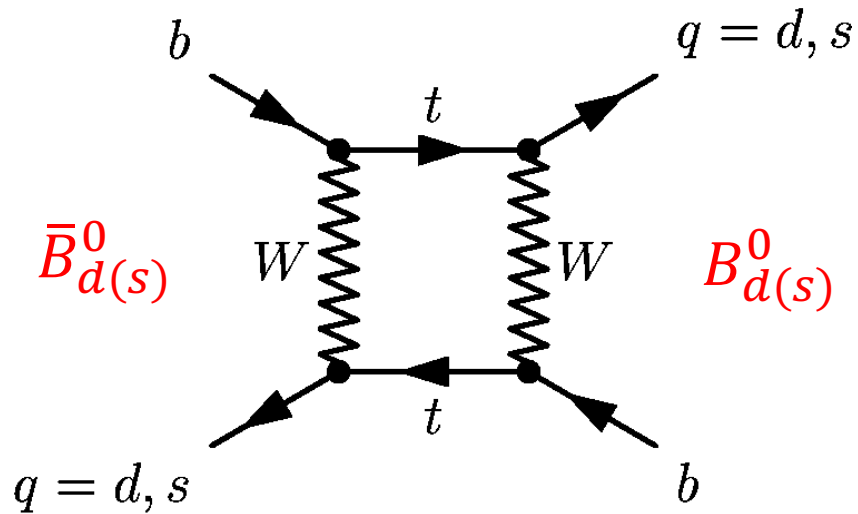
- Measurement
- $\Delta\alpha_{\text{had}}^{(5)} = 0.02758 \pm 0.00035$
- $\alpha_s = 0.118 \pm 0.003$
- $m_H = 114 \dots 1000 \text{ GeV}$

Phys. Rept. 427 (2006) 257

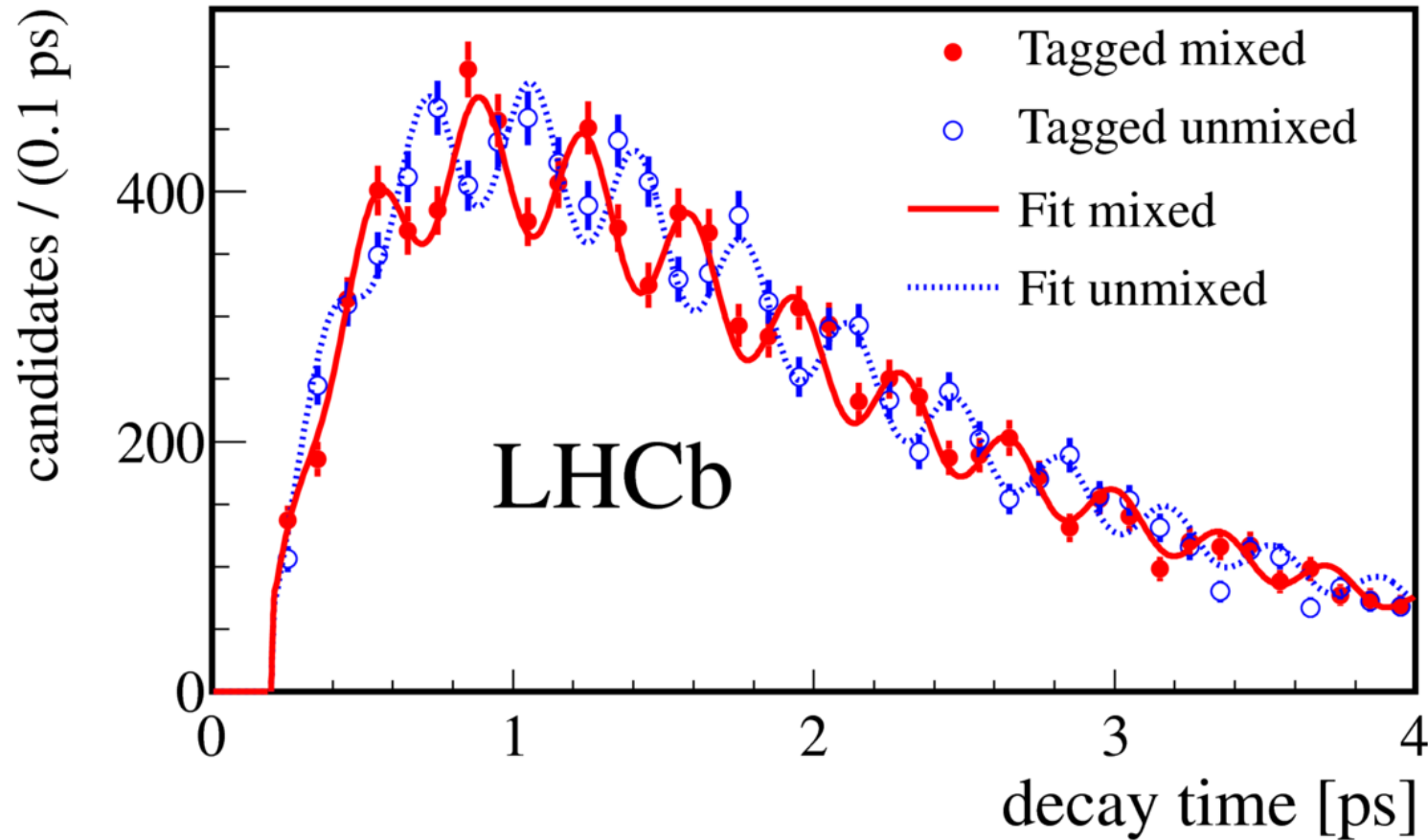
$$R_b^0 = \frac{\Gamma_{b\bar{b}}}{\Gamma_{\text{had}}}$$

The parameter R_b^0 depends strongly on the top-quark mass.

Top-quarks in loops: $B_{d(s)}^0 - \bar{B}_{d(s)}^0$ mixing



- Loops with top-quarks lead to main contribution.
- If all quark masses were degenerate, the amplitudes would cancel each other.



Tagged mixed =
different flavour at production and decay

Tagged unmixed =
same flavour at production and decay

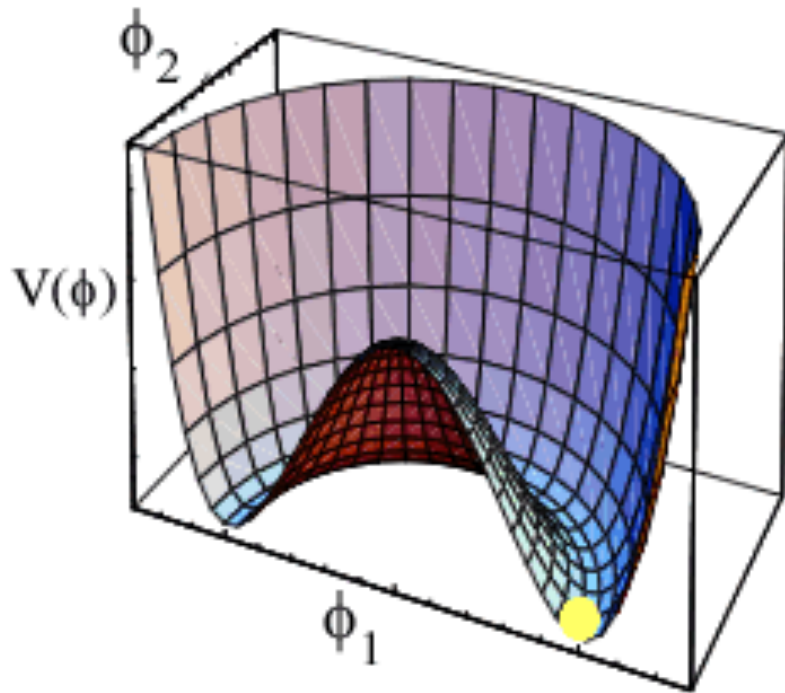
The mixing frequency is given by

$$\Delta m_s = 17.768 \pm 0.023 \text{ (stat.)} \pm 0.006 \text{ (syst.) ps}^{-1}$$

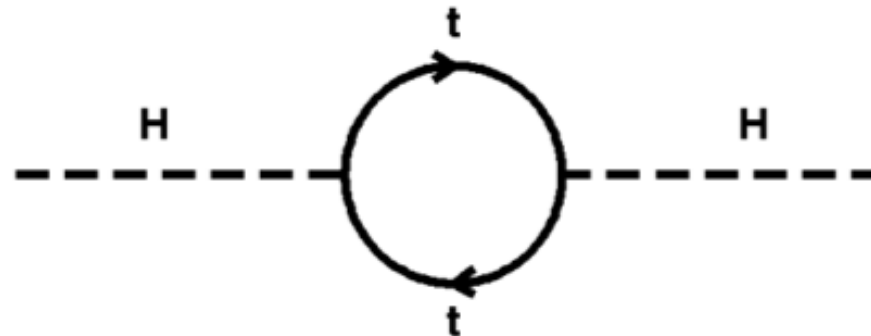
The top-quark and the Higgs

Potential of the Higgs field

$$V(\phi) = \frac{1}{2}\mu^2\phi^\dagger\phi + \frac{1}{4}\lambda(\phi^\dagger\phi)^2$$



Discovery of the Higgs boson in 2012 and subsequent measurements confirm the Brout-Englert-Higgs mechanism as the source of the mass of elementary particles.



Top-quark loops contribute to the Higgs propagator.

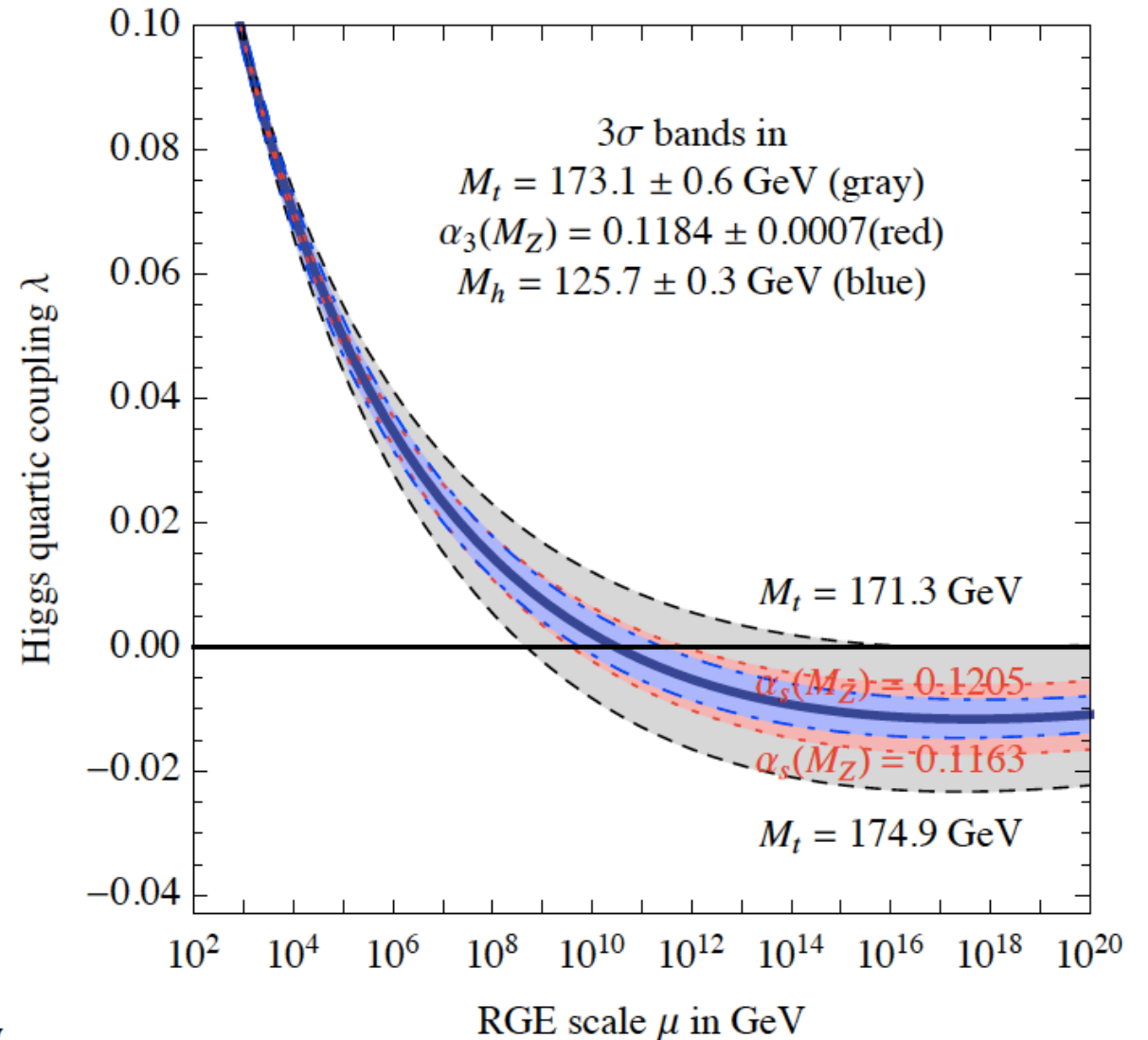
The running of the Higgs self-coupling

$$V(\phi) = \frac{1}{2}\mu^2\phi^\dagger\phi + \frac{1}{4}\lambda(\phi^\dagger\phi)^2$$

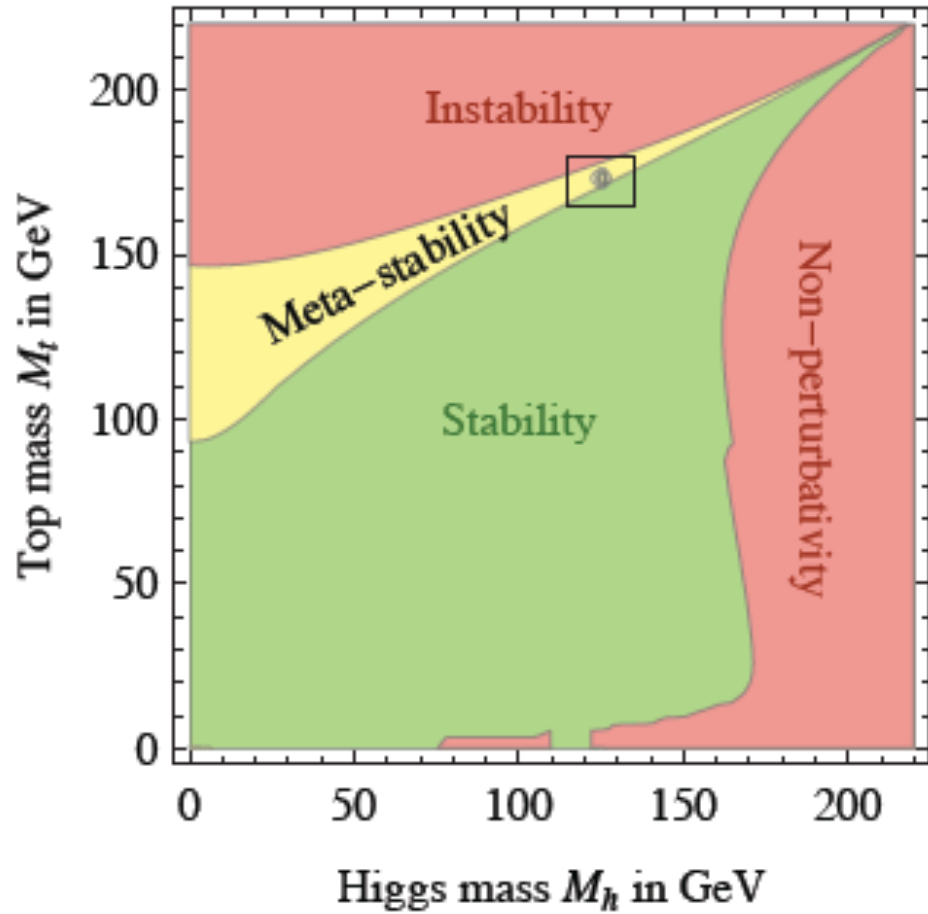
$$\lambda = \lambda(q^2)$$

- The Higgs self-coupling λ is not a constant.
- Loop corrections \rightarrow dependence on momentum scale μ
- Main contributions from top-quark
- Condition for absolute stability of the potential: $\lambda(q^2) > 0$

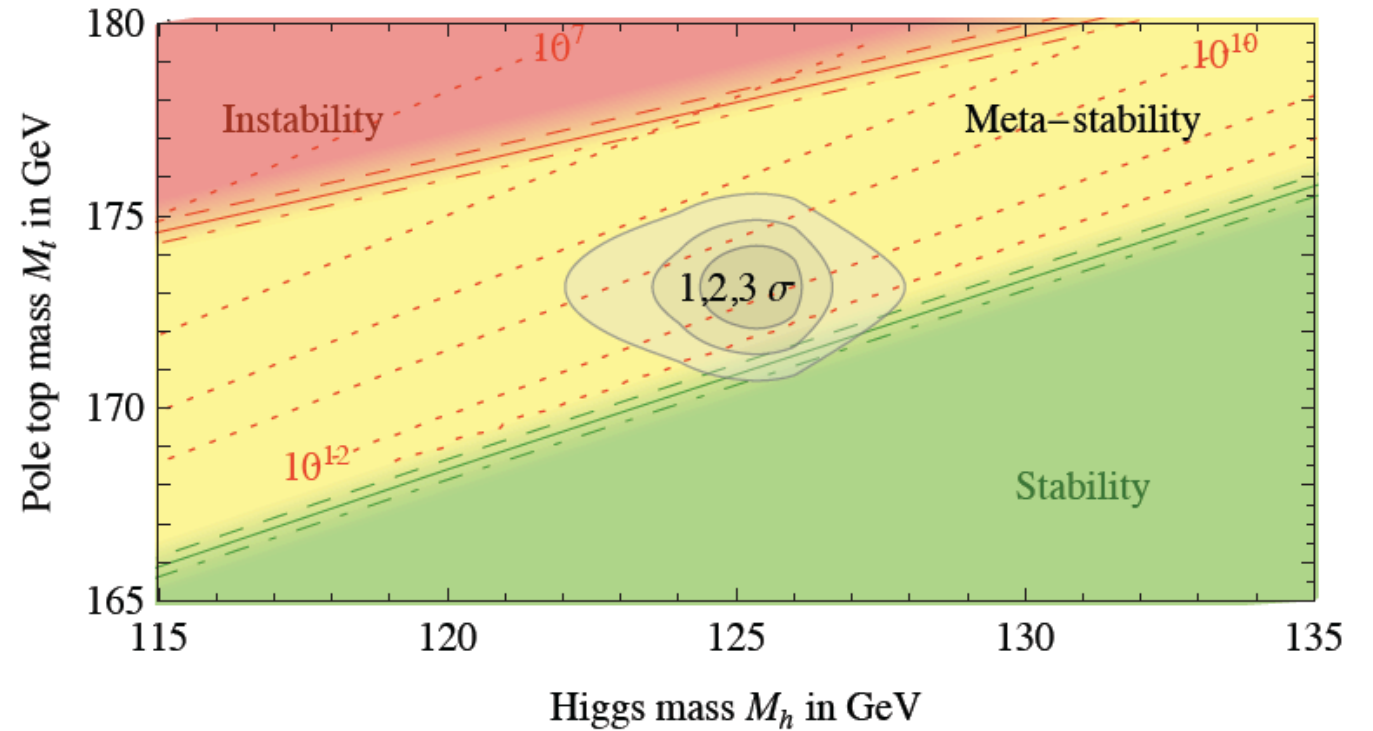
$$M_H \geq 129.2 + 1.8 \times \left(\frac{m_t^{\text{pole}} - 173.2 \text{ GeV}}{0.9 \text{ GeV}} \right) - 0.5 \times \left(\frac{\alpha_s(M_Z) - 0.1184}{0.0007} \right) \pm 1.0 \text{ GeV}$$



Vacuum stability



Degrassi et al., JHEP 1208 (2012) 098,
arXiv:1205.6497 [hep-ph] .

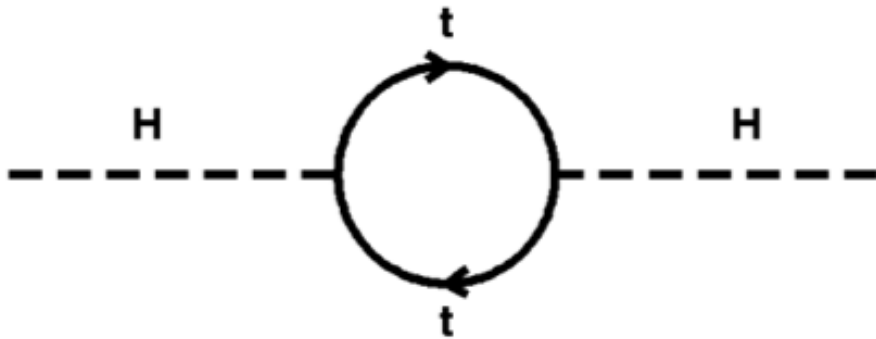


Top-quark mass is important parameter (value and uncertainty).

At leading order, the Higgs mass is given by the vacuum expectation value (minimum) of the potential of the Higgs field:

$$m_H \simeq v \simeq 10^2 \text{ GeV}$$

At higher orders, loop corrections shift the Higgs boson mass:



$$m_H^2 \rightarrow m_H^2 + \delta m_H^2$$

$$\delta m_H^2 = g^2 \int^\Lambda \frac{d^4 k}{k^2} \simeq g^2 \Lambda^2$$

Integral *diverges*, is regulated by a cut-off Λ .

- All fermions to which the Higgs field couples contribute to the loop corrections.
- There can be cancellations between different contributions.

- The Planck mass defines a maximum scale of validity for the Standard Model.
- At energies close to the Planck scale, gravity has similar strength as the other interactions.

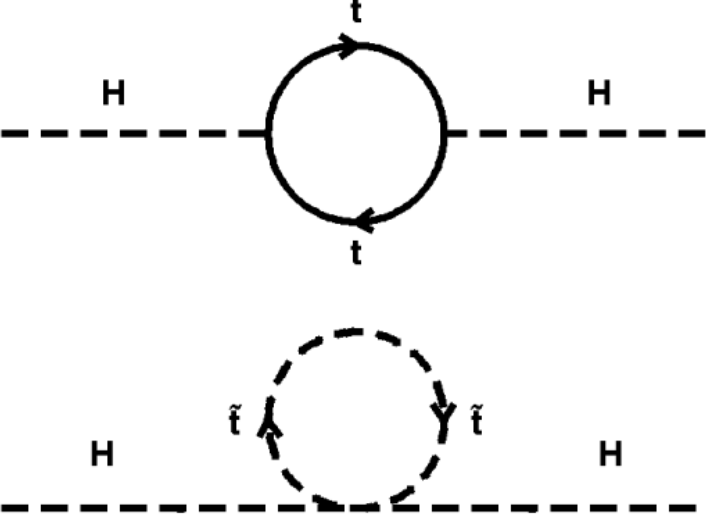
$$M_{\text{Planck}} \equiv (8\pi G_{\text{Newton}})^{-1/2} = 2.4 \cdot 10^{18} \text{ GeV}$$

- New physics laws have to kick in at M_{Planck} .
- In this sense $\Lambda \simeq M_{\text{Planck}}$ would be a *natural* choice.

- But
$$\frac{m_H}{m_{\text{Planck}}} \simeq 10^{-16} \text{ GeV}$$
 The hierarchy problem!

- Could be solved by introducing new physics at a lower scale, „close“ to the Higgs mass.

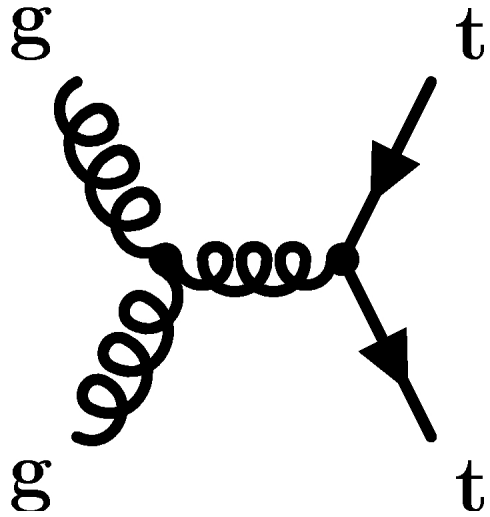
Regulation of the loop corrections



Addition of new particles lead to loop corrections which cancel the divergences.

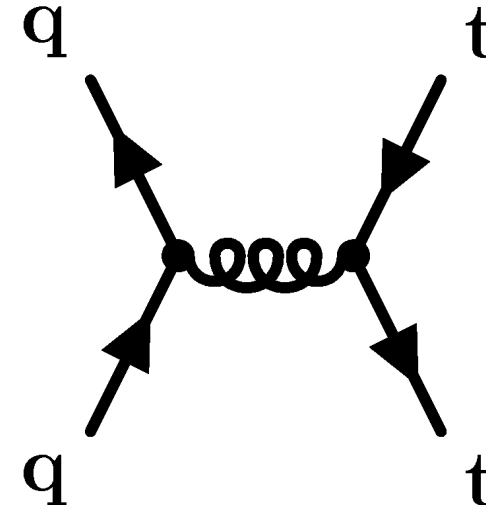
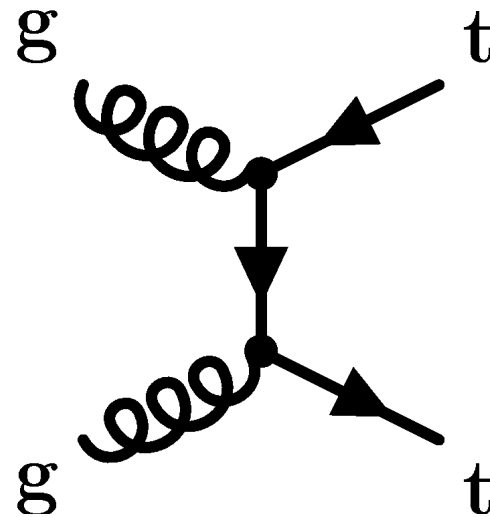
Top-quark-antiquark pair production

Gluon-gluon fusion



~10%

Quark-antiquark annihilation



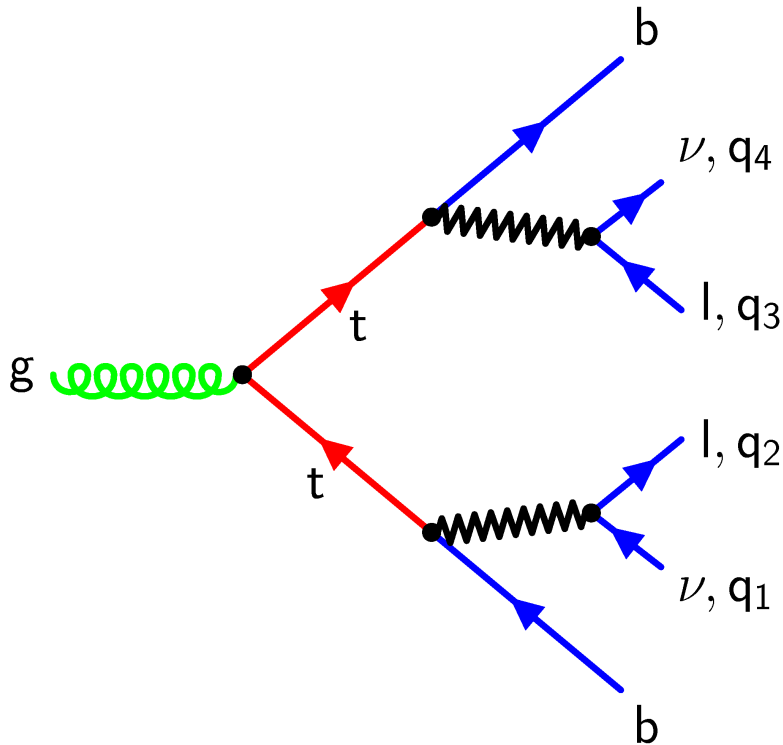
~90%

At the LHC at
 $\sqrt{s} = 13 \text{ TeV}$

Total cross-section: $\sigma = 832_{-30}^{+20} \text{ (scale)} \pm 35 \text{ (PDF and } \alpha_s)$

Relative uncertainty = 5.5%

Classification of top-quark events



Based on the decay modes of the W bosons from top-quark decay.

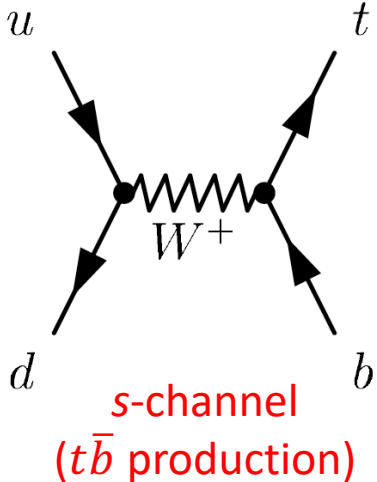
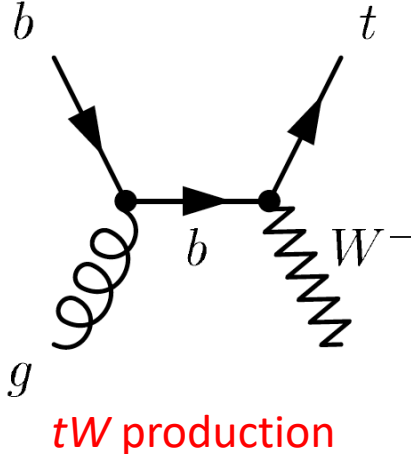
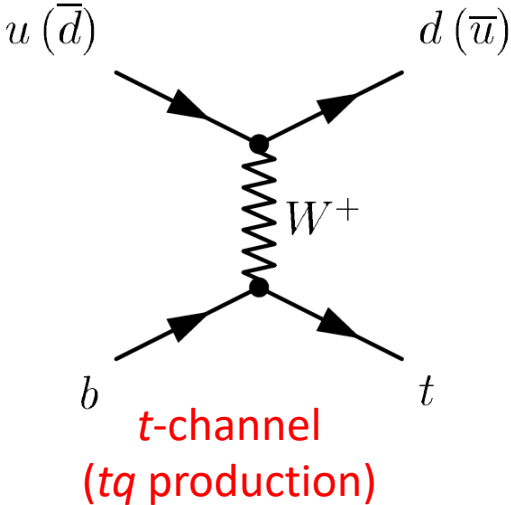
- 1) Di-lepton (e, μ)
- 2) Lepton + jets
- 3) Tau channels
- 4) All-hadronic

W decay	$e\nu/\mu\nu$	$\tau\nu$	$q\bar{q}'$
$e\nu/\mu\nu$	5%	5%	30%
$\tau\nu$	—	1%	15%
$q\bar{q}'$	—	—	44%

Top Pair Decay Channels

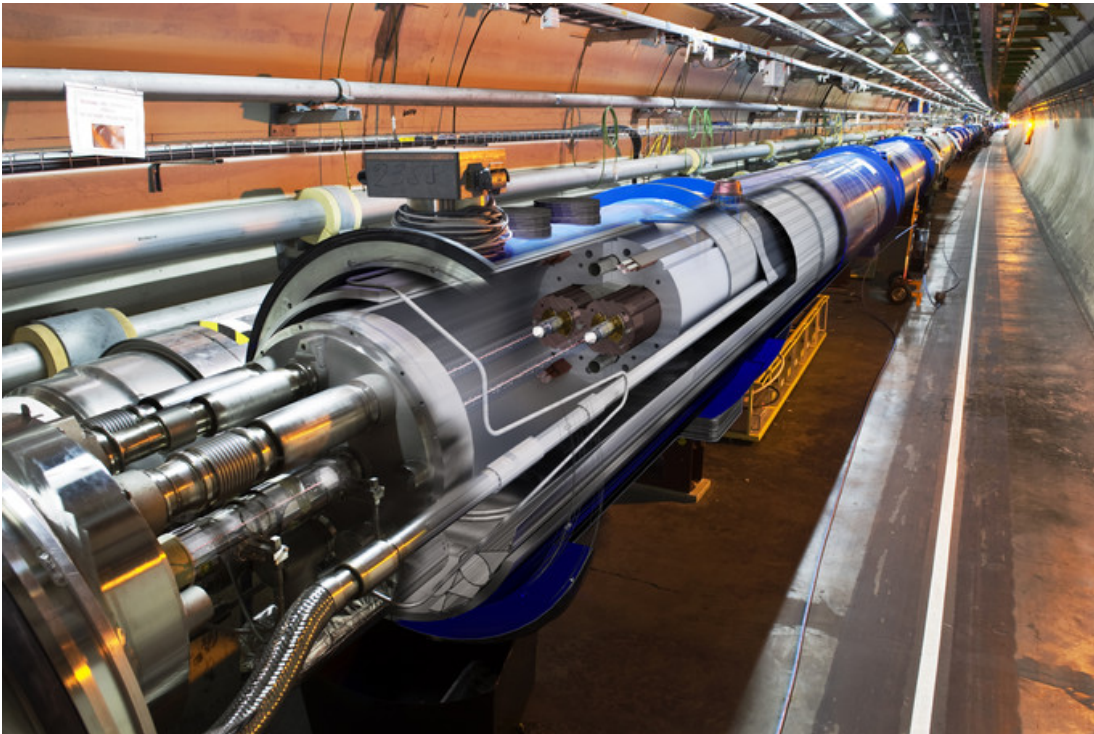
$\bar{c}s$	electron+jets	muon+jets	tau+jets	all-hadronic	
$\bar{u}d$					
τ^-	$e\tau$	$\mu\tau$	$\tau\tau$	tau+jets	
μ^-	$e\mu$	$\mu\mu$	$\mu\tau$	muon+jets	
e^-	ee	$e\mu$	$e\tau$	electron+jets	
W decay	e^+	μ^+	τ^+	$u\bar{d}$	$c\bar{s}$

Single top-quark production

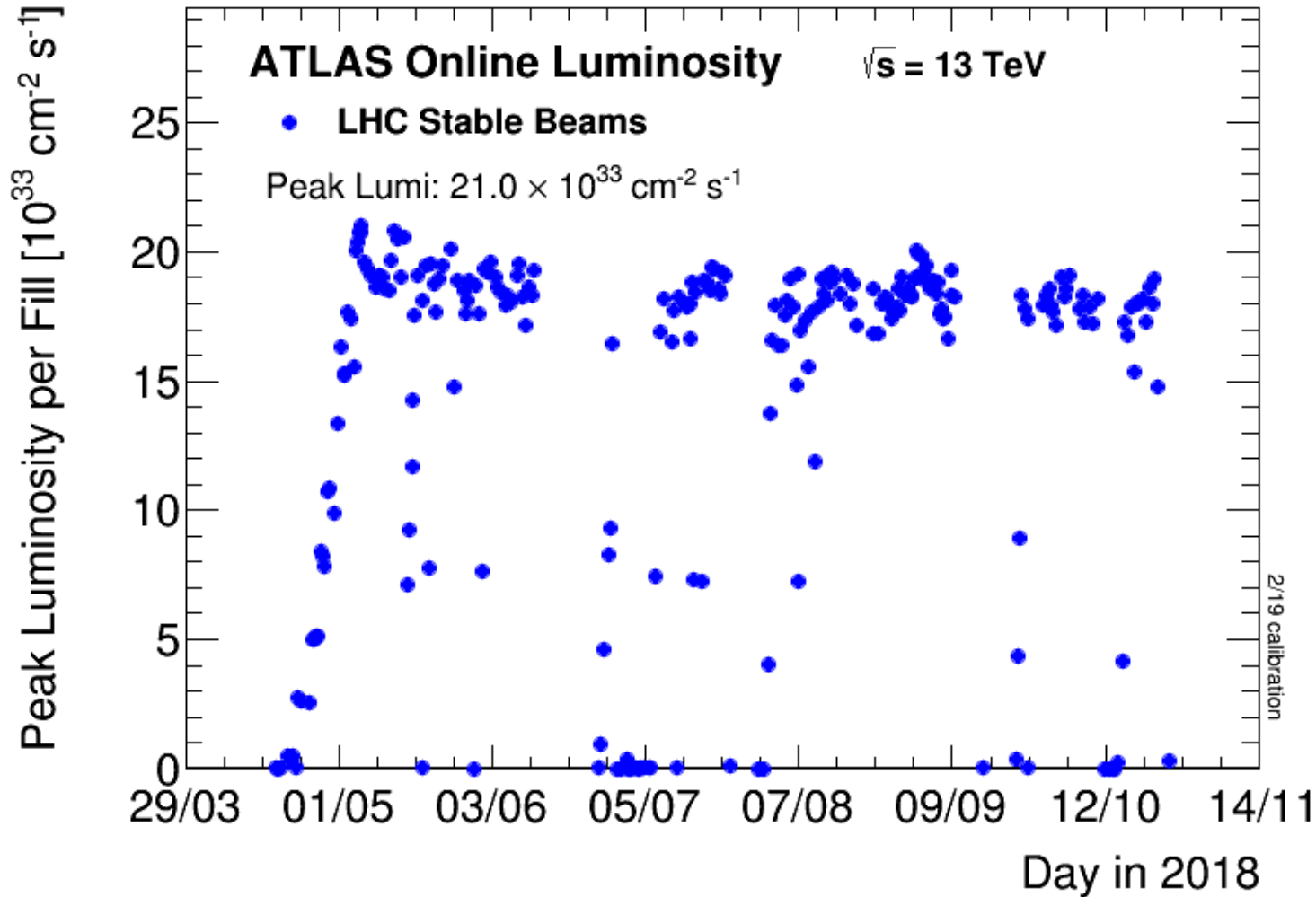


Chapter 2

The Large Hadron Collider and the ATLAS detector



Peak luminosity in 2018



$$\frac{dN}{dt} = L \cdot \sigma$$

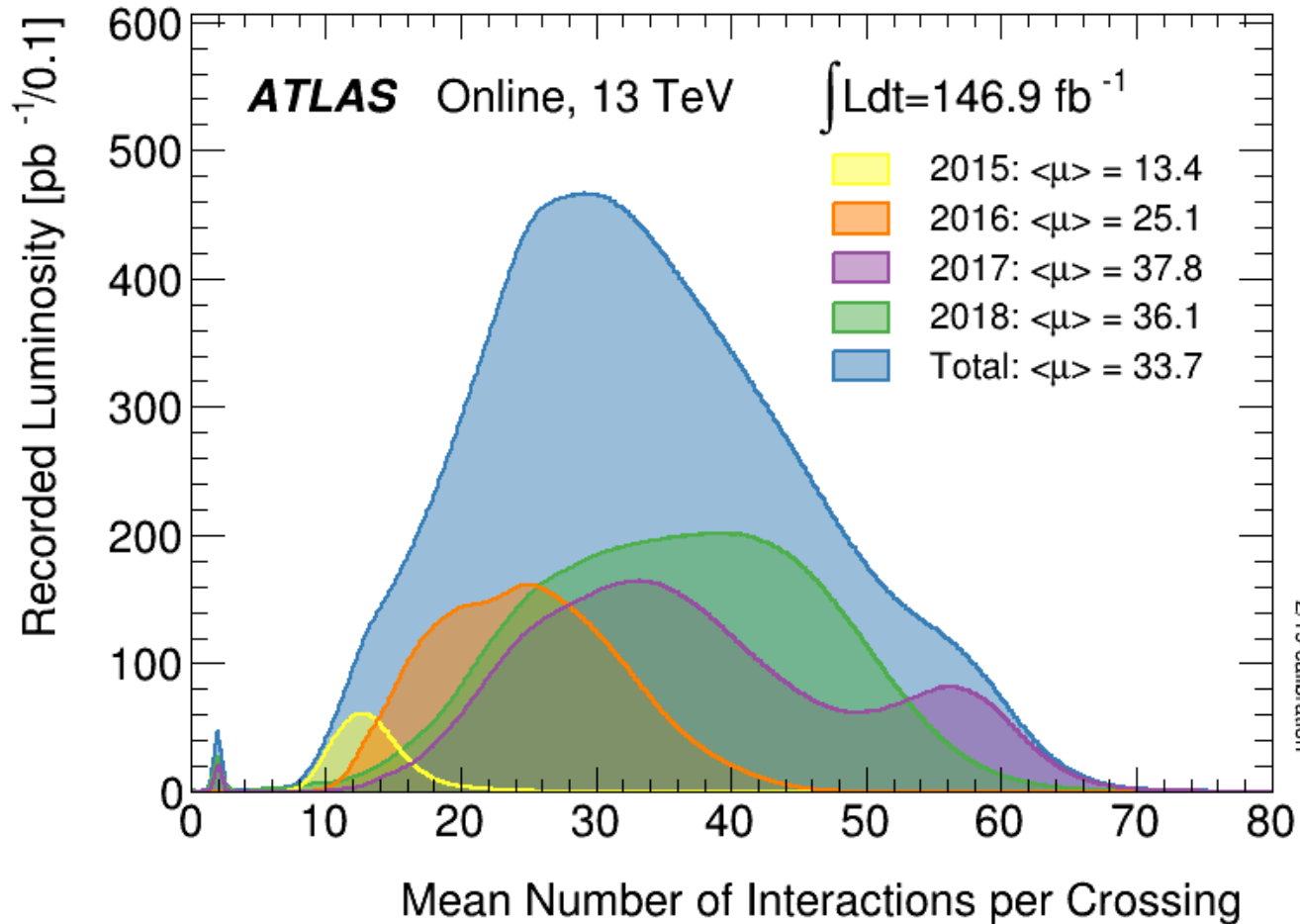
L: Luminosity

σ : Cross section

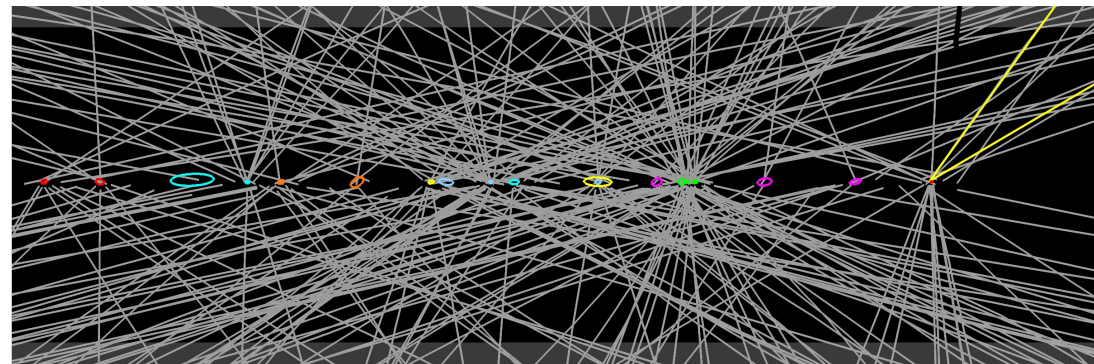
Units: $\text{cm}^{-2} \text{ s}^{-1}$

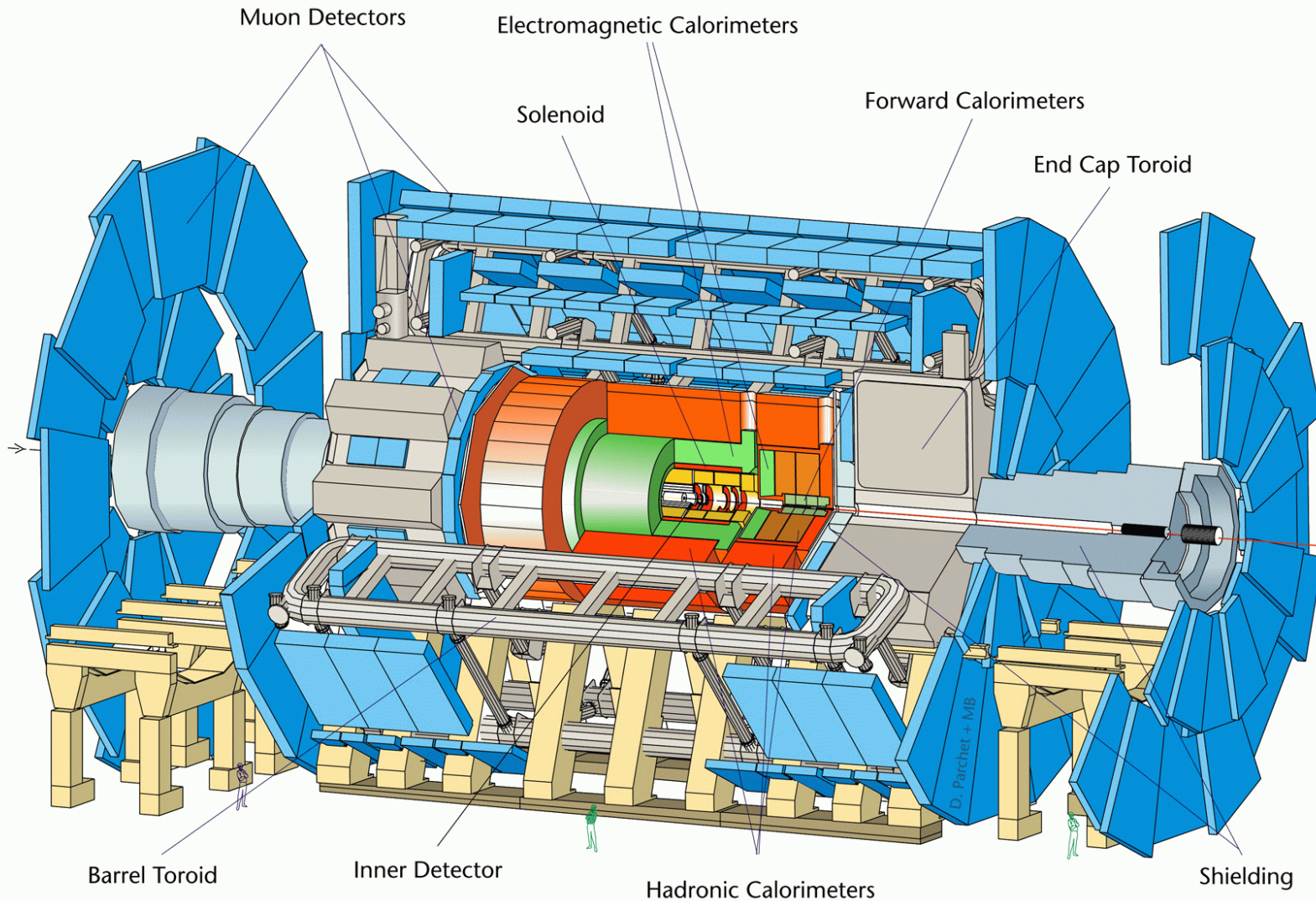
Same units as a particle current density.

Number of pp interactions per bunch crossing



Integrated luminosity „good for physics“ = 139 fb^{-1}



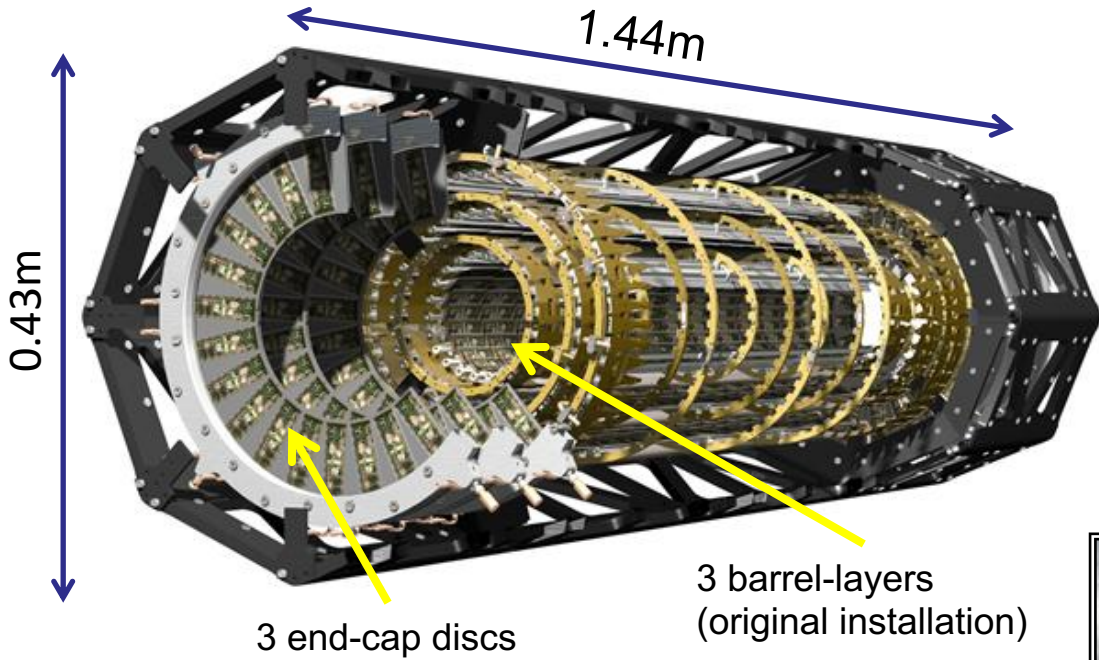


46 m long and 24 m high

Main components (= sub-detectors)

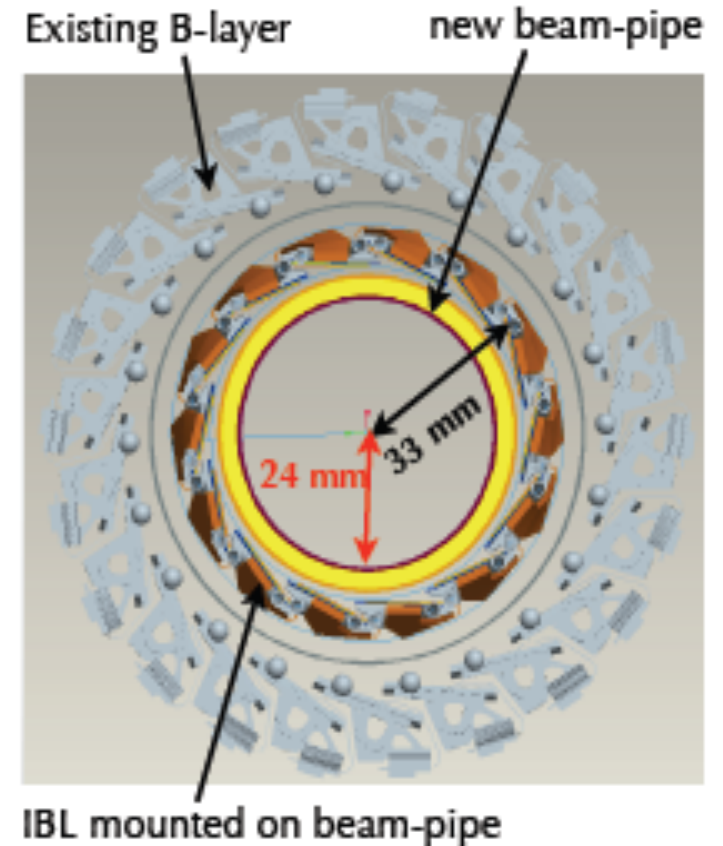
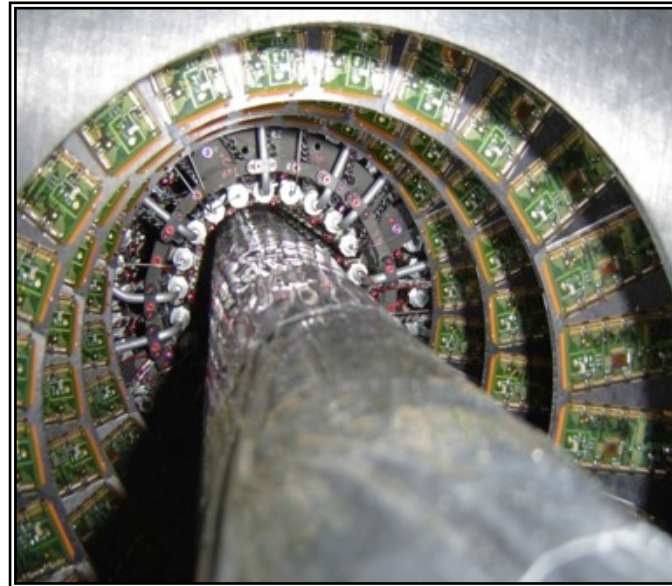
- Inner detector
→ tracks of charged particles
- Calorimeters
→ photons
→ electrons
→ hadronic jets (quarks and gluons)
- Muon system
→ muons
- Magnet systems
→ bending of charged particles

The ATLAS Pixel detector



- 3 to 4 precise track hits up to $|\eta| < 2.5$:
 - $R\Phi$ resolution: $10\ \mu\text{m}$
 - η (or z) resolution: $115\ \mu\text{m}$
- 4 shells in central region
- 3 discs in forward region
- 92 million pixel cells

- 4th layer installed in 2014.
- Radiation hard up to $2.4 \times 10^{16}\ \text{p/cm}^2$



Installation of the new pixel layer: the IBL

IBL =
Insertable B-Layer

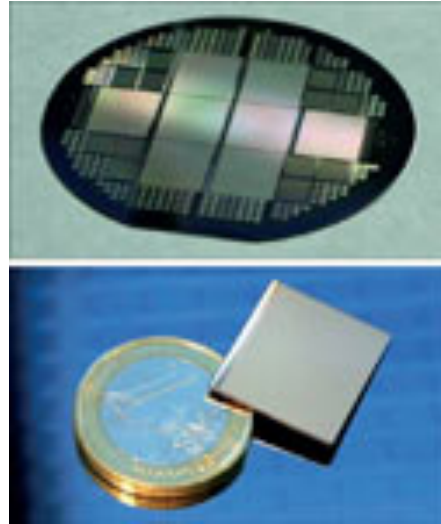
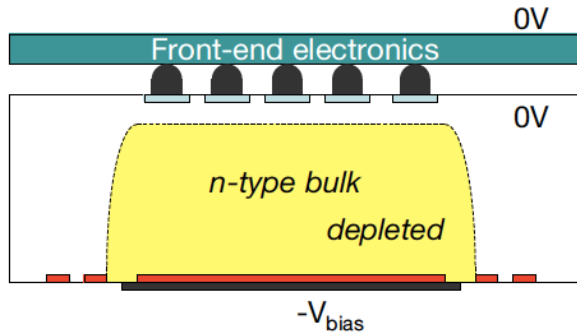
Designed and produced with vital contributions of the Wuppertal HEP group:

- 1) Support structures (carbon foam and carbon fibre compound)
- 2) Detector readout
- 3) Detector monitoring and control

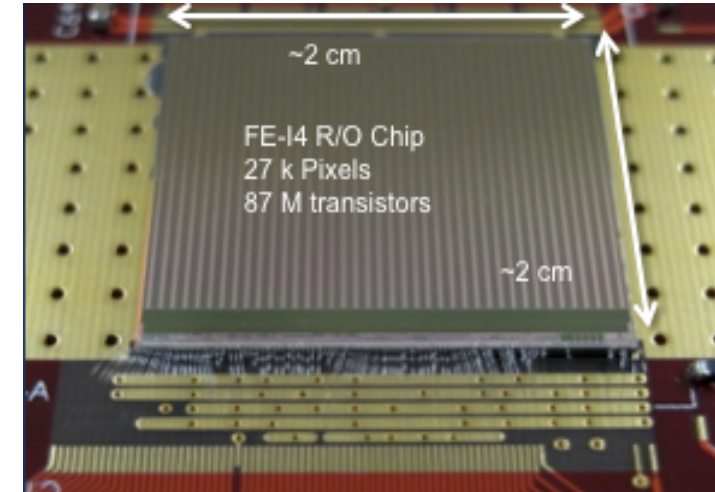
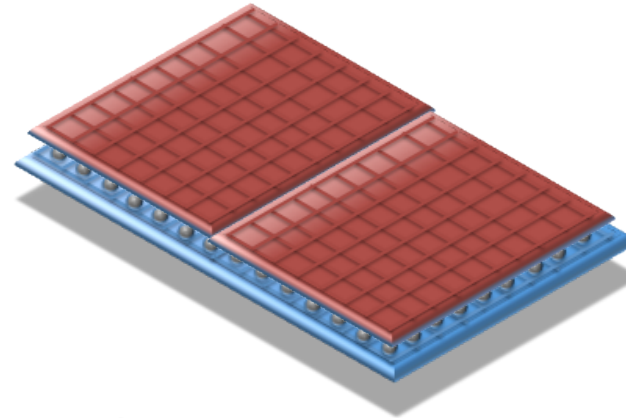
May 2014

Components of the Pixel detector

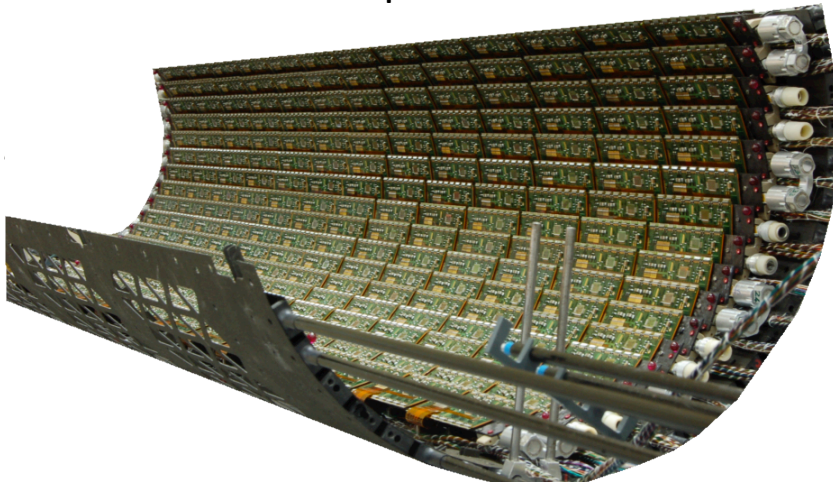
1) Sensors



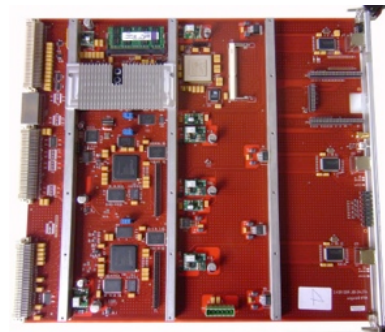
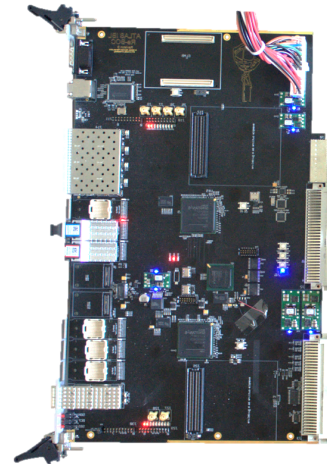
2) Front-end electronics



3) Mechanical support structures made of carbon fibre compounds



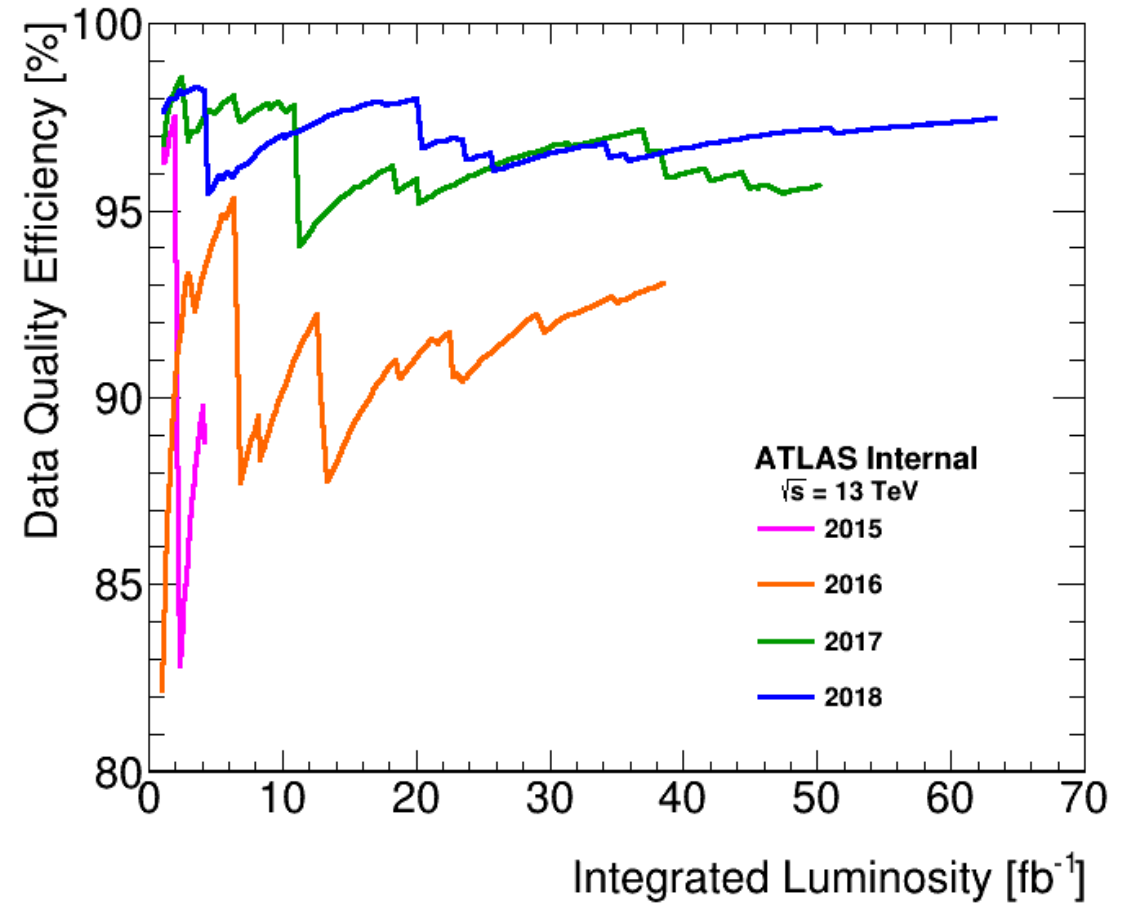
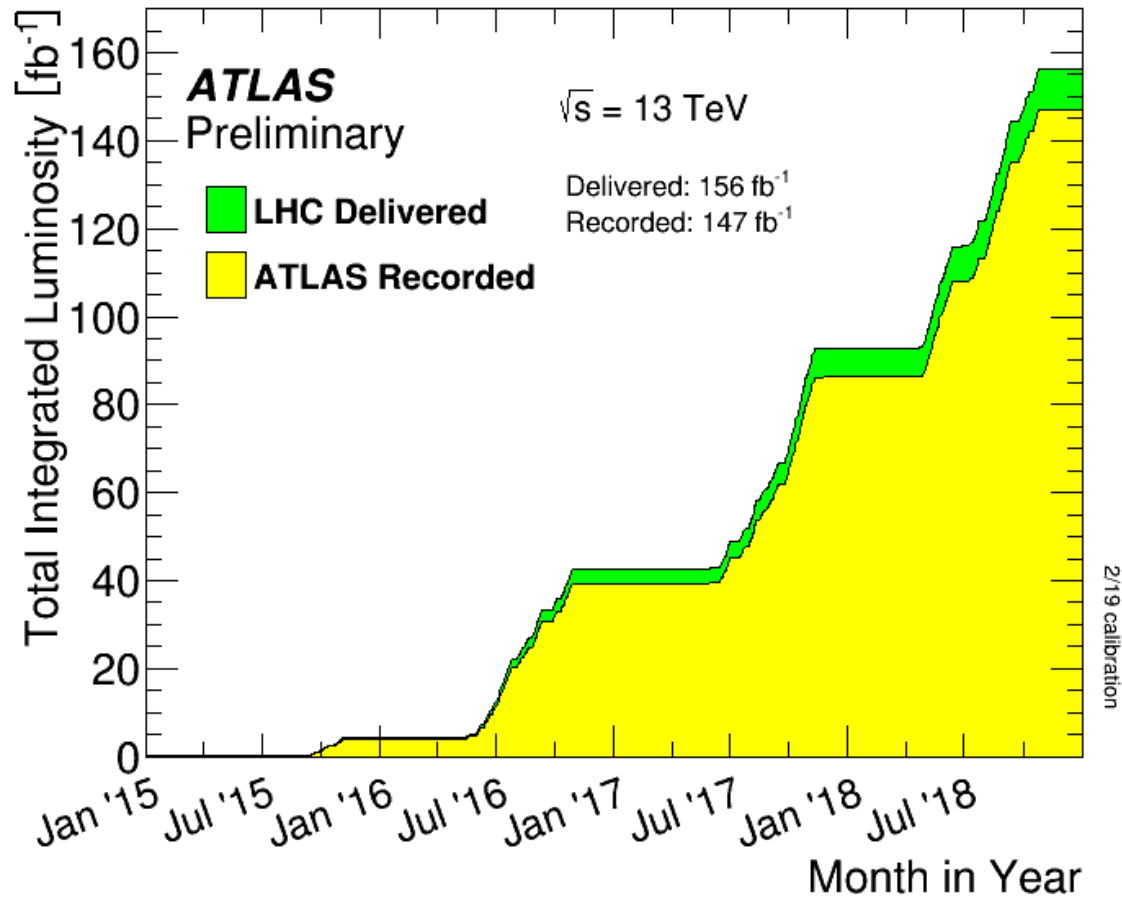
4) Readout and data acquisition system



5) Monitoring and control system



Integrated luminosity and data-taking efficiency



Secondary vertex reconstruction

- Important for top quark and Higgs boson physics

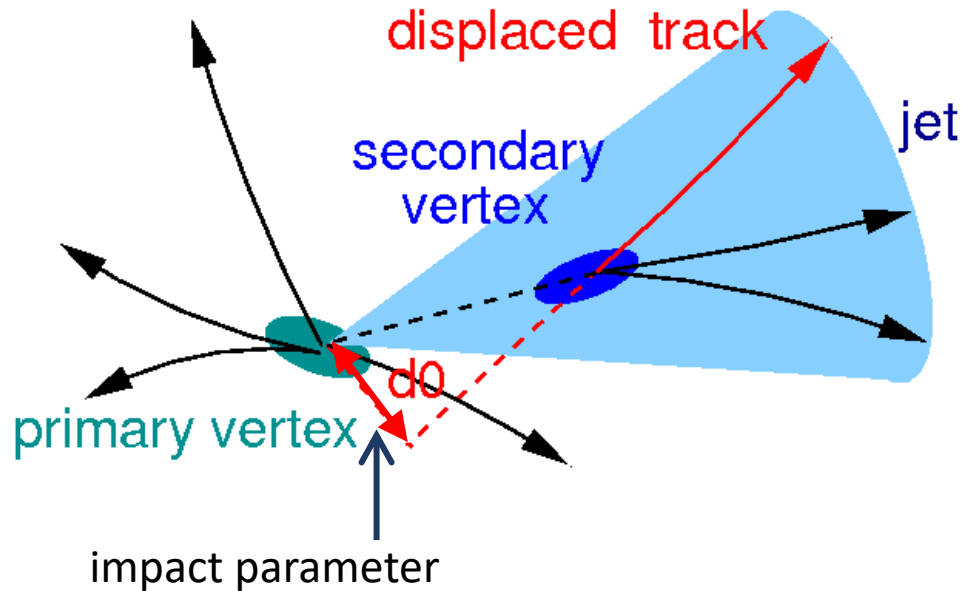
Identification of

- b-quark jets
- τ leptons

- Long lifetime: τ (b-Hadron) ≈ 1.5 ps $\rightarrow c\tau \approx 450$ μ m
 τ (τ -Lepton) ≈ 0.3 ps

Requirement of a secondary vertex:

\rightarrow strong reduction of the W + jets background in top-quark events



Impact parameter resolution is limited by multiple scattering:

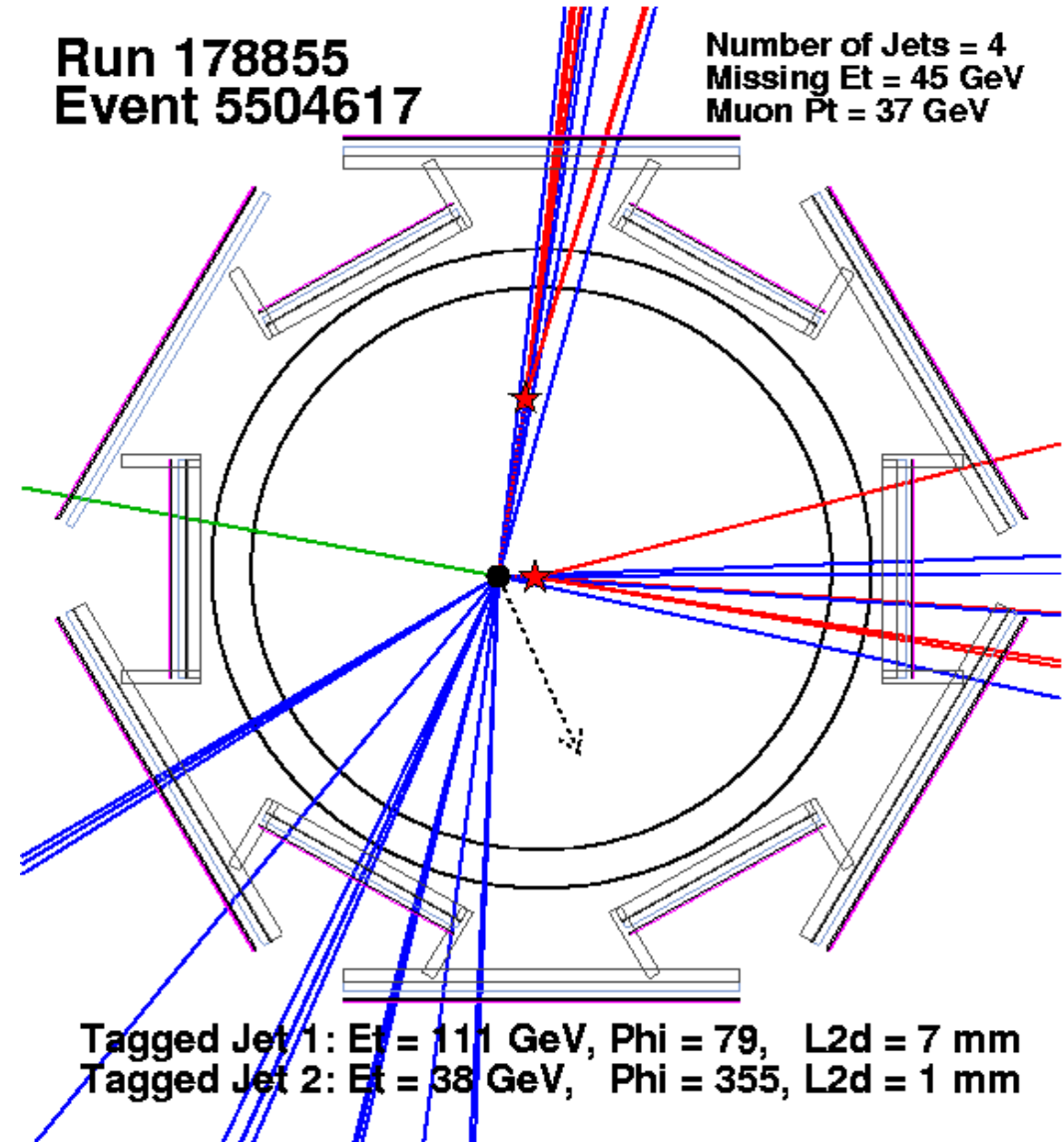
$$\propto \sqrt{\frac{x}{X_0}} \quad \text{Amount of material}$$

$$\propto L \quad \text{Distance of the first measurement layer}$$

Top-quark-antiquark pair candidate event ...

... with two reconstructed
secondary vertices

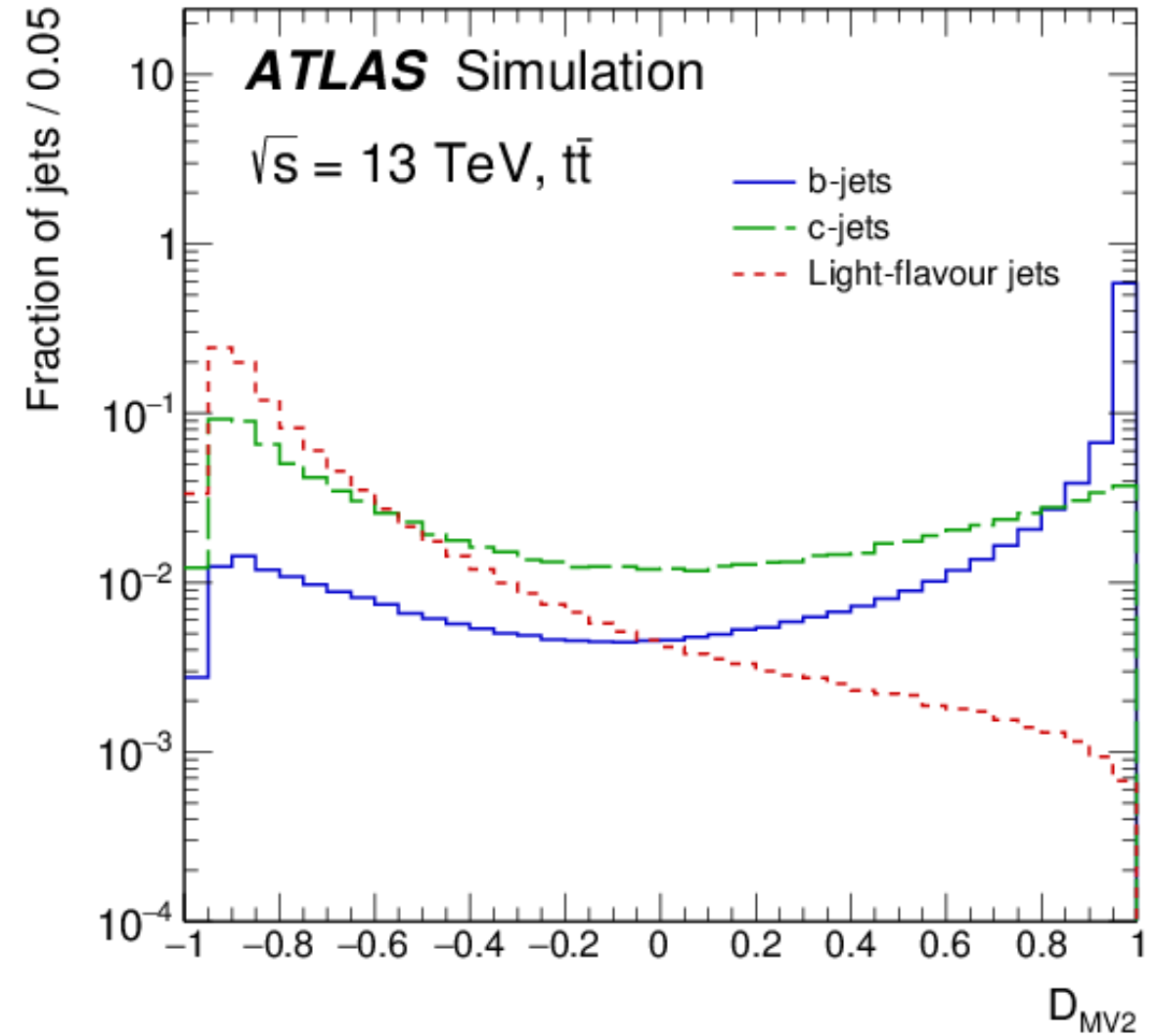
CDF experiment at Fermilab



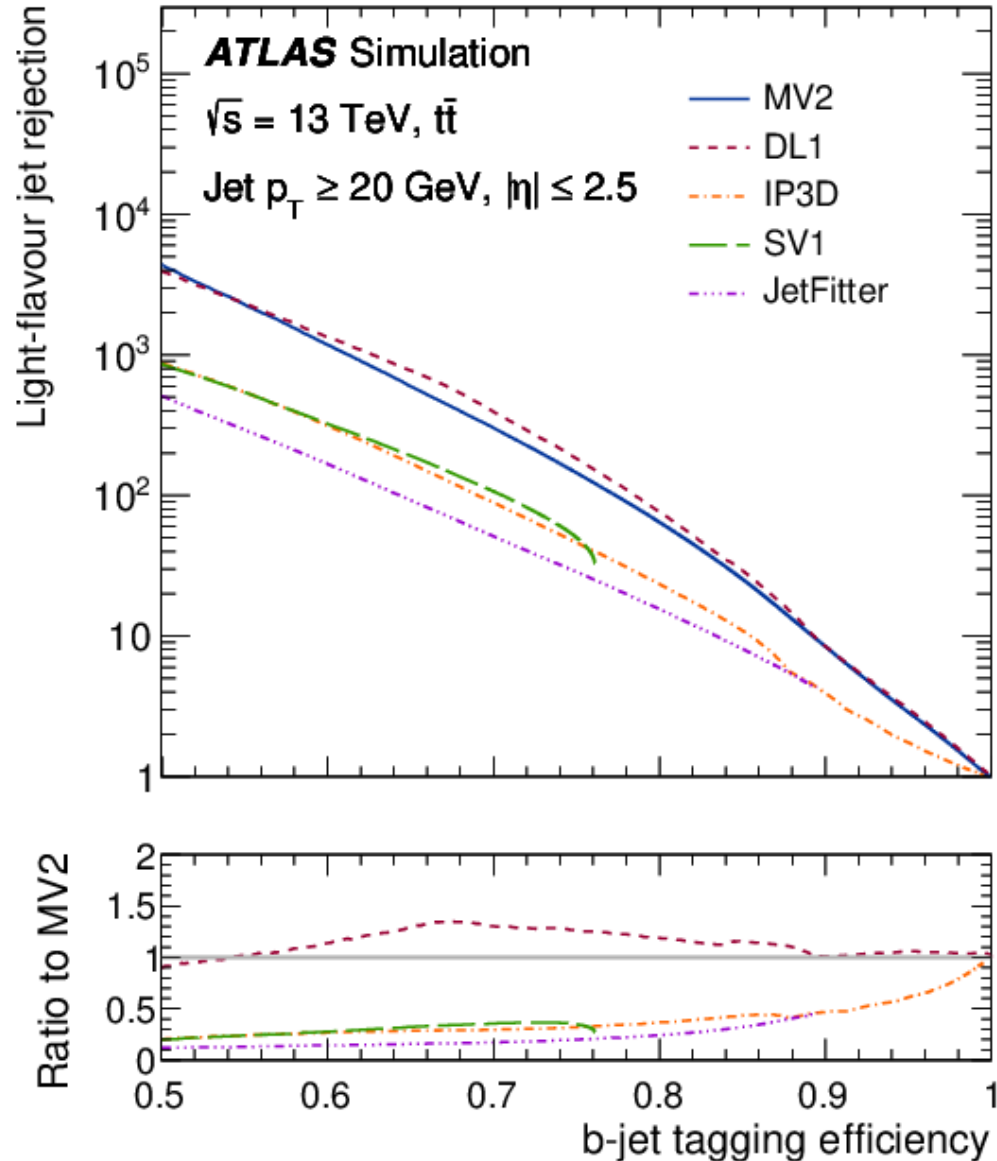
Flavour-tagging with multivariate techniques

Use many discriminating features of b-jets, c-jets and light-jets to identify them.

[arXiv:1907.05120](https://arxiv.org/abs/1907.05120)



Performance of flavour-tagging algorithms



Multivariate tagger algorithms improve rejection of light-flavour jets by more than one order of magnitude.

MV2 = Boosted Decision Tree (BDT)

DL1 = Deep Neural Network

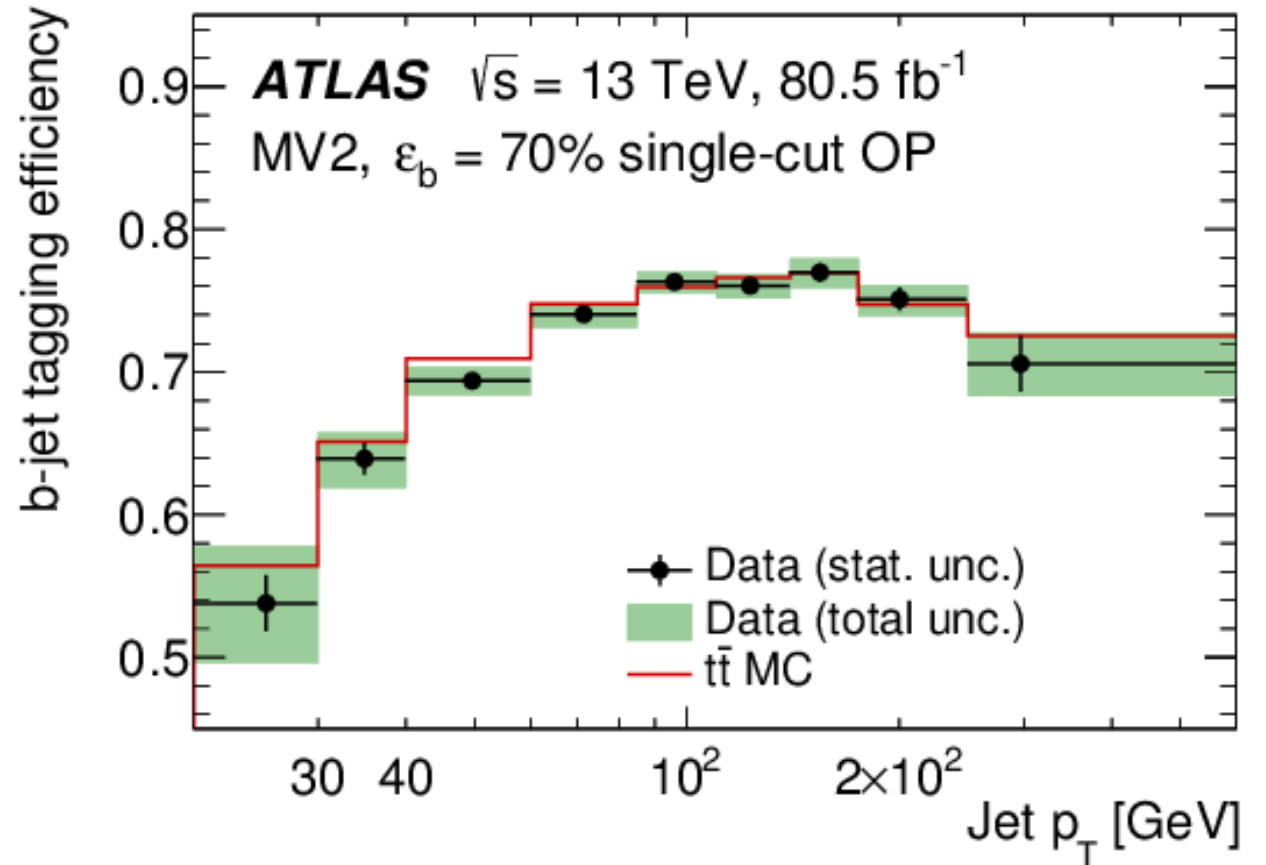
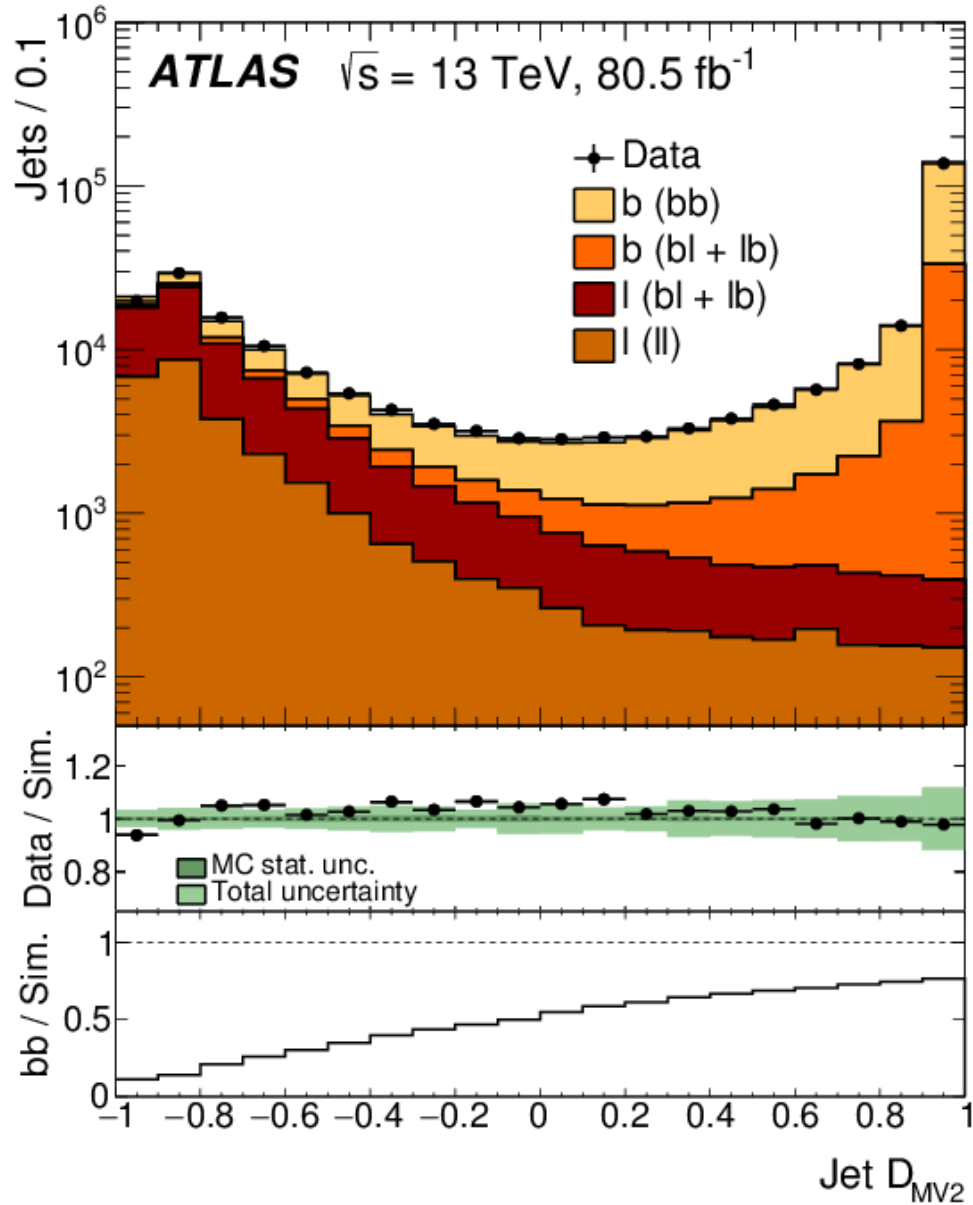
Conventional tagging algorithms:

IP3D = Track impact parameter based tagger

SV1 = Reconstruction of a secondary vertex

JetFitter =

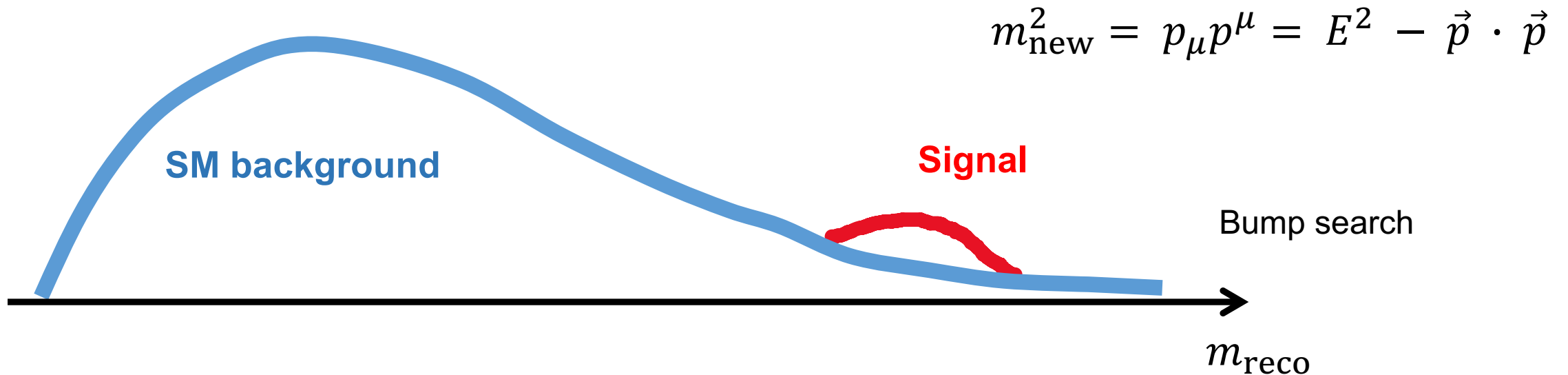
Data Monte-Carlo comparison (calibration)



MC-to-data scale factor is close to 1.

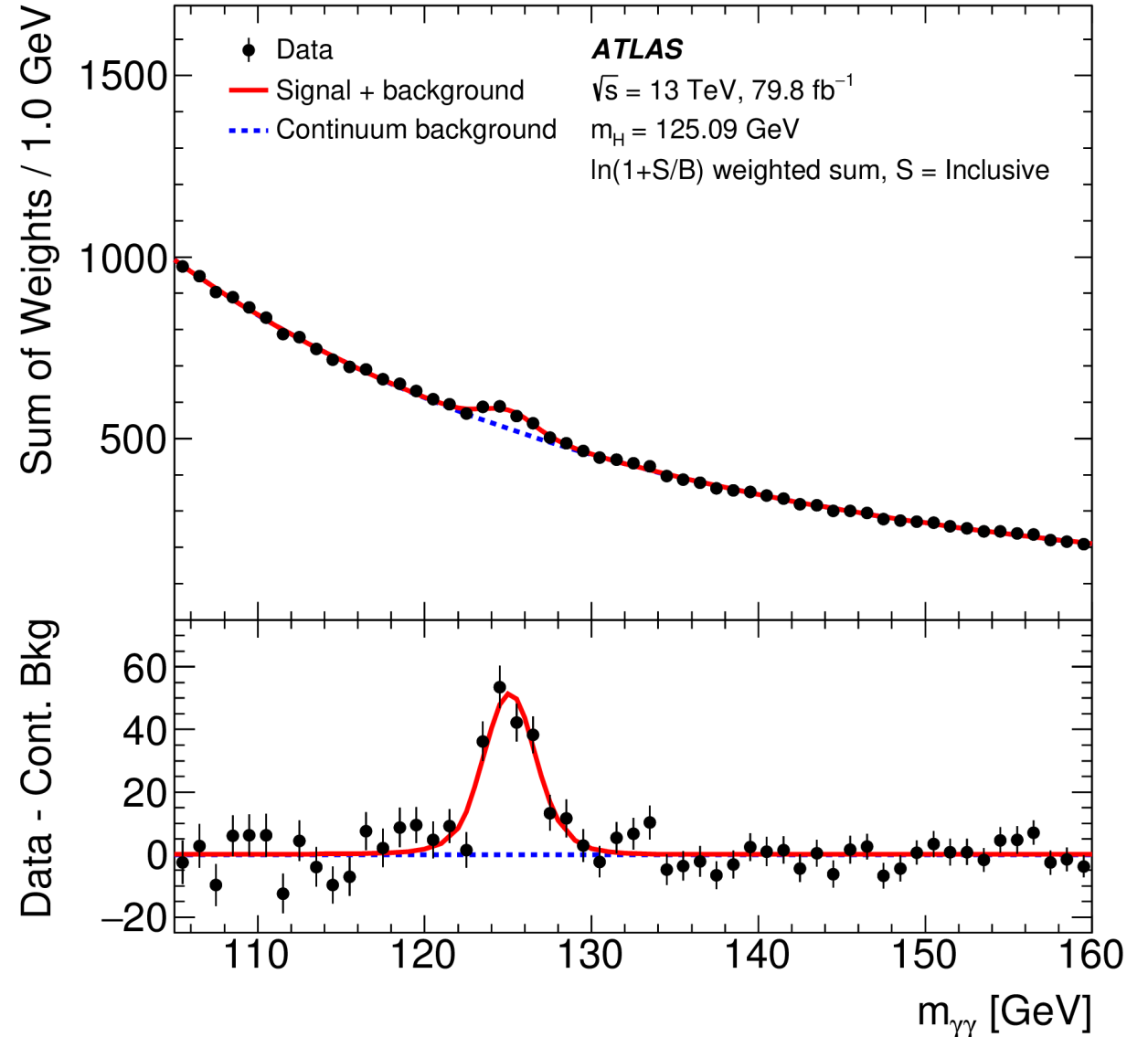
Chapter 3

Direct searches for new particles (So-called on-shell production)



Prime example of a bump search:

Observation and subsequent
measurement of the SM Higgs
boson in the
 $H \rightarrow \gamma\gamma$
decay channel.

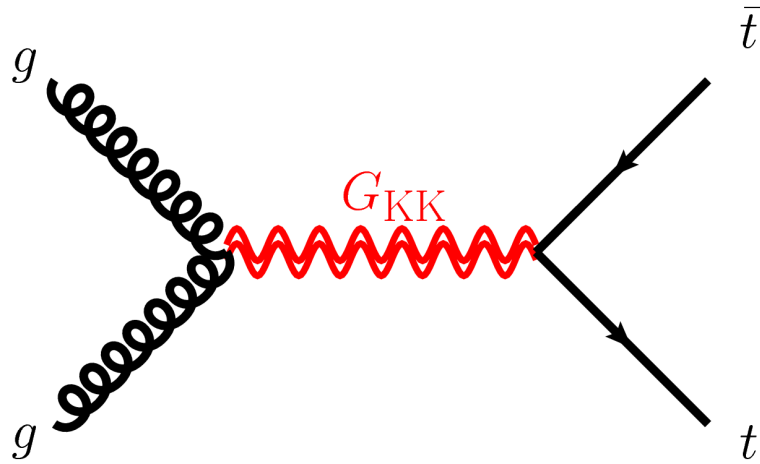


Direct searches for

- 1) $t\bar{t}$ resonances
- 2) Supersymmetric partners of top quarks, bottom quarks and gluons decaying to $t\bar{t}$ pairs
- 3) Vector-like top quarks
- 4) Lepto-quarks decaying to 3rd generation quarks and leptons

Search for $t\bar{t}$ resonances

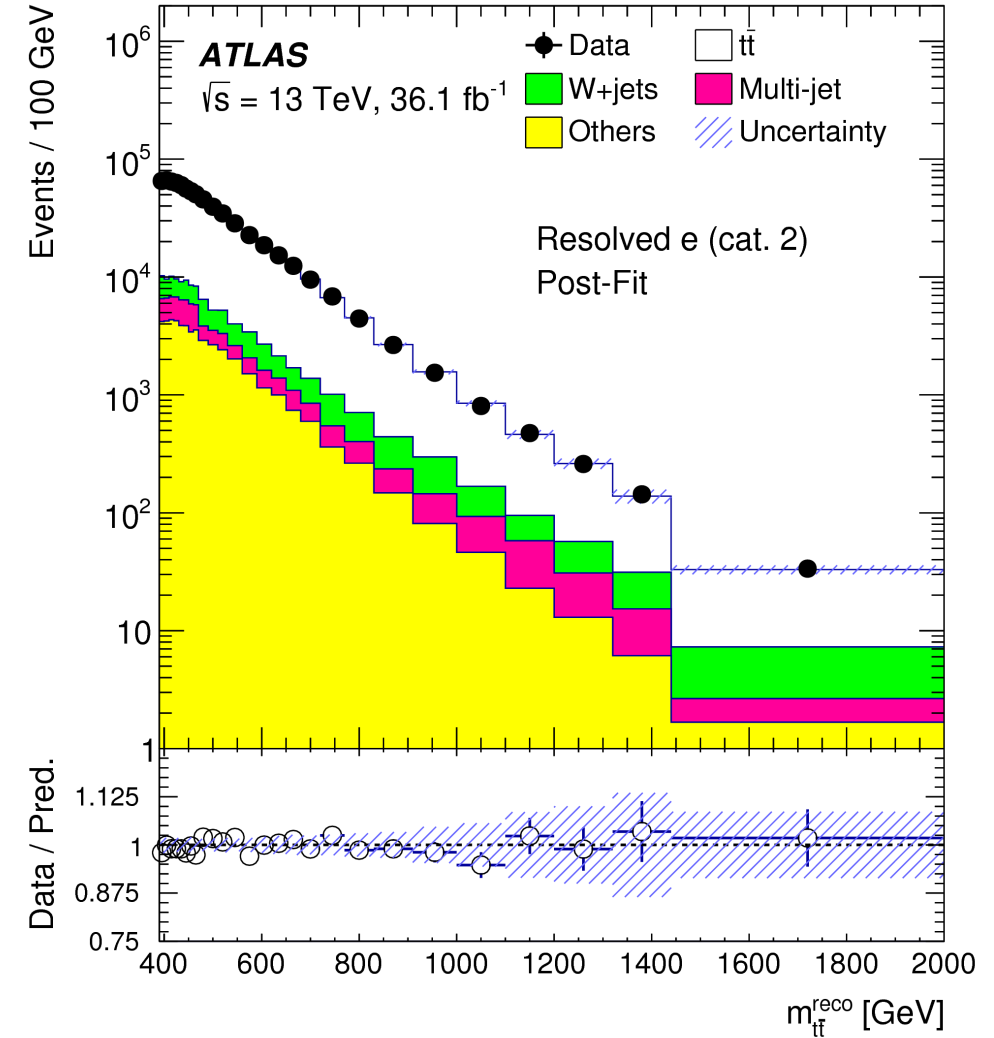
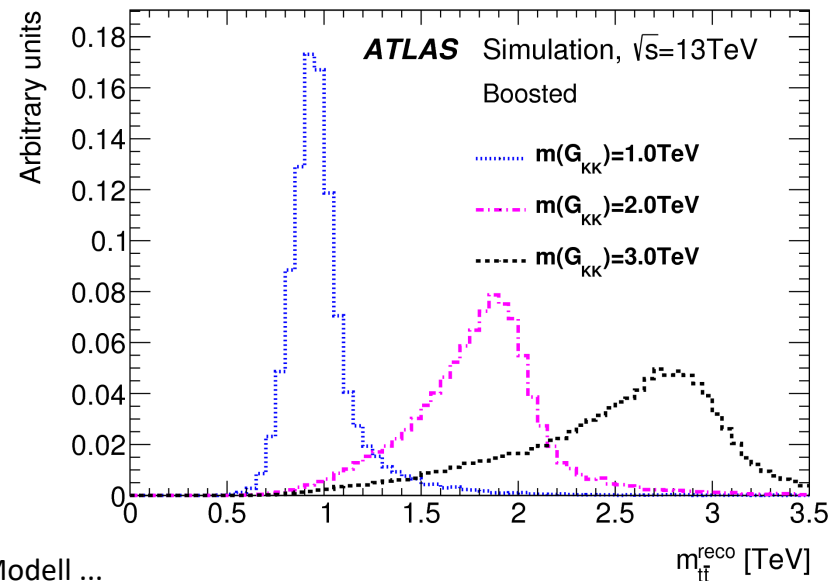
Higher symmetry than SM \rightarrow more gauge bosons



Important for discovery if decay to $t\bar{t}$ is enhanced.

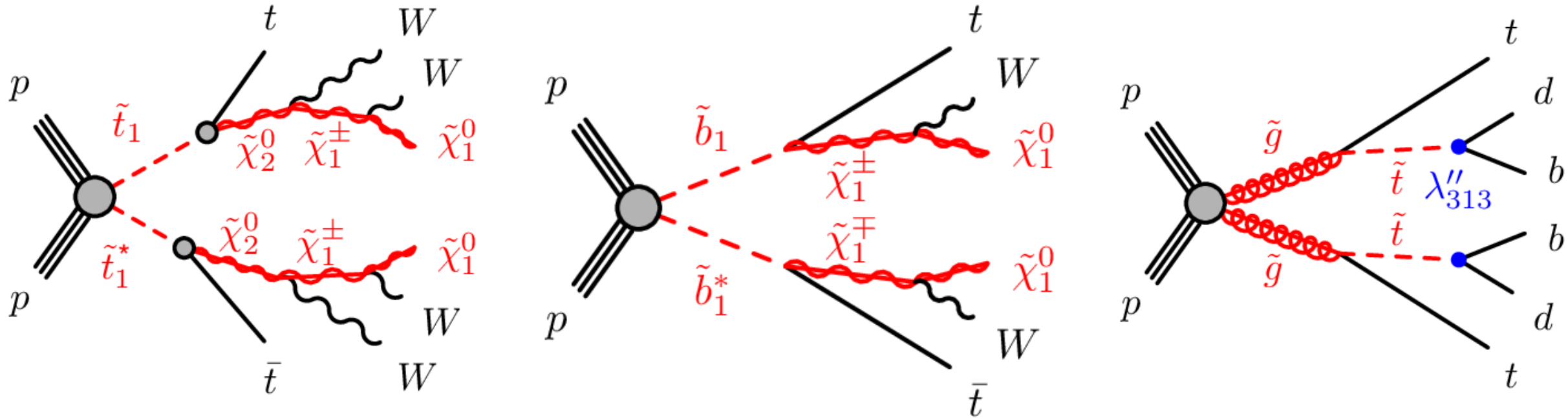
[arXiv: 1804.10823](https://arxiv.org/abs/1804.10823)

Eur. Phys. J. C 78 (2018) 565

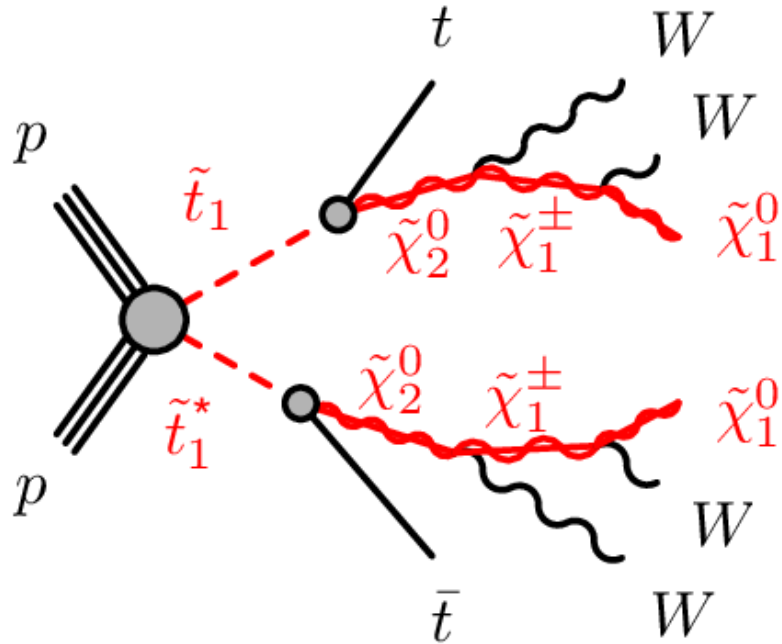


Search for top squarks and bottom squarks

\tilde{t}_1 and \tilde{b}_1 : the lightest eigenstates of the (scalar) supersymmetric top and bottom partners.



- Production of $t\bar{t} + X$
- Events contain multiple leptons and jets, and large missing transverse momentum.



- Do not attempt to reconstruct four-momentum of supersymmetric particle ($\tilde{t}_1, \tilde{b}_1, \tilde{g}, \dots$).
- Define global variables capturing the key features of the signal events:
 - Large missing transverse momentum E_T^{miss} due to neutralinos in R-parity conserving SUSY models.
 - Large effective mass

$$m_{\text{eff}} = \sum_{\text{jets}} p_T + \sum_{\text{leptons}} p_T + E_T^{\text{miss}}$$

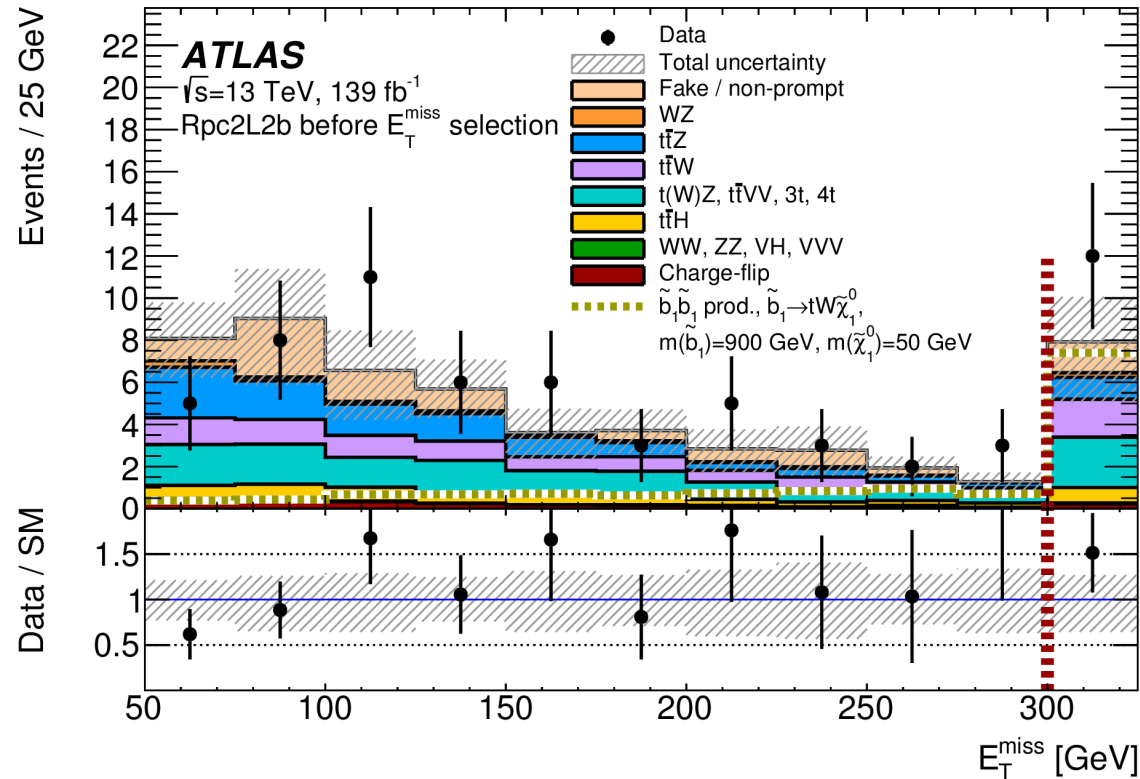
(scalar sum!)

ATLAS two-same-sign-leptons search

Define 5 signal regions with $\ell^\pm \ell^\pm$ pair and ≥ 6 jets.

SR Rpc2L2b:

$E_T^{\text{miss}} > 300$ GeV and $m_{\text{eff}} > 1600$ GeV

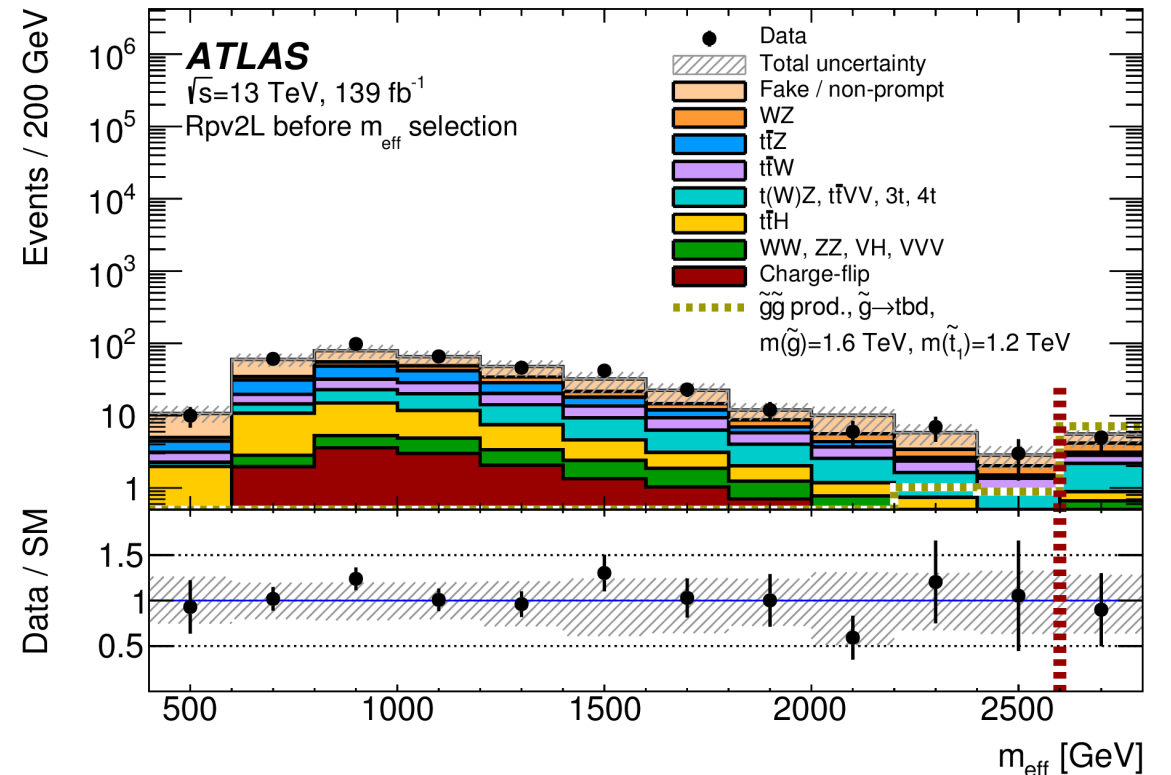


Sensitive to $\tilde{b}_1 \rightarrow tW\tilde{\chi}_1^0$ and $\tilde{g} \rightarrow t\bar{t}\tilde{\chi}_1^0$.

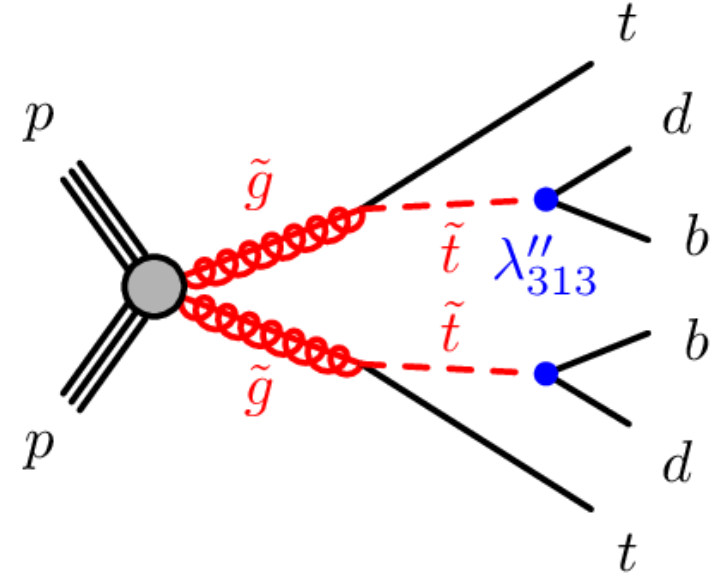
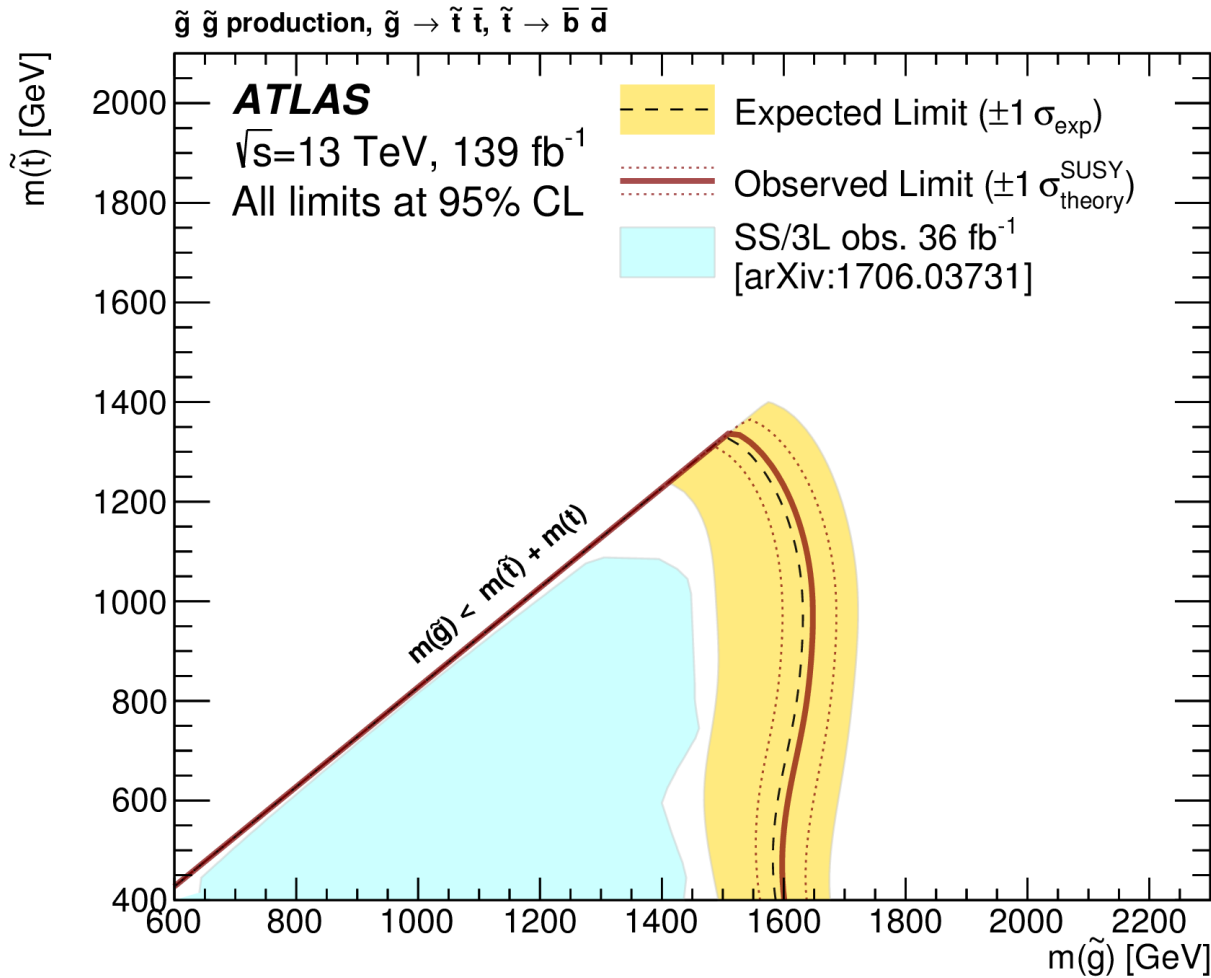
[arXiv: 1909.08457](https://arxiv.org/abs/1909.08457)

SR Rpv2L: $m_{\text{eff}} > 2600$ GeV

no E_T^{miss} requirement

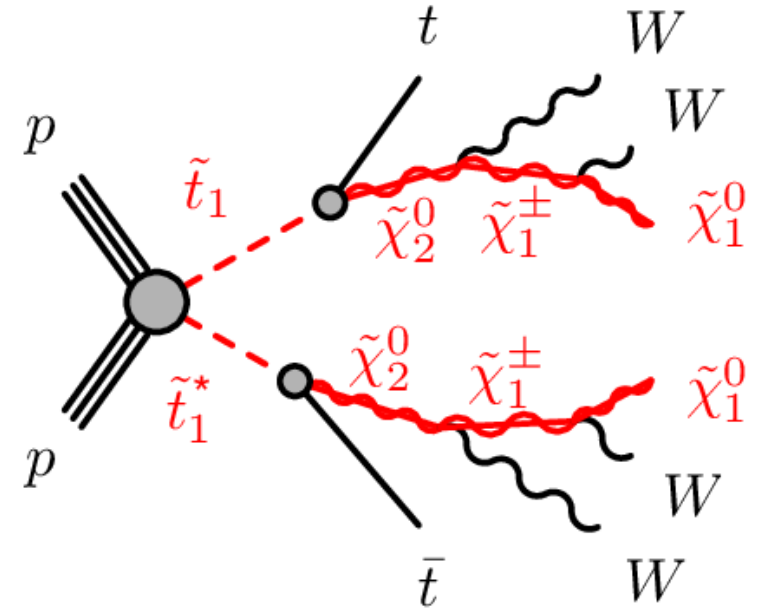
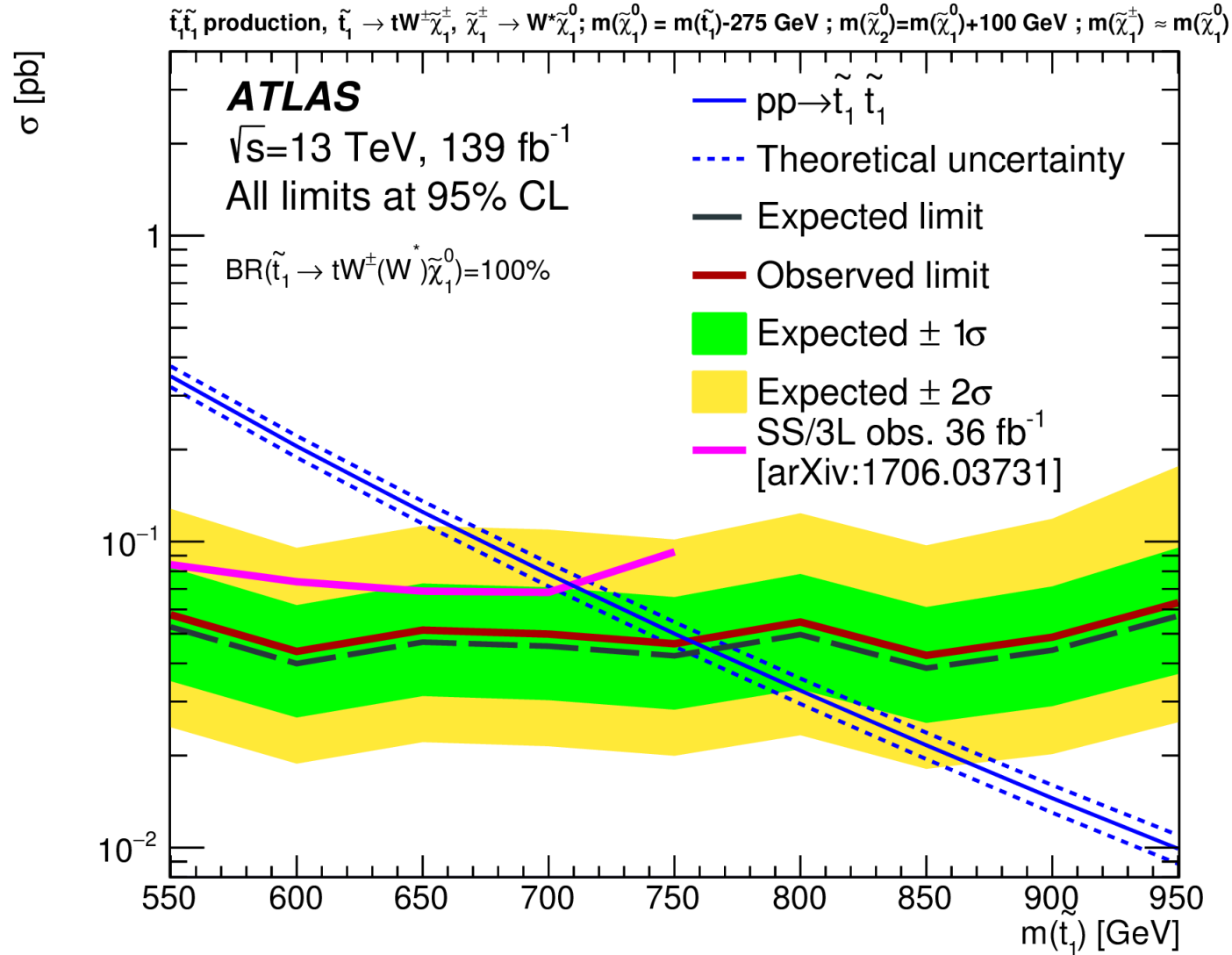


Sensitive to $\tilde{g} \rightarrow t\bar{t}\tilde{\chi}_1^0$ with $\tilde{\chi}_1^0 \rightarrow 3q$ and $\tilde{g} \rightarrow t\tilde{t}_1^*$.



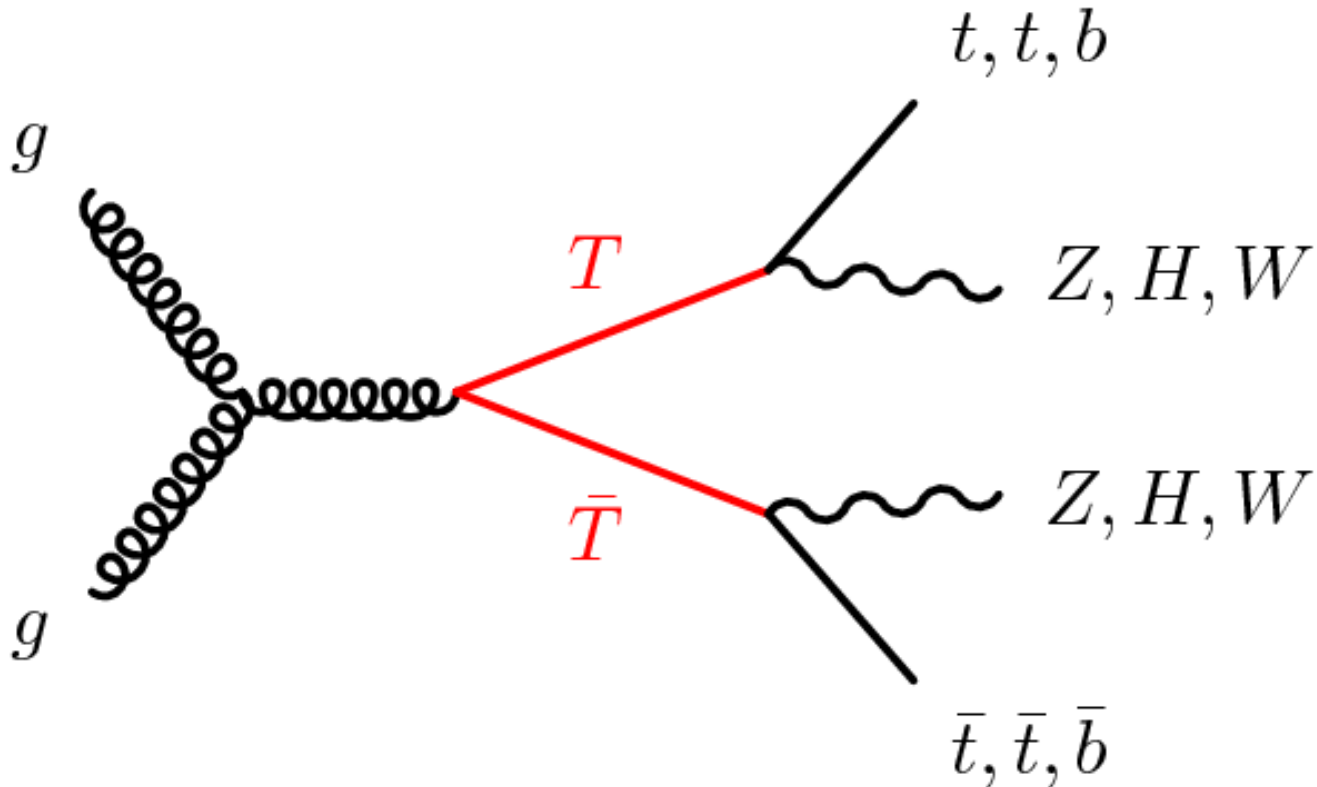
- R-parity violating model
- SR Rpv2L
- $\tilde{g} \rightarrow t b d$

Exclusion limits



- R-parity conserving model
- SR Rpc3LSS1b
- $\tilde{t}_1 \rightarrow tW^{\mp}\tilde{\chi}_1^{\pm}$

Pair production of vector-like top quark partners (T)



Pair production cross section does not depend on any BSM couplings. It is pure QCD.

- T quarks have spin $\frac{1}{2}$
- Left-handed and right-handed states have the same electroweak coupling = no need to consider chiral states
- Avoids exclusion of a simple sequential 4th generation as obtained from Higgs production cross sections at the LHC.
- Contributions by T quarks dampen large quadratic corrections to the Higgs boson mass (propagator).
→ Solution to the naturalness problem
- Occur in Little Higgs or Composite Higgs models.

Search in the $T\bar{T} \rightarrow Zt + X$ with $Z \rightarrow \nu\bar{\nu}$ channel

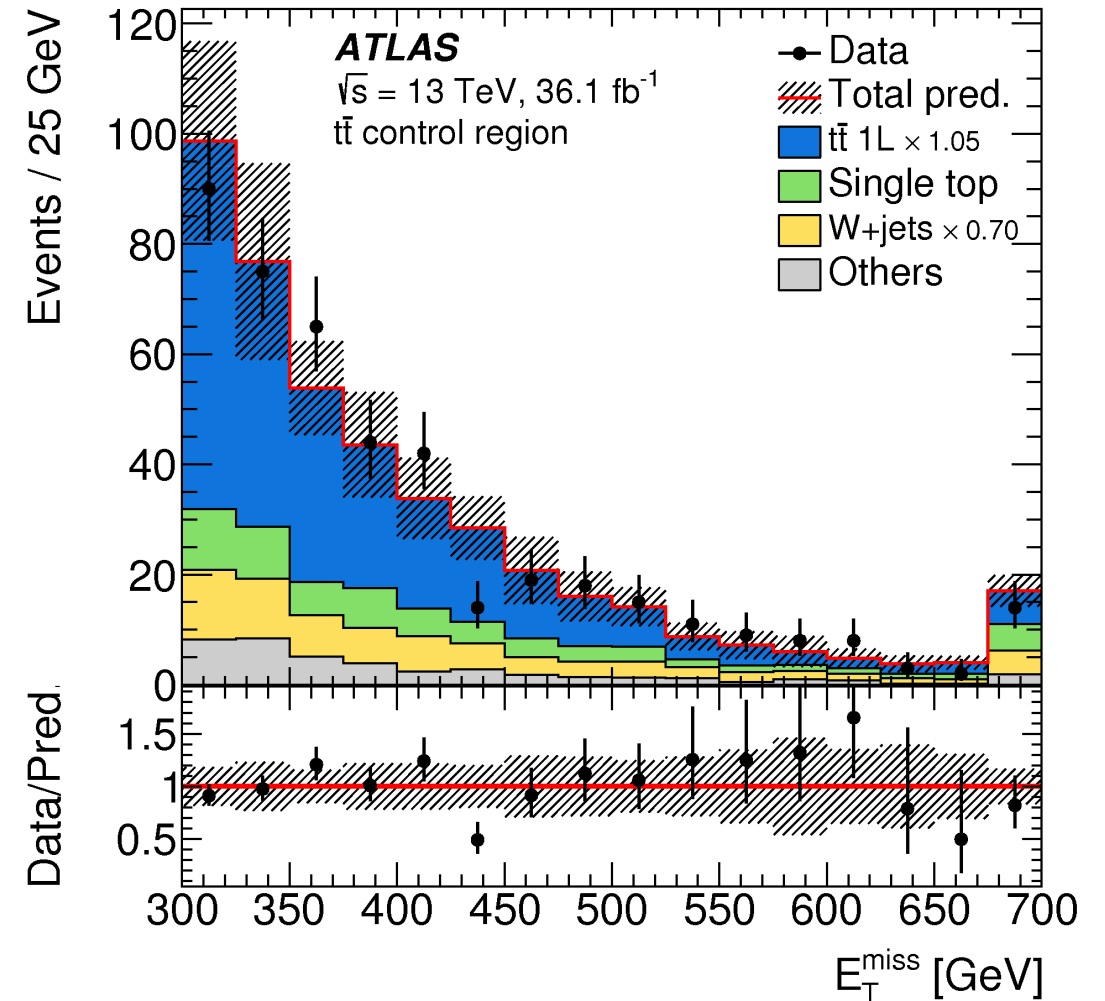
[arXiv:1705.10751](https://arxiv.org/abs/1705.10751)

JHEP 08 (2017) 052

$t\bar{t}$ control region with $30 \text{ GeV} \leq m_T(W) \leq 90 \text{ GeV}$

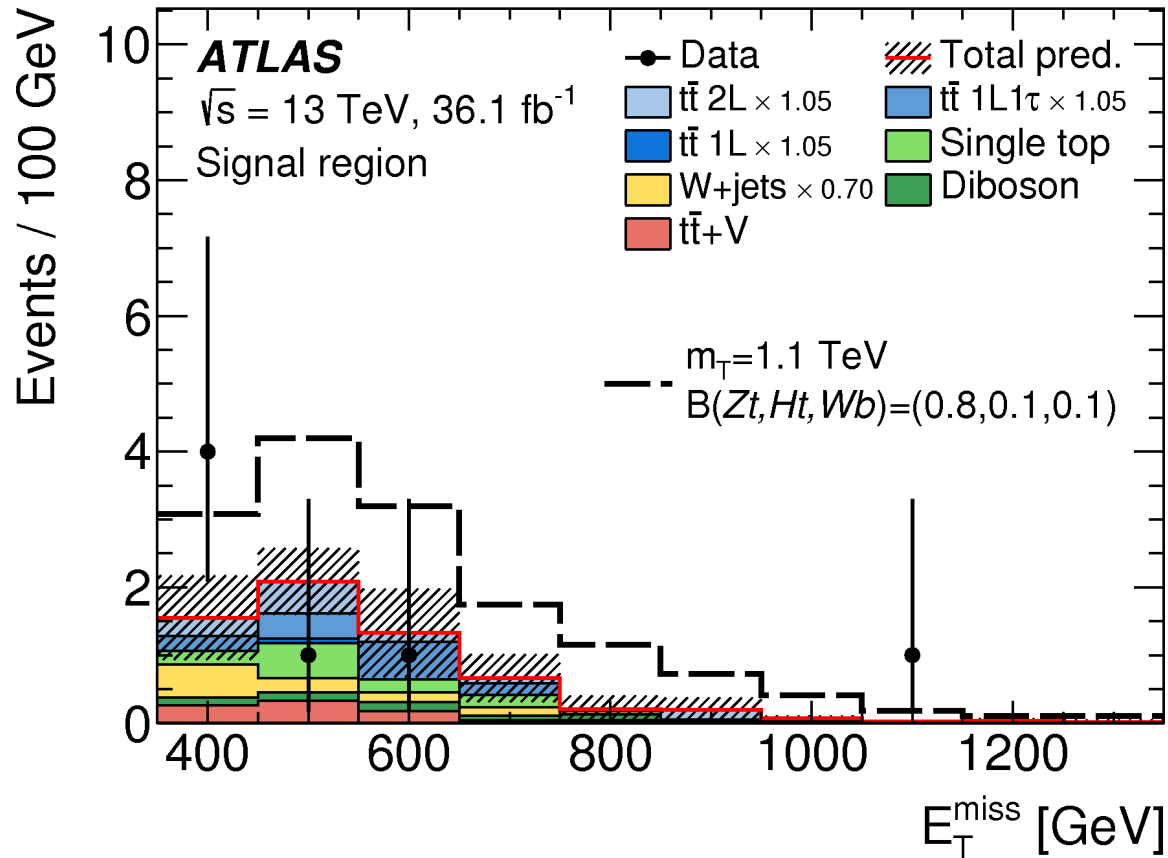
Basic event selection:

- $E_T^{\text{miss}} > 300 \text{ GeV}$
- exactly 1 charged lepton
- ≥ 4 jets with (small) $R = 0.4$
- Re-cluster jets to large-R jets with $R = 1.0$:
 ≥ 2 large-R jets



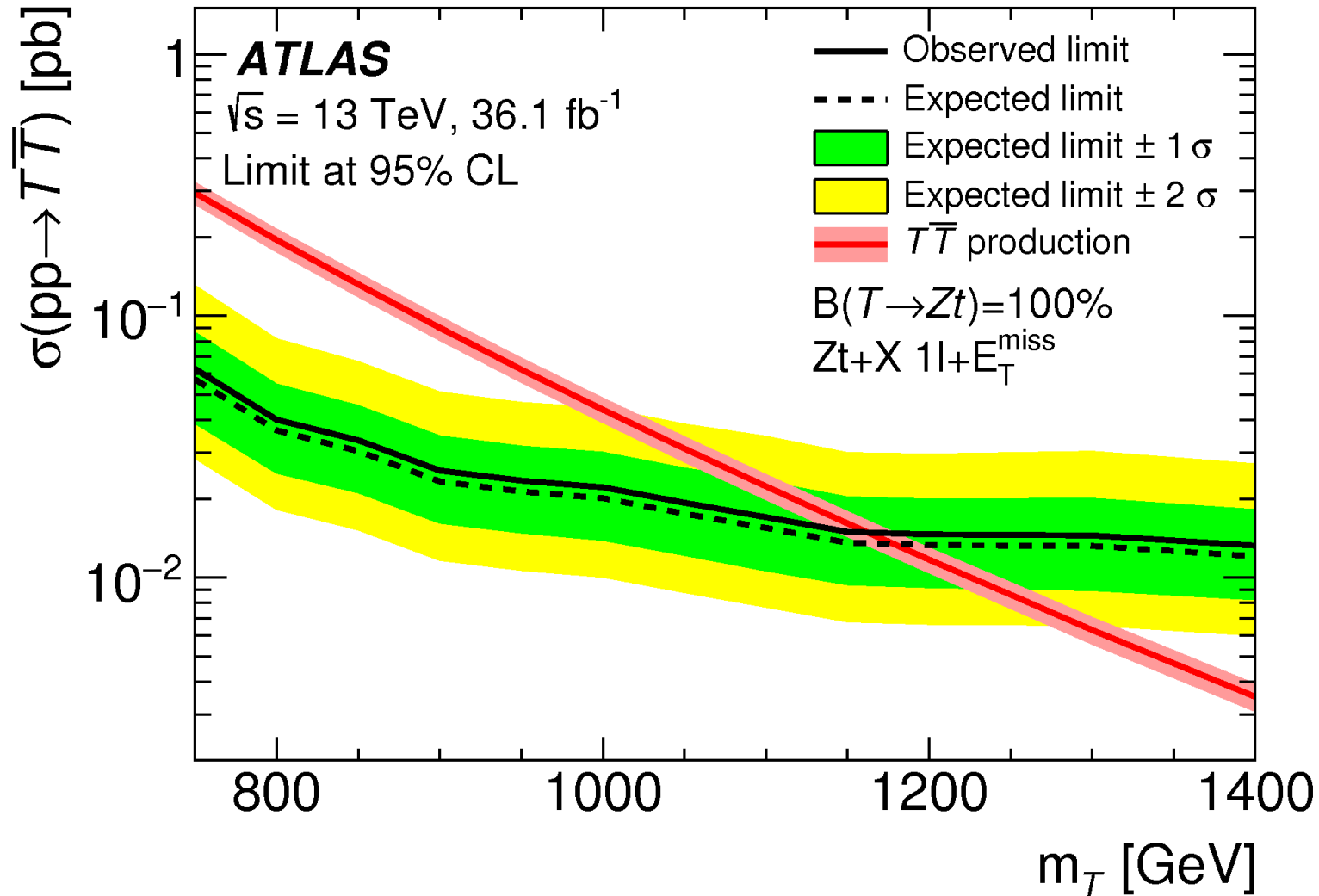
Signal region

with $m_T(W) \geq 170$ GeV



Region	SR
Observed events	7
Fitted bkg events	6.1 ± 1.9
Fitted $t\bar{t}$ events	2.5 ± 1.7
Fitted W + jets events	1.1 ± 0.7
Fitted singletop events	1.1 ± 0.7
Fitted $t\bar{t} + V$ events	0.91 ± 0.20
Fitted diboson events	0.6 ± 0.6
MC exp. bkg events	6.5

Exclusion limits on $T\bar{T} \rightarrow Zt + X$



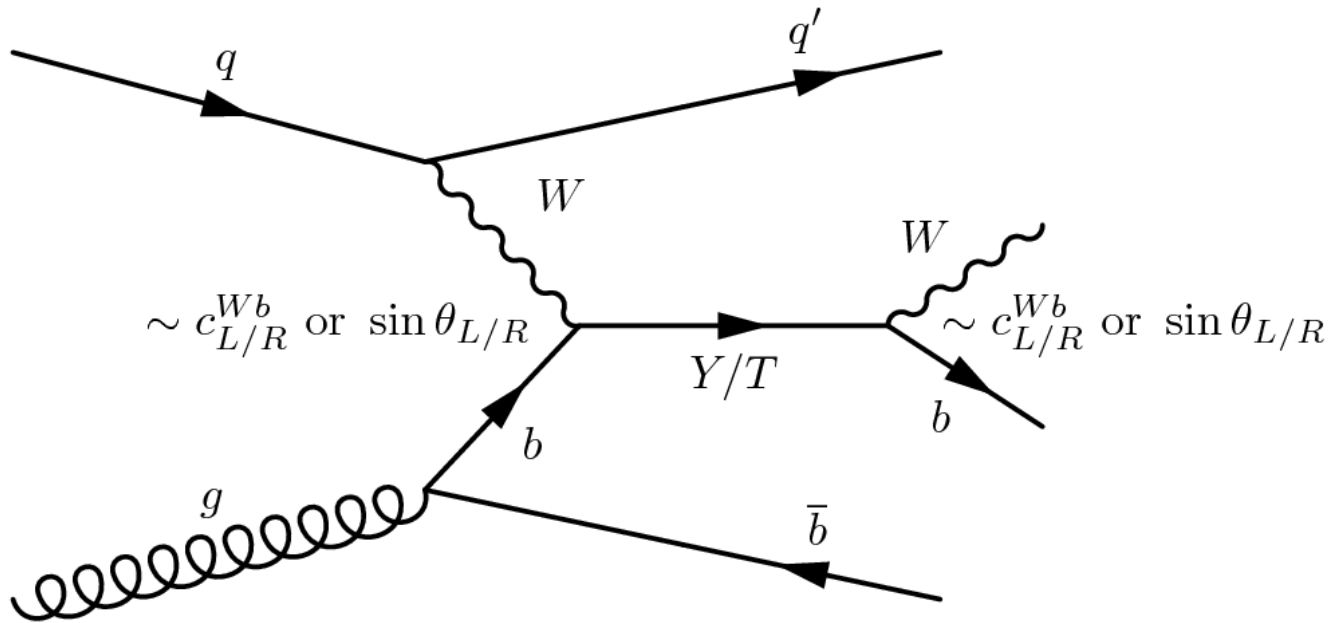
- T quarks with $m_T < 1.16 \text{ TeV}$ are excluded if $B(T \rightarrow Zt) = 100\%$ is assumed.
- Account for other decay modes ($T \rightarrow Ht$ and $T \rightarrow Wb$):
 - Single model:
 $m_T < 0.87 \text{ TeV}$
 - Double model:
 $m_T < 1.05 \text{ TeV}$

Single production of vector-like top quarks

[arXiv: 1812.07343](https://arxiv.org/abs/1812.07343)

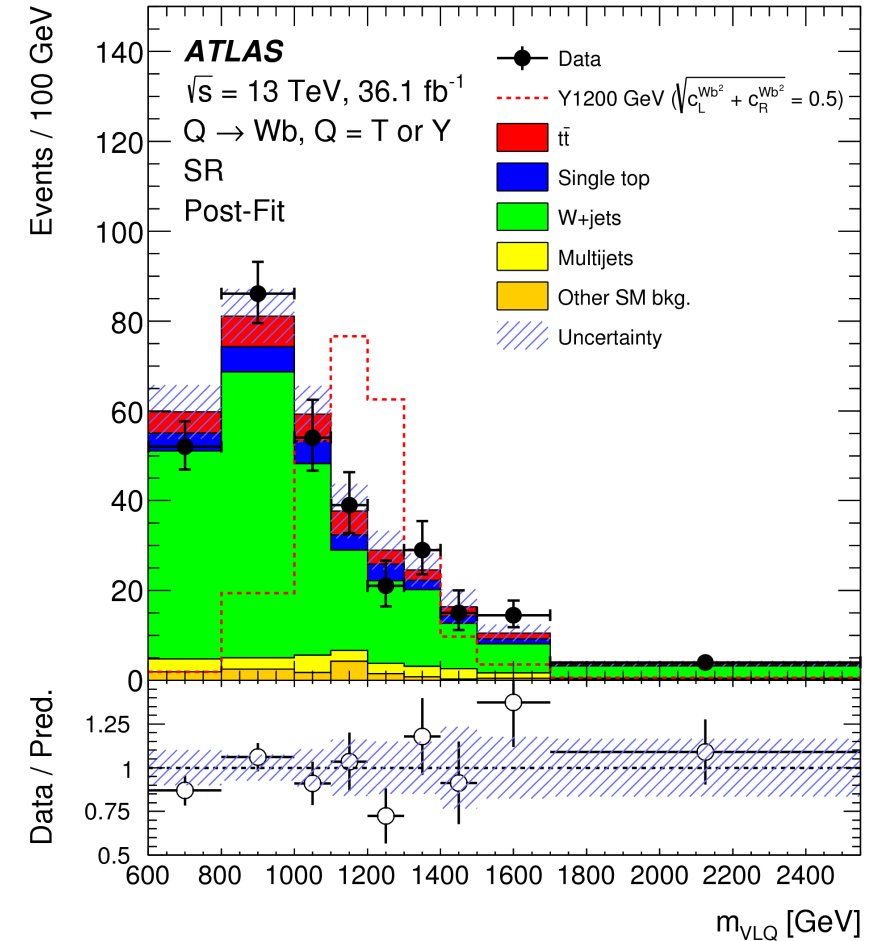
JHEP 05 (2019) 164

$T \rightarrow Wb$ channel (and Y quarks with $Q_Y = -\frac{4}{3}$)



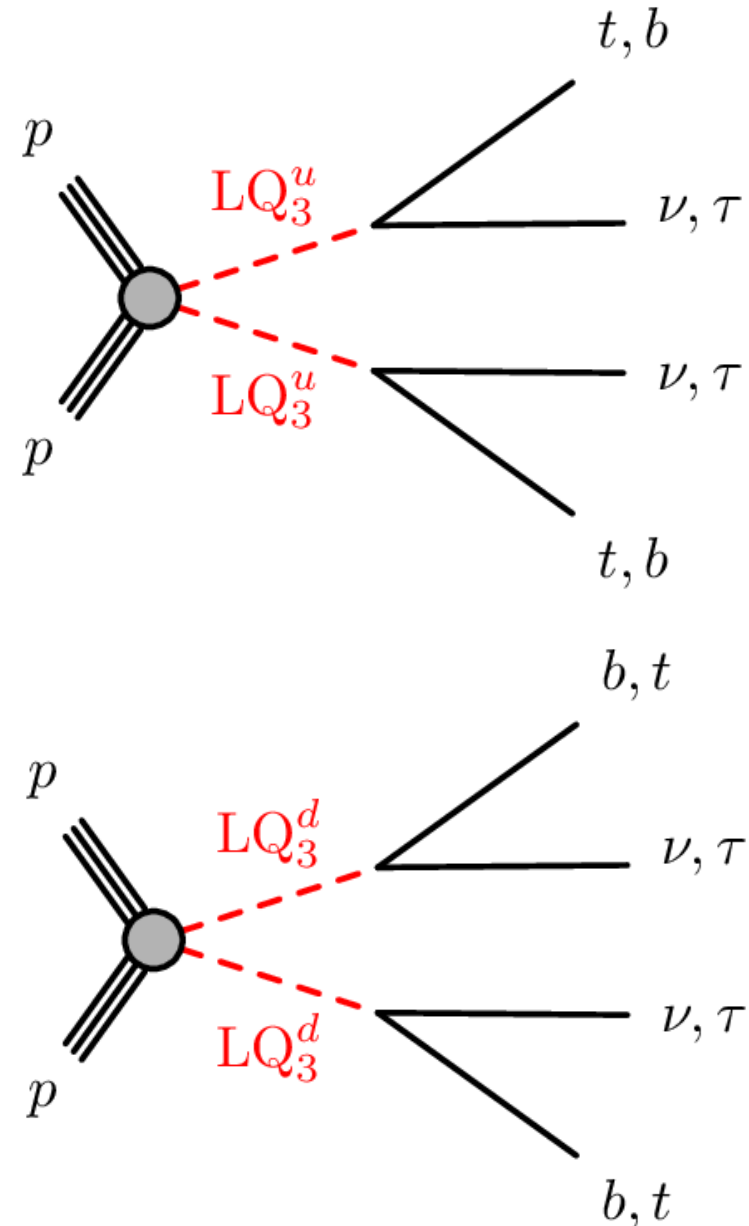
Production cross section scales with a coupling squared.

Reconstructed mass distribution of the T(Y) candidate



Searches for lepto-quarks

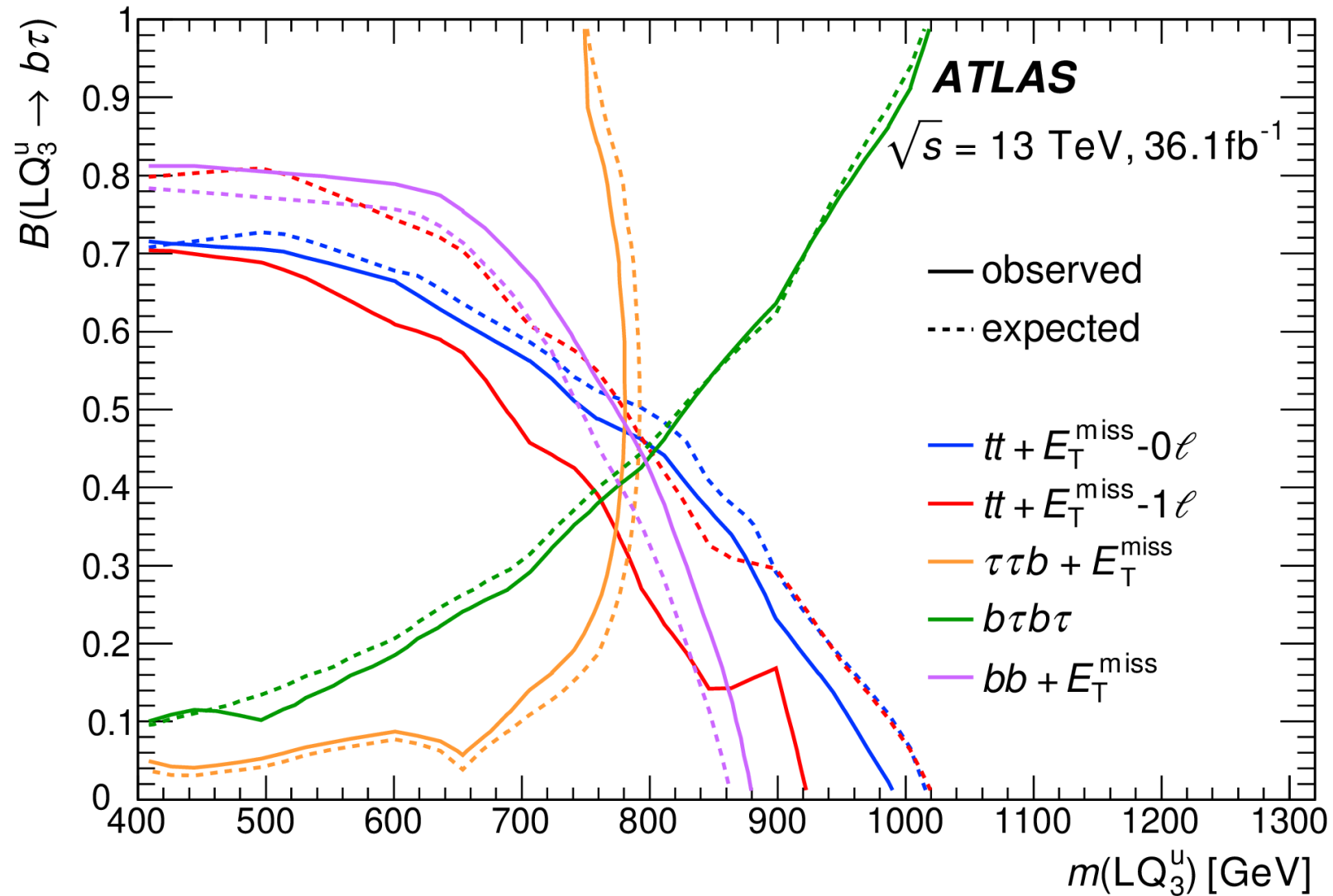
- Lepto-quarks occur in many extensions of the SM based on a larger symmetry group.
- Bosons
- Carry colour charge and electrical charge.
- Connect quark and lepton sector.
- Carry non-zero baryon and lepton numbers.
- Decay into a lepton-quark pair.
- Consider up-type lepto-quark LQ_3^u and down-type lepto-quark LQ_3^d
- Decay into fermions of the 3rd generation.



Exclusion limits

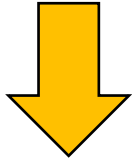
[arXiv: 1902.08103](https://arxiv.org/abs/1902.08103)

JHEP 06 (2019) 144



Indirect vs. direct Searches for New Physics

- No evidence (yet) for *on-shell* production of new particles.
- Lower limits are growing.
- Will (soon) face steep drop i parton luminosity.



Access higher mass scales by deviations in coupling measurements and search for rare processes.

ATLAS Exotics Searches* - 95% CL Upper Exclusion Limits

Status: May 2019

ATLAS Preliminary
 $\int \mathcal{L} dt = (3.2 - 139) \text{ fb}^{-1}$
 $\sqrt{s} = 8, 13 \text{ TeV}$

Model	ℓ, γ	Jets [†]	E_T^{miss}	$\int \mathcal{L} dt [\text{fb}^{-1}]$	Limit	Reference		
Extra dimensions	ADD $G_{KK} + g/q$	$0 e, \mu$	$1-4 j$	Yes	36.1	M_D 7.7 TeV	$n = 2$	1711.03301
	ADD non-resonant $\gamma\gamma$	2γ	-	-	36.7	M_S 8.6 TeV	$n = 3 \text{ HLZ NLO}$	1707.04147
	ADD QBH	-	$2 j$	-	37.0	M_{th} 8.9 TeV	$n = 6$	1703.09127
	ADD BH high Σp_T	$\geq 1 e, \mu$	$\geq 2 j$	-	3.2	M_{th} 8.2 TeV	$n = 6, M_D = 3 \text{ TeV, rot BH}$	1606.02265
	ADD BH multijet	-	$\geq 3 j$	-	3.6	M_{th} 9.55 TeV	$n = 6, M_D = 3 \text{ TeV, rot BH}$	1512.02586
	RS1 $G_{KK} \rightarrow \gamma\gamma$	2γ	-	-	36.7	$G_{KK} \text{ mass}$ 4.1 TeV	$k/\bar{M}_{Pl} = 0.1$	1707.04147
	Bulk RS $G_{KK} \rightarrow WW/ZZ$	multi-channel	-	-	36.1	$G_{KK} \text{ mass}$ 2.3 TeV	$k/\bar{M}_{Pl} = 1.0$	1808.02380
	Bulk RS $G_{KK} \rightarrow WW \rightarrow qqqq$	$0 e, \mu$	$2 j$	-	139	$G_{KK} \text{ mass}$ 1.6 TeV	$k/\bar{M}_{Pl} = 1.0$	ATLAS-CONF-2019-003
	Bulk RS $g_{KK} \rightarrow tt$	$1 e, \mu$	$\geq 1 b, \geq 1J/2j$	Yes	36.1	$g_{KK} \text{ mass}$ 3.8 TeV	$\Gamma/m = 15\%$	1804.10823
	2UED / RPP	$1 e, \mu$	$\geq 2 b, \geq 3 j$	Yes	36.1	$KK \text{ mass}$ 1.8 TeV	Tier (1,1), $\mathcal{B}(A^{(1,1)} \rightarrow tt) = 1$	1803.09678
Gauge bosons	SSM $Z' \rightarrow \ell\ell$	$2 e, \mu$	-	-	139	$Z' \text{ mass}$ 5.1 TeV	-	1903.06248
	SSM $Z' \rightarrow \tau\tau$	2τ	-	-	36.1	$Z' \text{ mass}$ 2.42 TeV	-	1709.07242
	Leptophobic $Z' \rightarrow bb$	-	$2 b$	-	36.1	$Z' \text{ mass}$ 2.1 TeV	-	1805.09299
	Leptophobic $Z' \rightarrow tt$	$1 e, \mu$	$\geq 1 b, \geq 1J/2j$	Yes	36.1	$Z' \text{ mass}$ 3.0 TeV	$\Gamma/m = 1\%$	1804.10823
	SSM $W' \rightarrow \ell\nu$	$1 e, \mu$	-	Yes	139	$W' \text{ mass}$ 6.0 TeV	-	CERN-EP-2019-100
	SSM $W' \rightarrow \tau\nu$	1τ	-	Yes	36.1	$W' \text{ mass}$ 3.7 TeV	-	1801.06992
	HVT $V' \rightarrow WZ \rightarrow qqqq$ model B	$0 e, \mu$	$2 j$	-	139	$V' \text{ mass}$ 3.6 TeV	$g_V = 3$	ATLAS-CONF-2019-003
	HVT $V' \rightarrow WH/ZH$ model B	multi-channel	-	-	36.1	$V' \text{ mass}$ 2.93 TeV	$g_V = 3$	1712.06518
	LRSM $W_R \rightarrow tb$	multi-channel	-	-	36.1	$W_R \text{ mass}$ 3.25 TeV	-	1807.10473
LRSM $W_R \rightarrow \mu N_R$	2μ	$1 j$	-	80	$W_R \text{ mass}$ 5.0 TeV	$m(N_R) = 0.5 \text{ TeV, } g_L = g_R$	1904.12679	
CI	CI $qqqq$	-	$2 j$	-	37.0	Λ 21.8 TeV	η_{LL}	1703.09127
	CI $\ell\ell qq$	$2 e, \mu$	-	-	36.1	Λ 40.0 TeV	η_{LL}	1707.02424
	CI $tttt$	$\geq 1 e, \mu$	$\geq 1 b, \geq 1 j$	Yes	36.1	Λ 2.57 TeV	$ C_{4\ell} = 4\pi$	1811.02305
DM	Axial-vector mediator (Dirac DM)	$0 e, \mu$	$1-4 j$	Yes	36.1	m_{med} 1.55 TeV	$g_q = 0.25, g_\ell = 1.0, m(\chi) = 1 \text{ GeV}$	1711.03301
	Colored scalar mediator (Dirac DM)	$0 e, \mu$	$1-4 j$	Yes	36.1	m_{med} 1.67 TeV	$g = 1.0, m(\chi) = 1 \text{ GeV}$	1711.03301
	VV $\chi\chi$ EFT (Dirac DM)	$0 e, \mu$	$1 j, \leq 1 j$	Yes	3.2	M_χ 700 GeV	$m(\chi) < 150 \text{ GeV}$	1608.02372
	Scalar reson. $\phi \rightarrow t\chi$ (Dirac DM)	$0-1 e, \mu$	$1 b, 0-1 j$	Yes	36.1	m_ϕ 3.4 TeV	$y = 0.4, \lambda = 0.2, m(\chi) = 10 \text{ GeV}$	1812.09743
LQ	Scalar LQ 1 st gen	$1, 2 e$	$\geq 2 j$	Yes	36.1	$LQ \text{ mass}$ 1.4 TeV	$\beta = 1$	1902.00377
	Scalar LQ 2 nd gen	$1, 2 \mu$	$\geq 2 j$	Yes	36.1	$LQ \text{ mass}$ 1.56 TeV	$\beta = 1$	1902.00377
	Scalar LQ 3 rd gen	2τ	$2 b$	-	36.1	$LQ^u \text{ mass}$ 1.03 TeV	$\mathcal{B}(LQ^u \rightarrow b\tau) = 1$	1902.08103
	Scalar LQ 3 rd gen	$0-1 e, \mu$	$2 b$	Yes	36.1	$LQ^d \text{ mass}$ 970 GeV	$\mathcal{B}(LQ^d \rightarrow t\tau) = 0$	1902.08103
Heavy quarks	VLQ $TT \rightarrow Ht/Zt/Wb + X$	multi-channel	-	-	36.1	$T \text{ mass}$ 1.37 TeV	SU(2) doublet	1808.02343
	VLQ $BB \rightarrow Wt/Zb + X$	multi-channel	-	-	36.1	$B \text{ mass}$ 1.34 TeV	SU(2) doublet	1808.02343
	VLQ $T_{5/3} T_{5/3} T_{5/3} \rightarrow Wt + X$	$2(SS) \geq 3 e, \mu \geq 1 b, \geq 1 j$	Yes	36.1	$T_{5/3} \text{ mass}$ 1.64 TeV	$\mathcal{B}(T_{5/3} \rightarrow Wt) = 1, c(T_{5/3} Wt) = 1$	1807.11883	
	VLQ $Y \rightarrow Wb + X$	$1 e, \mu \geq 1 b, \geq 1 j$	Yes	36.1	$Y \text{ mass}$ 1.85 TeV	$\mathcal{B}(Y \rightarrow Wb) = 1, c_Y(Wb) = 1$	1812.07343	
	VLQ $B \rightarrow Hb + X$	$0 e, \mu, 2 \gamma \geq 1 b, \geq 1 j$	Yes	79.8	$B \text{ mass}$ 1.21 TeV	$\kappa_B = 0.5$	ATLAS-CONF-2018-024	
VLQ $QQ \rightarrow WqWq$	$1 e, \mu \geq 4 j$	Yes	20.3	$Q \text{ mass}$ 690 GeV	-	1509.04261		
Excited fermions	Excited quark $q^* \rightarrow qg$	-	$2 j$	-	139	$q^* \text{ mass}$ 6.7 TeV	only u^* and $d^*, \Lambda = m(q^*)$	ATLAS-CONF-2019-007
	Excited quark $q^* \rightarrow q\gamma$	1γ	$1 j$	-	36.7	$q^* \text{ mass}$ 5.3 TeV	only u^* and $d^*, \Lambda = m(q^*)$	1709.10440
	Excited quark $b^* \rightarrow bg$	-	$1 b, 1 j$	-	36.1	$b^* \text{ mass}$ 2.6 TeV	-	1805.09299
	Excited lepton ℓ^*	$3 e, \mu$	-	-	20.3	$\ell^* \text{ mass}$ 3.0 TeV	$\Lambda = 3.0 \text{ TeV}$	1411.2921
	Excited lepton ν^*	$3 e, \mu, \tau$	-	-	20.3	$\nu^* \text{ mass}$ 1.6 TeV	$\Lambda = 1.6 \text{ TeV}$	1411.2921
Other	Type III Seesaw	$1 e, \mu$	$\geq 2 j$	Yes	79.8	$N^c \text{ mass}$ 560 GeV	-	ATLAS-CONF-2018-020
	LRSM Majorana ν	2μ	$2 j$	-	36.1	$N_R \text{ mass}$ 3.2 TeV	$m(W_R) = 4.1 \text{ TeV, } g_L = g_R$	1809.11105
	Higgs triplet $H^{\pm\pm} \rightarrow \ell\ell$	$2, 3, 4 e, \mu$ (SS)	-	-	36.1	$H^{\pm\pm} \text{ mass}$ 870 GeV	DY production	1710.09748
	Higgs triplet $H^{\pm\pm} \rightarrow \ell\tau$	$3 e, \mu, \tau$	-	-	20.3	$H^{\pm\pm} \text{ mass}$ 400 GeV	DY production, $\mathcal{B}(H^{\pm\pm} \rightarrow \ell\tau) = 1$	1411.2921
	Multi-charged particles	-	-	-	36.1	multi-charged particle mass 1.22 TeV	DY production, $ q = 5e$	1812.03673
	Magnetic monopoles	-	-	-	34.4	monopole mass 2.37 TeV	DY production, $ g = 1g_D, \text{spin } 1/2$	1905.10130

*Only a selection of the available mass limits on new states or phenomena is shown.

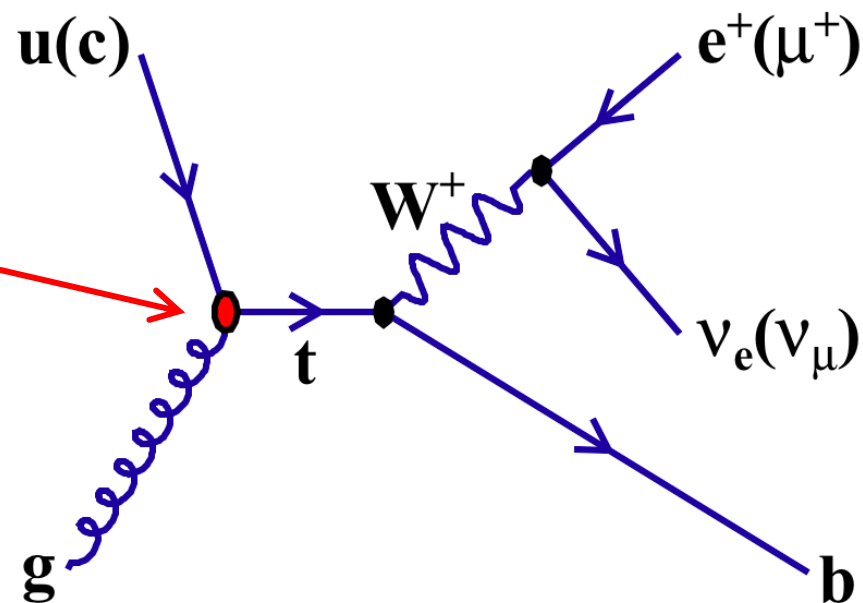
†Small-radius (large-radius) jets are denoted by the letter j (J).

Chapter 4

Indirect searches / searches for anomalous couplings

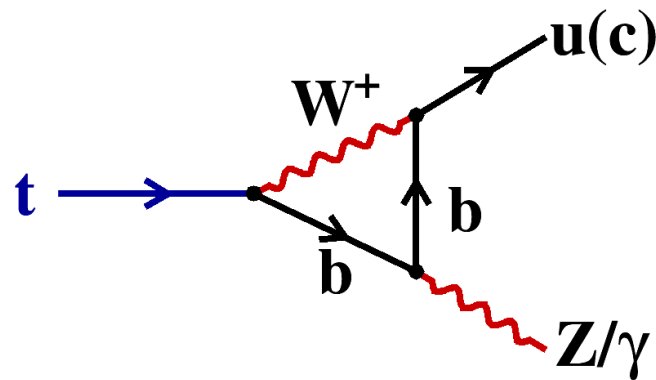
Parameterise new physics (full theory) by effective couplings at vertices.

→ Recall Fermi theory of nuclear beta decay



Decays via flavour-changing neutral currents (FCNC)

- Do not exist at tree (Born) level in the SM
- Very strongly suppressed at next-to-leading order (loop level): GIM mechanism = CKM unitarity
- Suppression is lifted by non-degenerate quark masses.
- Branching ratios are extremely small.



	$Br(t \rightarrow q\gamma)$	$Br(t \rightarrow qZ)$	$Br(t \rightarrow qq)$
$q = u$	3.7×10^{-16}	8×10^{-17}	3.7×10^{-14}
$q = c$	4.6×10^{-14}	1×10^{-14}	4.6×10^{-12}

FCNC in theories beyond the SM

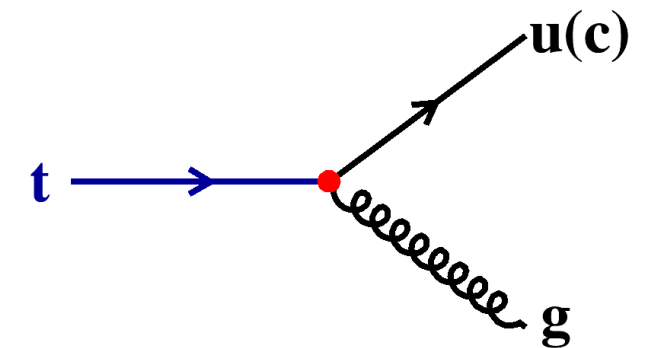
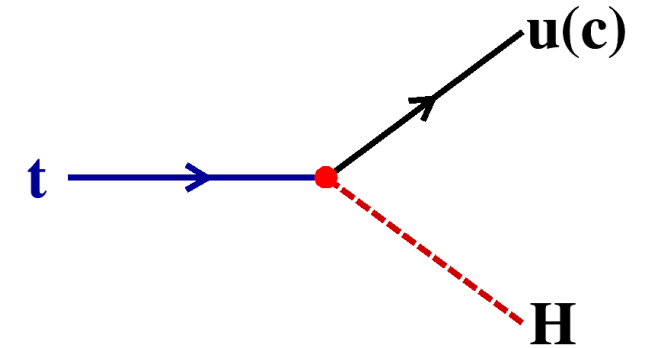
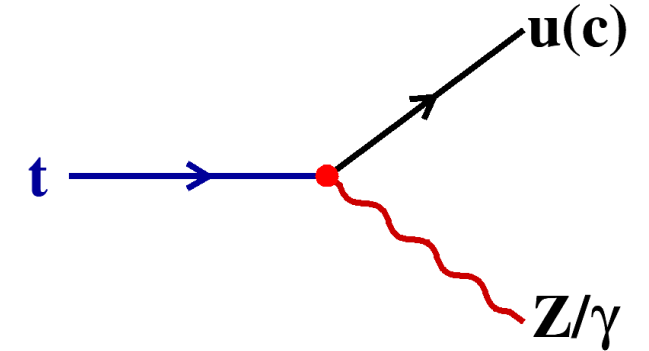
Branching ratios of top-quark decays in SM and BSM theories:

Process	SM	2HDM(FV)	2HDM(FC)	MSSM	RPV	RS
$t \rightarrow Zu$	7×10^{-17}	–	–	$\leq 10^{-7}$	$\leq 10^{-6}$	–
$t \rightarrow Zc$	1×10^{-14}	$\leq 10^{-6}$	$\leq 10^{-10}$	$\leq 10^{-7}$	$\leq 10^{-6}$	$\leq 10^{-5}$
$t \rightarrow gu$	4×10^{-14}	–	–	$\leq 10^{-7}$	$\leq 10^{-6}$	–
$t \rightarrow gc$	5×10^{-12}	$\leq 10^{-4}$	$\leq 10^{-8}$	$\leq 10^{-7}$	$\leq 10^{-6}$	$\leq 10^{-10}$
$t \rightarrow \gamma u$	4×10^{-16}	–	–	$\leq 10^{-8}$	$\leq 10^{-9}$	–
$t \rightarrow \gamma c$	5×10^{-14}	$\leq 10^{-7}$	$\leq 10^{-9}$	$\leq 10^{-8}$	$\leq 10^{-9}$	$\leq 10^{-9}$
$t \rightarrow hu$	2×10^{-17}	6×10^{-6}	–	$\leq 10^{-5}$	$\leq 10^{-9}$	–
$t \rightarrow hc$	3×10^{-15}	2×10^{-3}	$\leq 10^{-5}$	$\leq 10^{-5}$	$\leq 10^{-9}$	$\leq 10^{-4}$

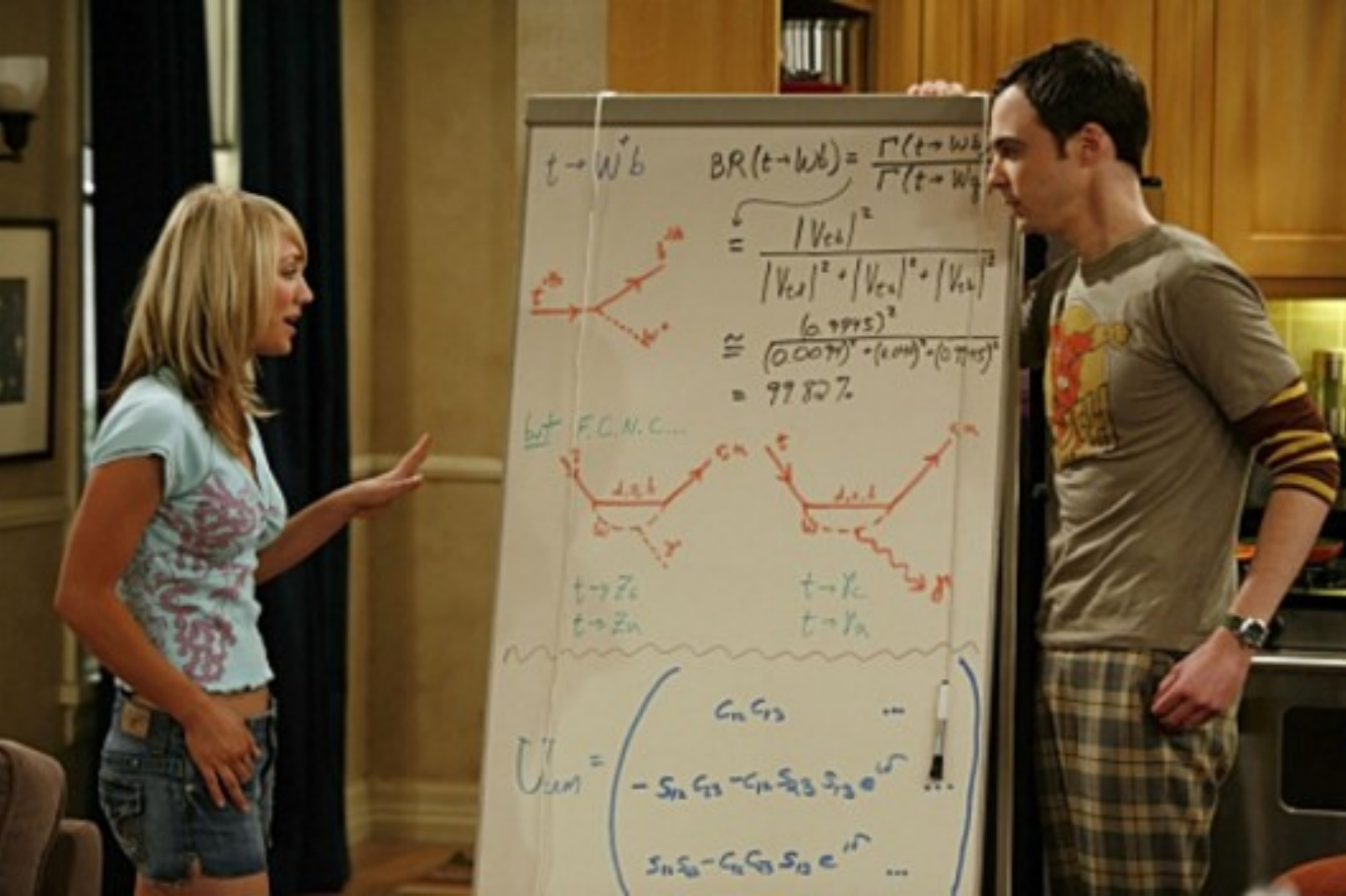
Snowmass Workshop 2013, arXiv: 1311.2028

Strong enhancement!

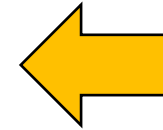
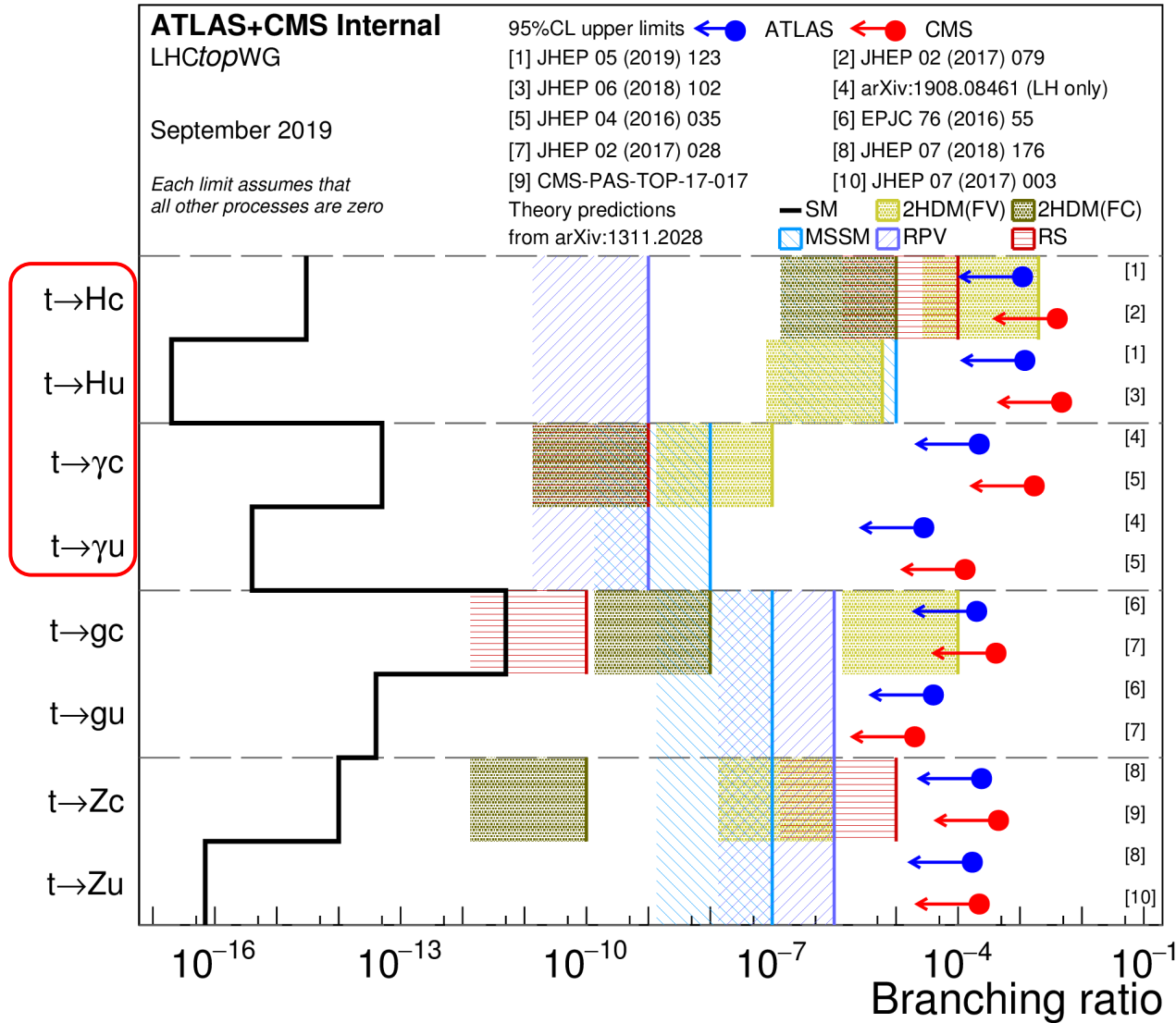
Any FCNC signal is evidence for BSM physics!



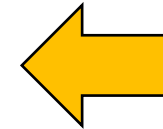
Even Hollywood knows: FCNC are exiting!



Status of FCNC limits



Latest ATLAS analysis

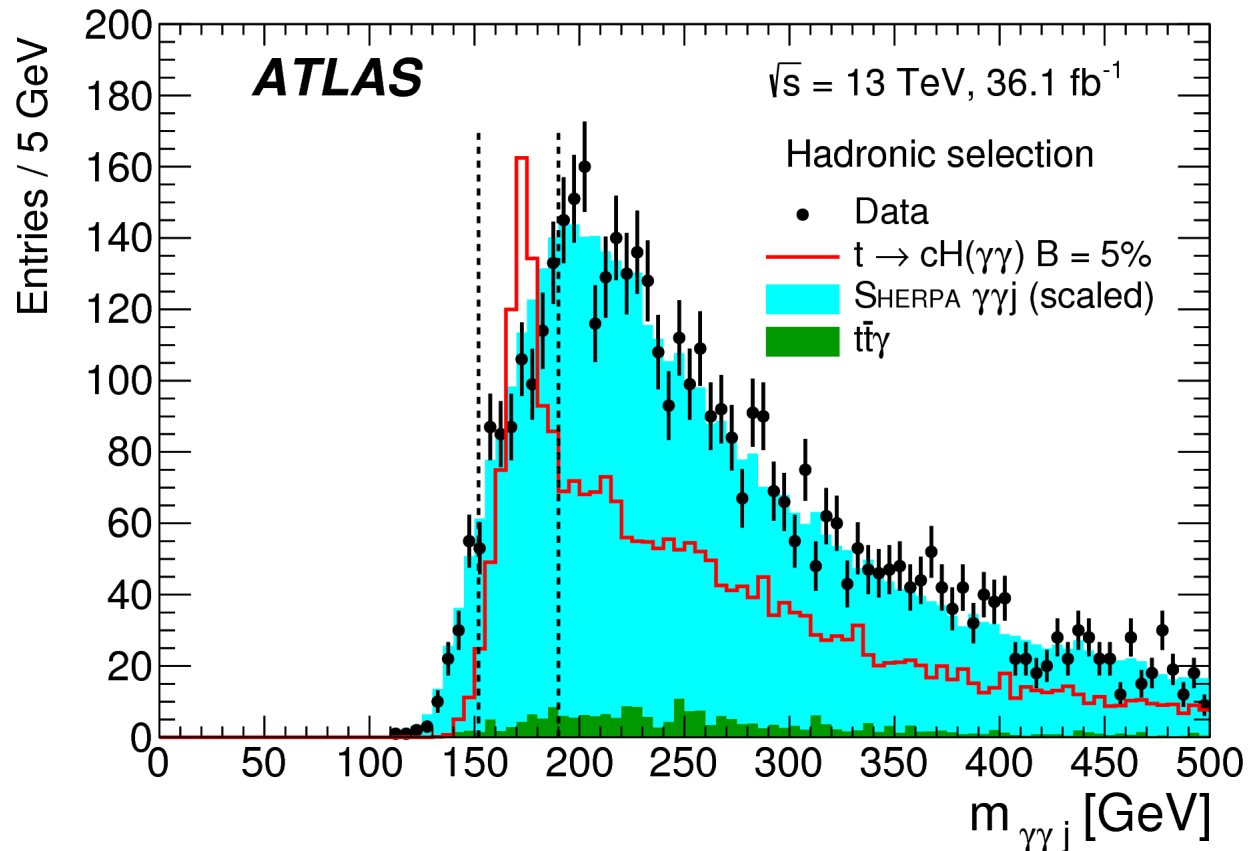


Search for $t \rightarrow qH$ with $H \rightarrow \gamma\gamma$

- Select $t\bar{t}$ candidate events.
- Assume one top-quark decays via $t \rightarrow q\gamma\gamma$ and one via the SM mode $t \rightarrow Wb$
- Consider $W \rightarrow q\bar{q}'$ and $W \rightarrow \ell\nu$

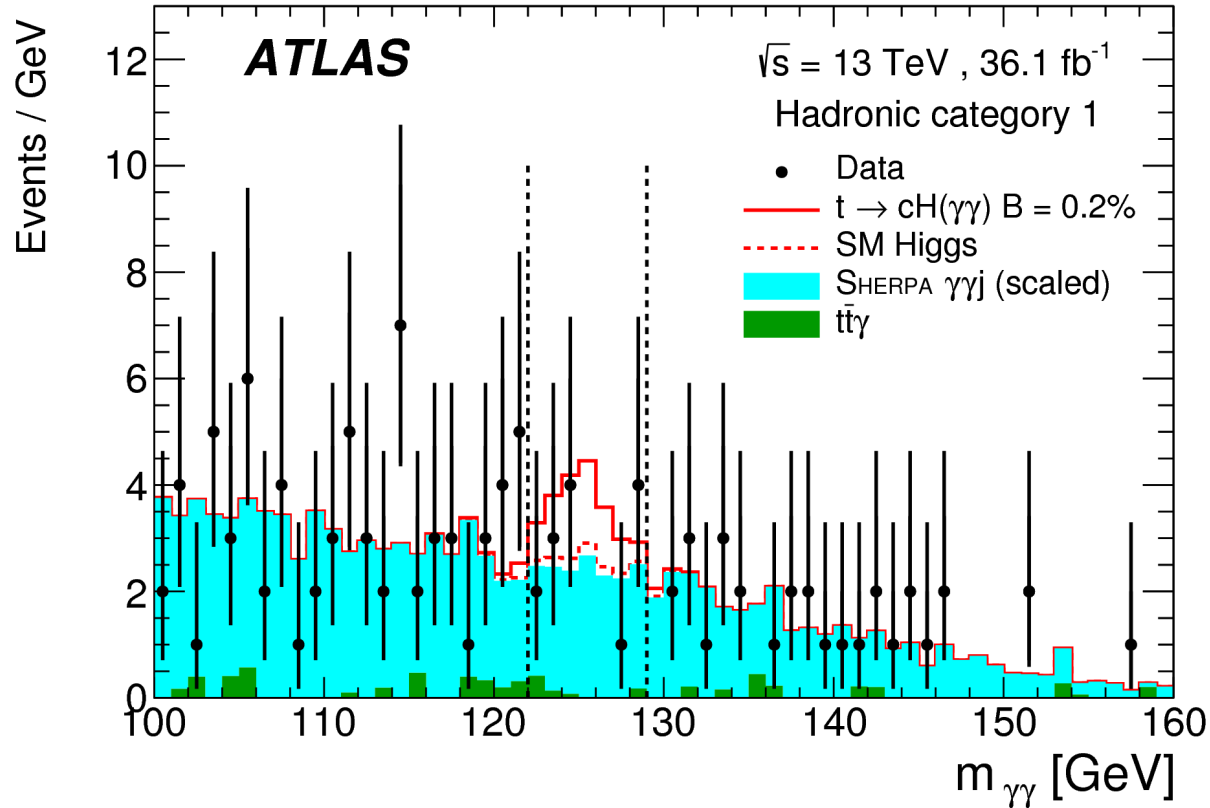
[arXiv: 1707.01404](https://arxiv.org/abs/1707.01404)

JHEP 10 (2017) 129



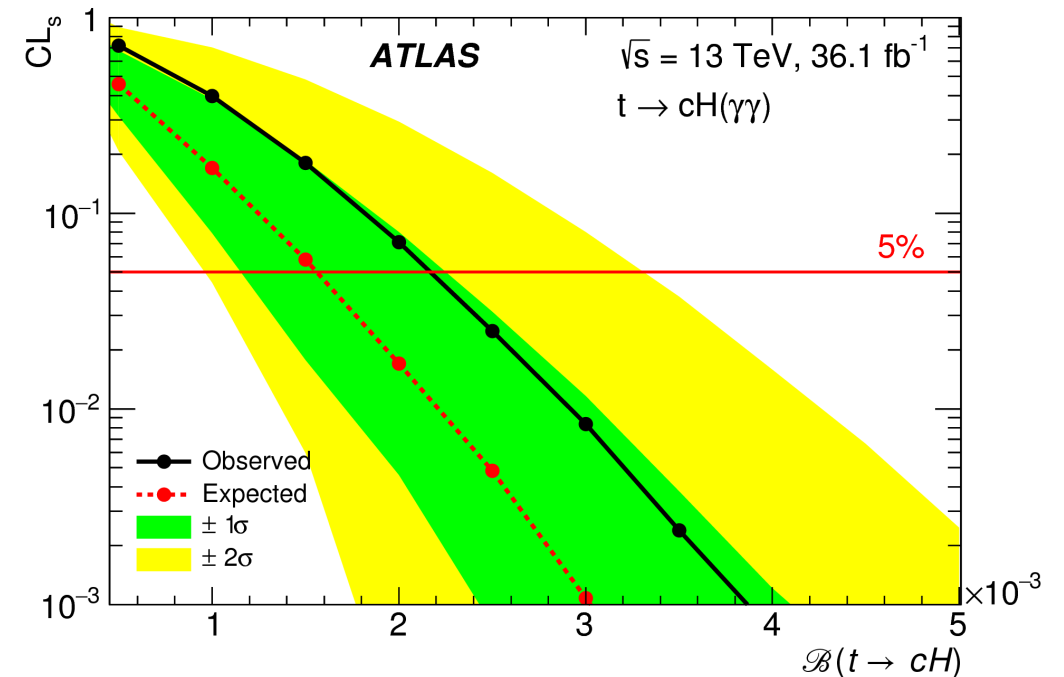
- Reconstruct top-quark mass:
 $m(\gamma\gamma j)$ and $m(jjj)$
- Place mass window cuts.

Limits on $t \rightarrow qH$ with $H \rightarrow \gamma\gamma$



- Look at $m(\gamma\gamma)$ spectrum.
- Normalise background to data in side bands.
- Obtained limits:

$$\mathcal{B}(t \rightarrow cH) \leq 2.2 \cdot 10^{-3} \text{ and } \mathcal{B}(t \rightarrow uH) \leq 2.4 \cdot 10^{-3}$$



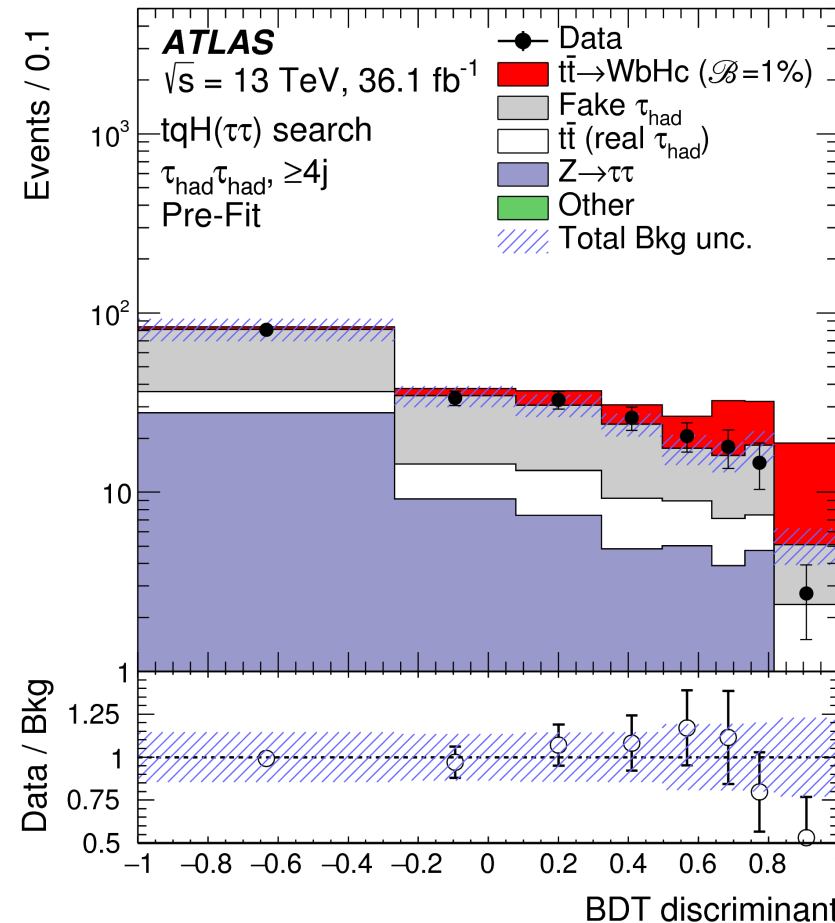
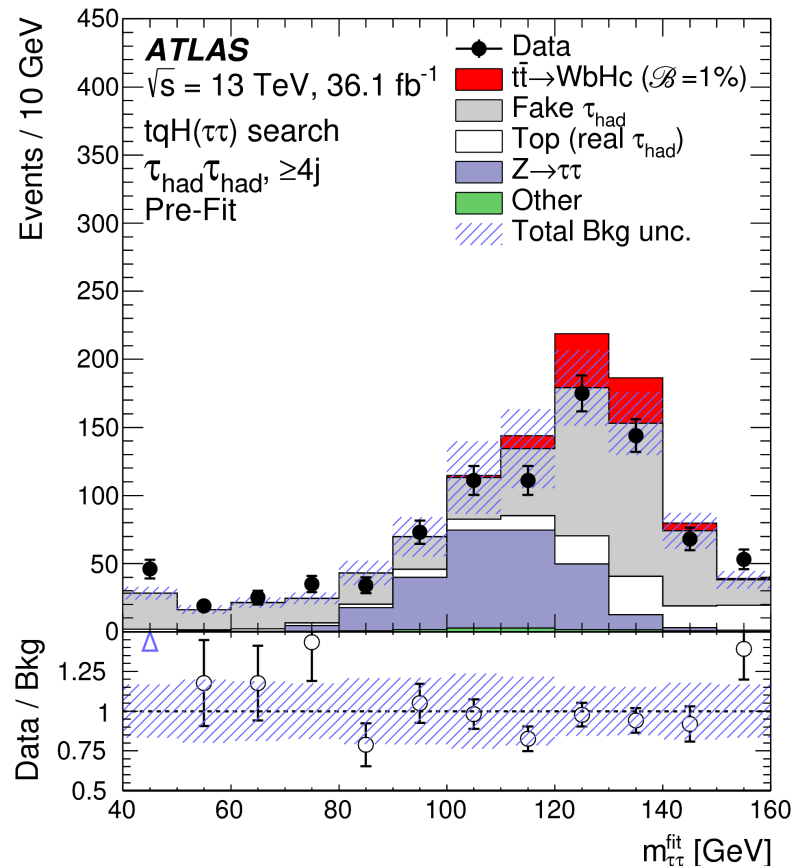
Search for $t \rightarrow qH$ with $H \rightarrow \tau^+ \tau^-$

- τ leptons are reconstructed in their leptonic and hadronic decay modes
- Boosted decision trees (BDTs) are used to separate signal and background.

[arXiv: 1812.11568](https://arxiv.org/abs/1812.11568)

JHEP 05 (2019) 123

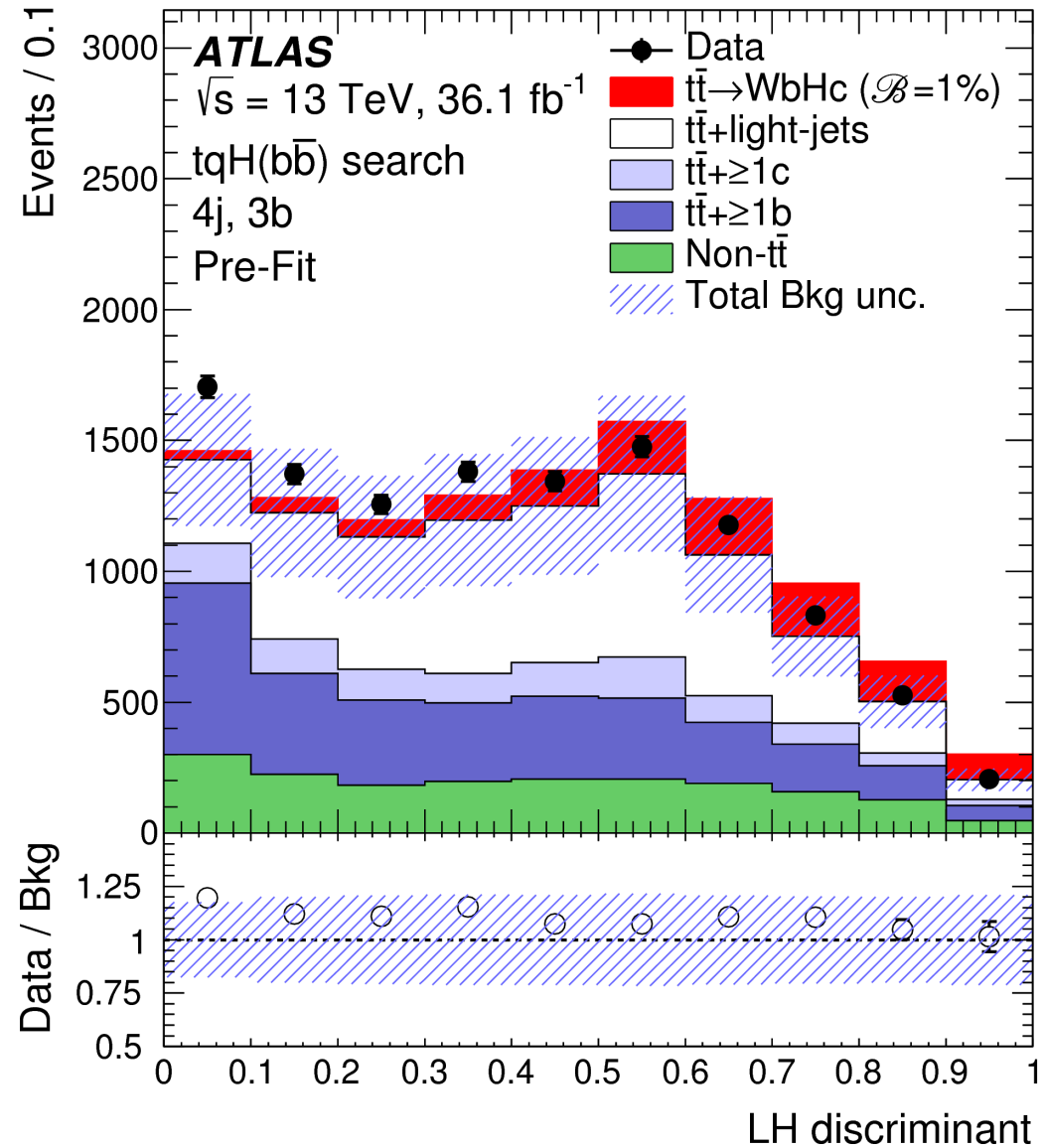
One of the input variables to the BDT:
The reconstructed Higgs boson mass.



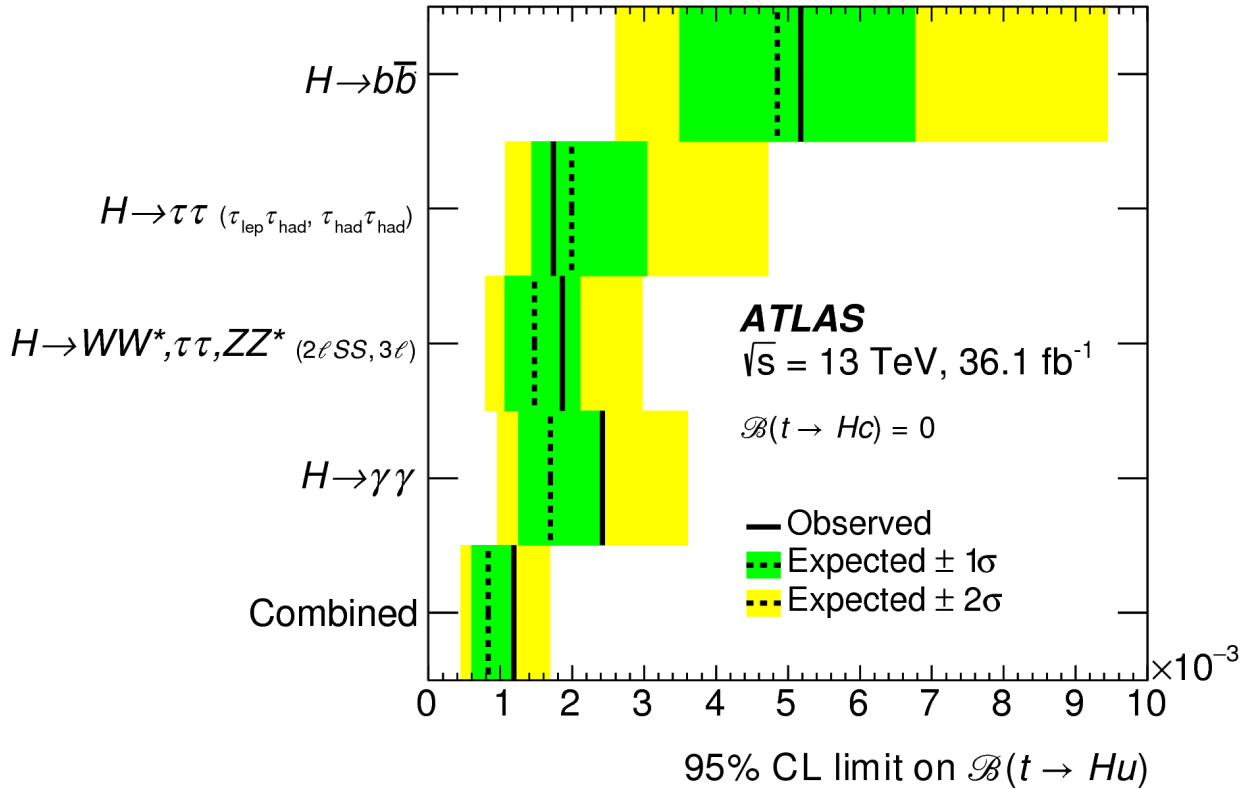
Search for $t \rightarrow qH$ with $H \rightarrow b\bar{b}$

Combine several kinematic variables with a likelihood ratio.

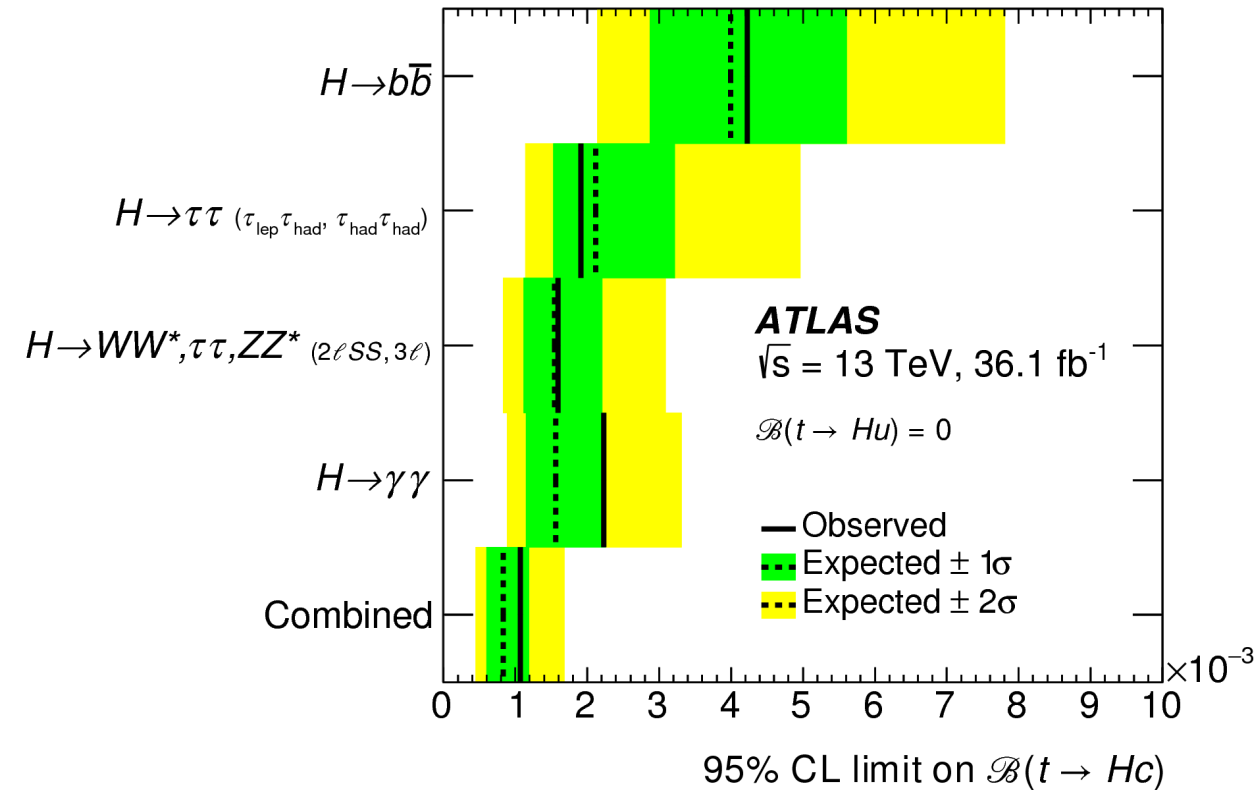
$$L(\vec{x}) = \frac{p_{\text{sig}}(\vec{x})}{p_{\text{sig}}(\vec{x}) + p_{\text{bkg}}(\vec{x})}$$



Upper limits on $\mathcal{B}(t \rightarrow qH)$



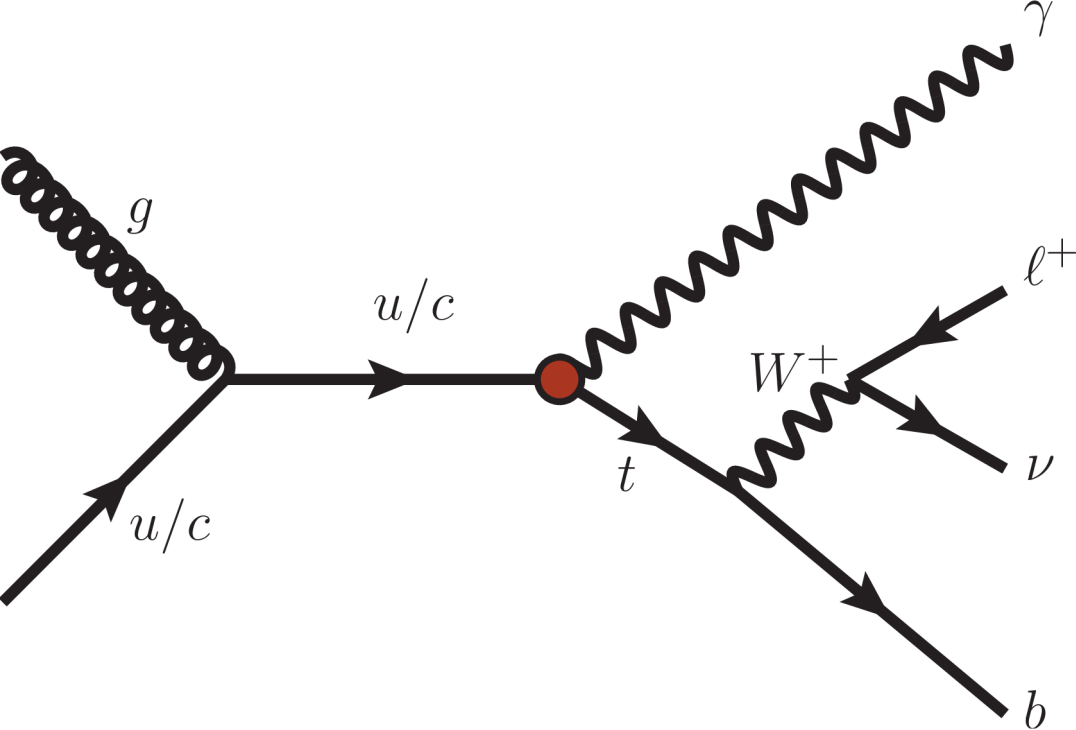
$$\mathcal{B}(t \rightarrow uH) < 1.2 \cdot 10^{-3}$$



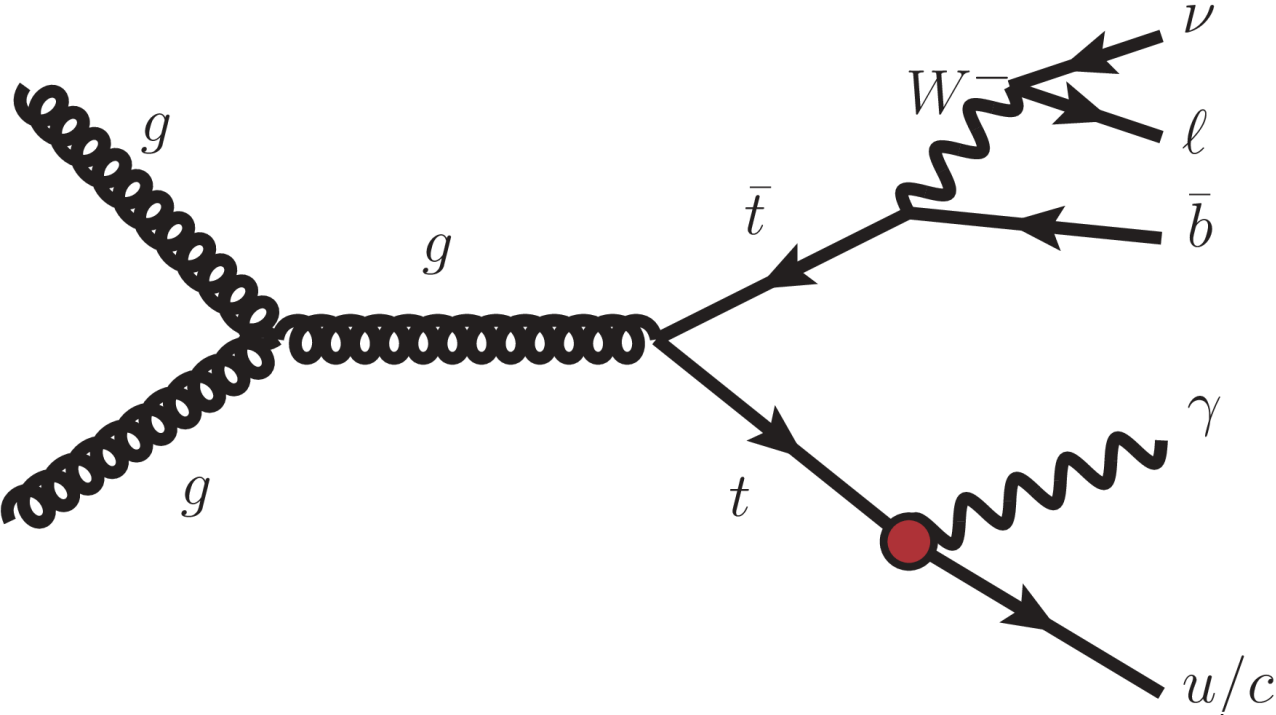
$$\mathcal{B}(t \rightarrow cH) < 1.1 \cdot 10^{-3}$$

Search for $t\gamma$ FCNC

$t\gamma$ production



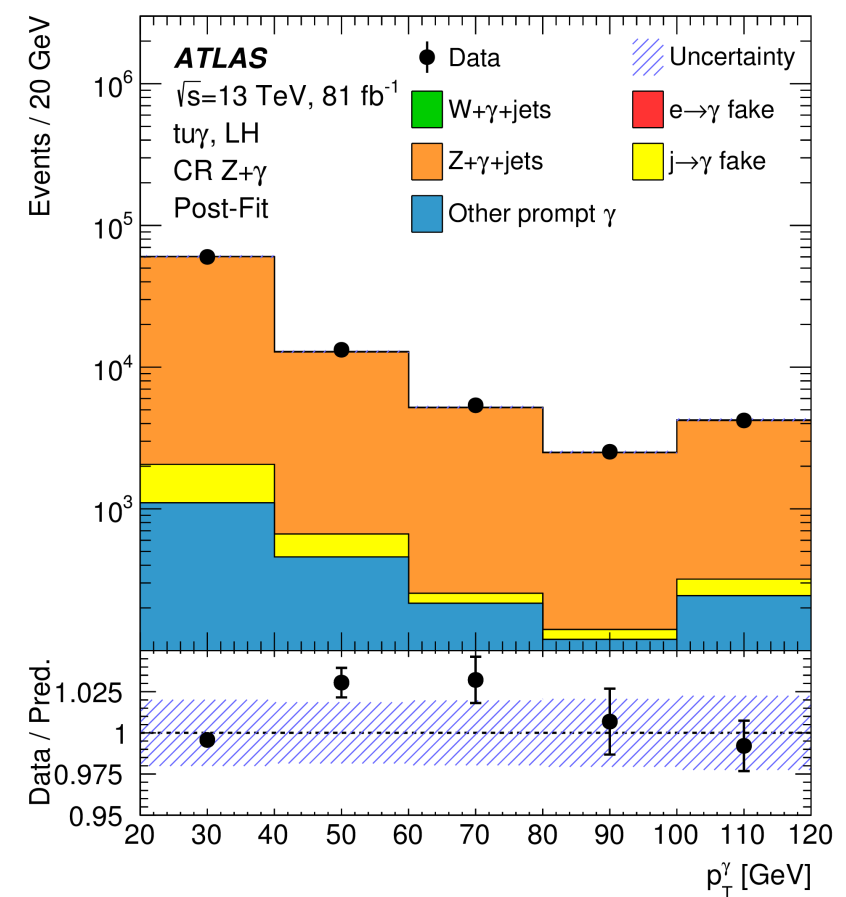
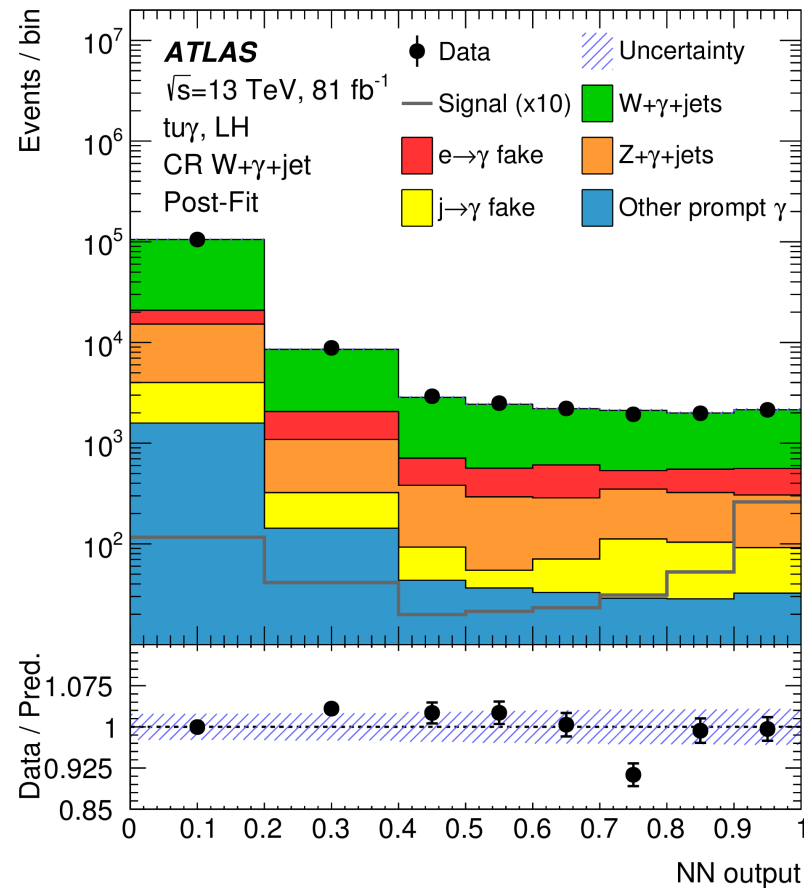
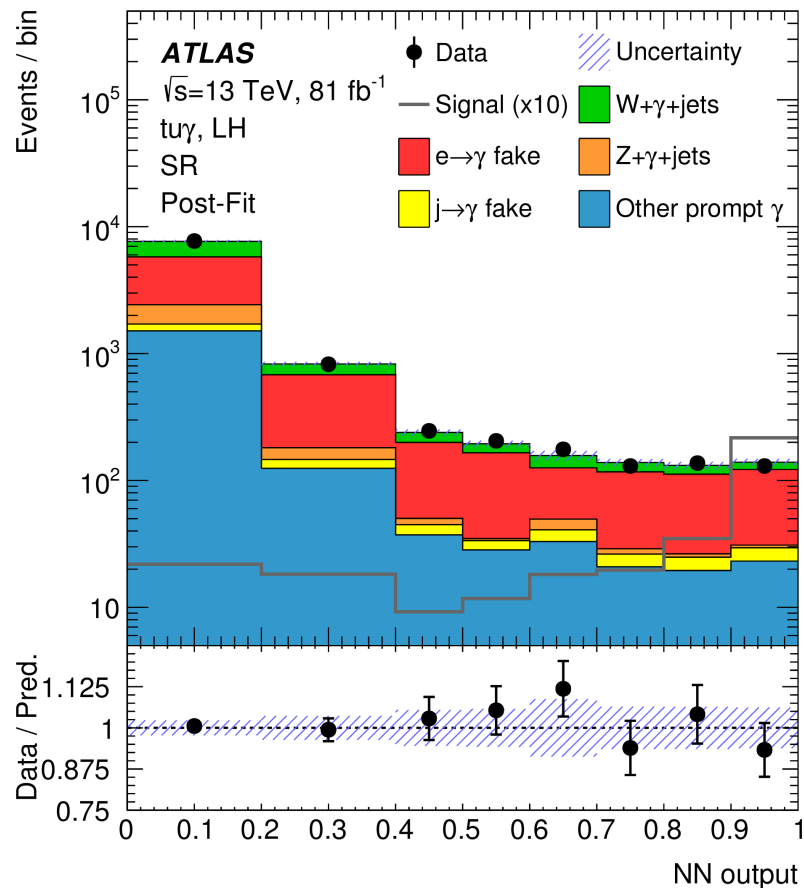
$t \rightarrow q\gamma$ decay



Postfit distributions

- Train neural networks wot separate signal and background.
- Use control regions for two backgrounds.
- Consider different chiral couplings: left-handed and right-handed.

[arXiv: 1908.08461](https://arxiv.org/abs/1908.08461)



Observable	Vertex	Coupling	Obs.	Exp.
$ C_{uW}^{(13)*} + C_{uB}^{(13)*} $	tuy	LH	0.19	$0.22^{+0.04}_{-0.03}$
$ C_{uW}^{(31)} + C_{uB}^{(31)} $	tuy	RH	0.27	$0.27^{+0.05}_{-0.04}$
$ C_{uW}^{(23)*} + C_{uB}^{(23)*} $	$tc\gamma$	LH	0.52	$0.57^{+0.11}_{-0.09}$
$ C_{uW}^{(32)} + C_{uB}^{(32)} $	$tc\gamma$	RH	0.48	$0.59^{+0.12}_{-0.09}$
$\sigma(pp \rightarrow t\gamma)$ [fb]	tuy	LH	36	52^{+21}_{-14}
$\sigma(pp \rightarrow t\gamma)$ [fb]	tuy	RH	78	75^{+31}_{-21}
$\sigma(pp \rightarrow t\gamma)$ [fb]	$tc\gamma$	LH	40	49^{+20}_{-14}
$\sigma(pp \rightarrow t\gamma)$ [fb]	$tc\gamma$	RH	33	52^{+22}_{-14}
$\mathcal{B}(t \rightarrow q\gamma)$ [10^{-5}]	tuy	LH	2.8	$4.0^{+1.6}_{-1.1}$
$\mathcal{B}(t \rightarrow q\gamma)$ [10^{-5}]	tuy	RH	6.1	$5.9^{+2.4}_{-1.6}$
$\mathcal{B}(t \rightarrow q\gamma)$ [10^{-5}]	$tc\gamma$	LH	22	27^{+11}_{-7}
$\mathcal{B}(t \rightarrow q\gamma)$ [10^{-5}]	$tc\gamma$	RH	18	28^{+12}_{-8}

Upper limits on ...

Effective operator coefficients

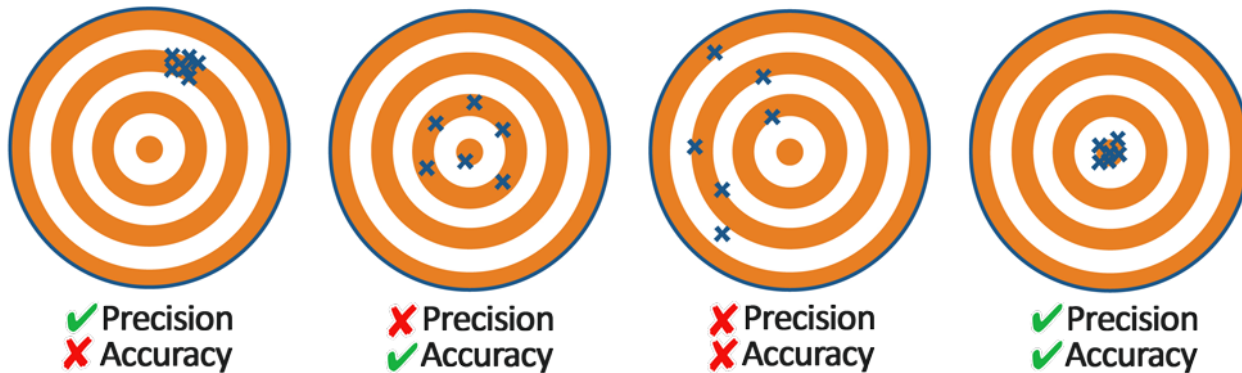
Cross sections

Branching ratios

Chapter 5

Precision measurements of top-quark properties

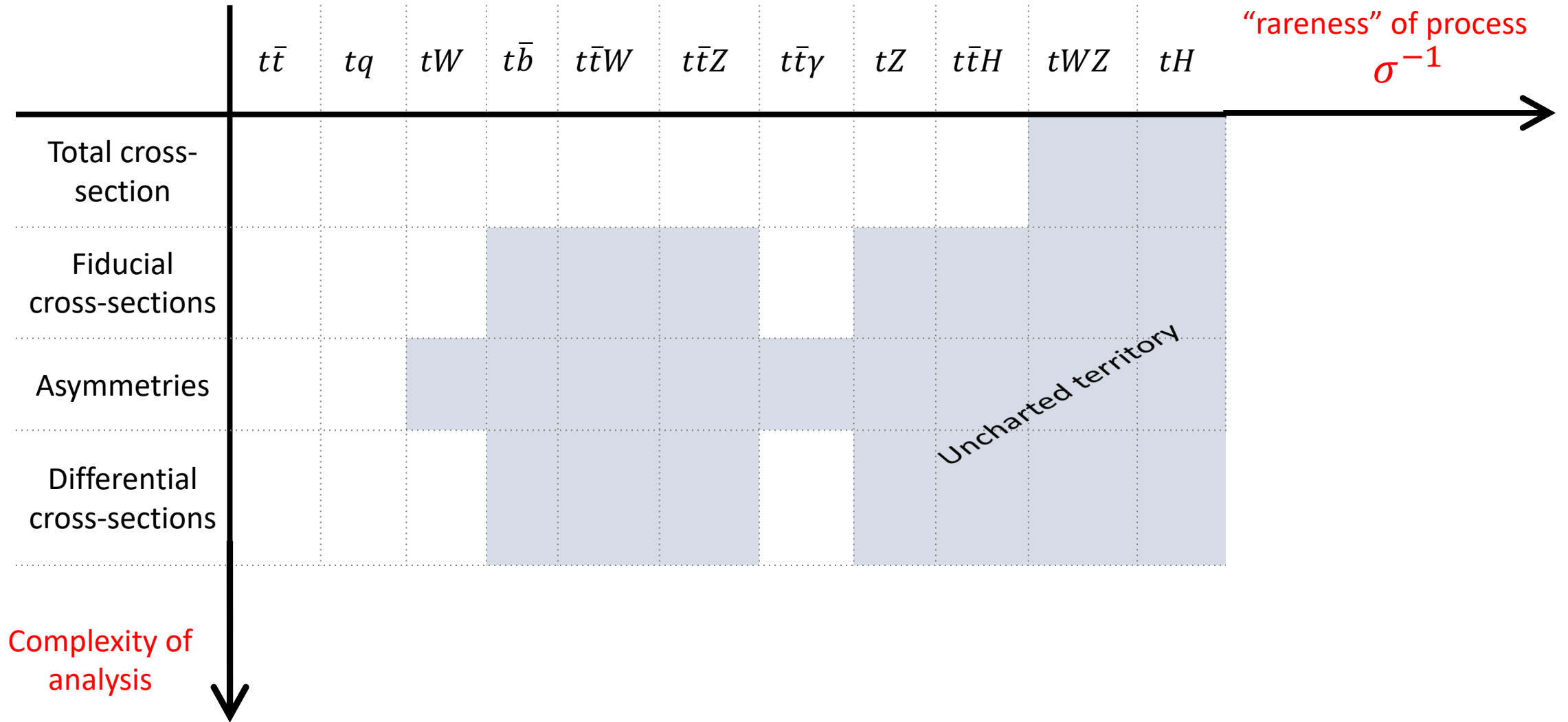
PRECISION VS ACCURACY



Discussed analyses:

- 1) Measurement of $t\bar{t}$ cross-section in the electron muon channel
- 2) Measurement of $t\bar{t}$ cross-section in the lepton+jets channel
- 3) Charge asymmetry in $t\bar{t}$ events
- 4) Spin correlations in $t\bar{t}$ events

Pushing the frontiers of complexity



Precision measurement of $\sigma(t\bar{t})$

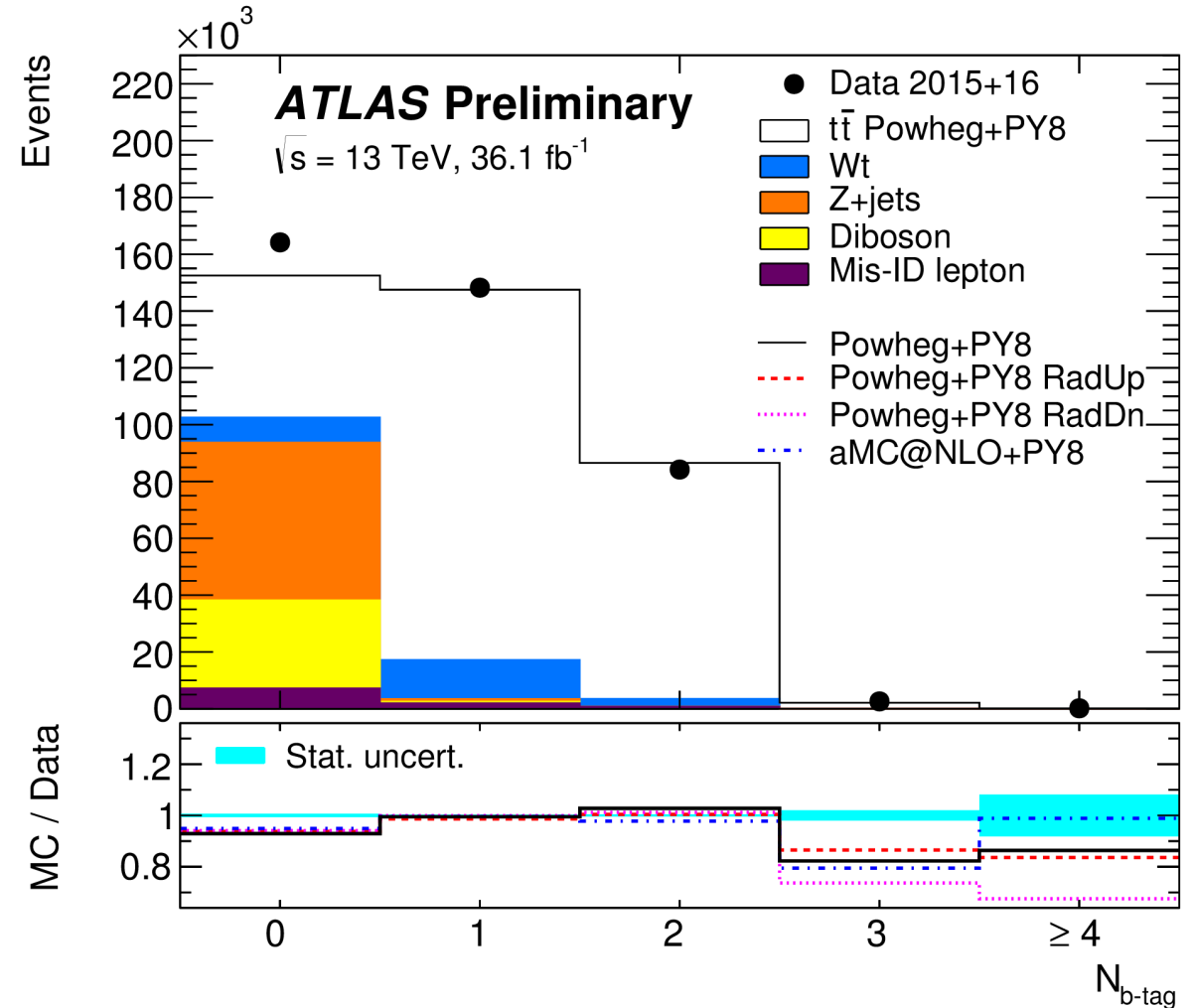
- Use electron-muon final state.
- Low background
- Counting experiment
- Determine b-tagging efficiency by using the 1-tag and 2-tag rates.

$$N_1 = \mathcal{L}_{\text{int}} \sigma(t\bar{t}) \epsilon_{e\mu} 2 \epsilon_b (1 - C_b \epsilon_b) + N_1^{\text{bkg}}$$

$$N_2 = \mathcal{L}_{\text{int}} \sigma(t\bar{t}) \epsilon_{e\mu} C_b \epsilon_b^2 + N_2^{\text{bkg}}$$

- The lepton isolation efficiency is recalibrated in the context of this analysis.

[ATLAS-CONF-2019-041](#)

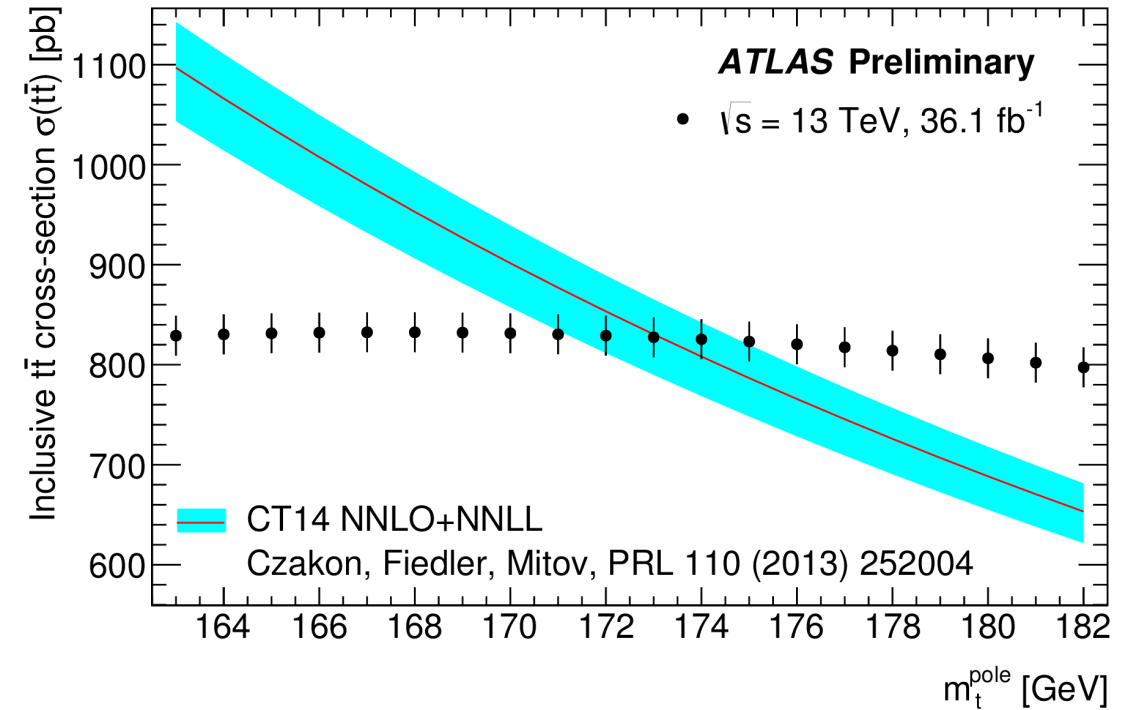
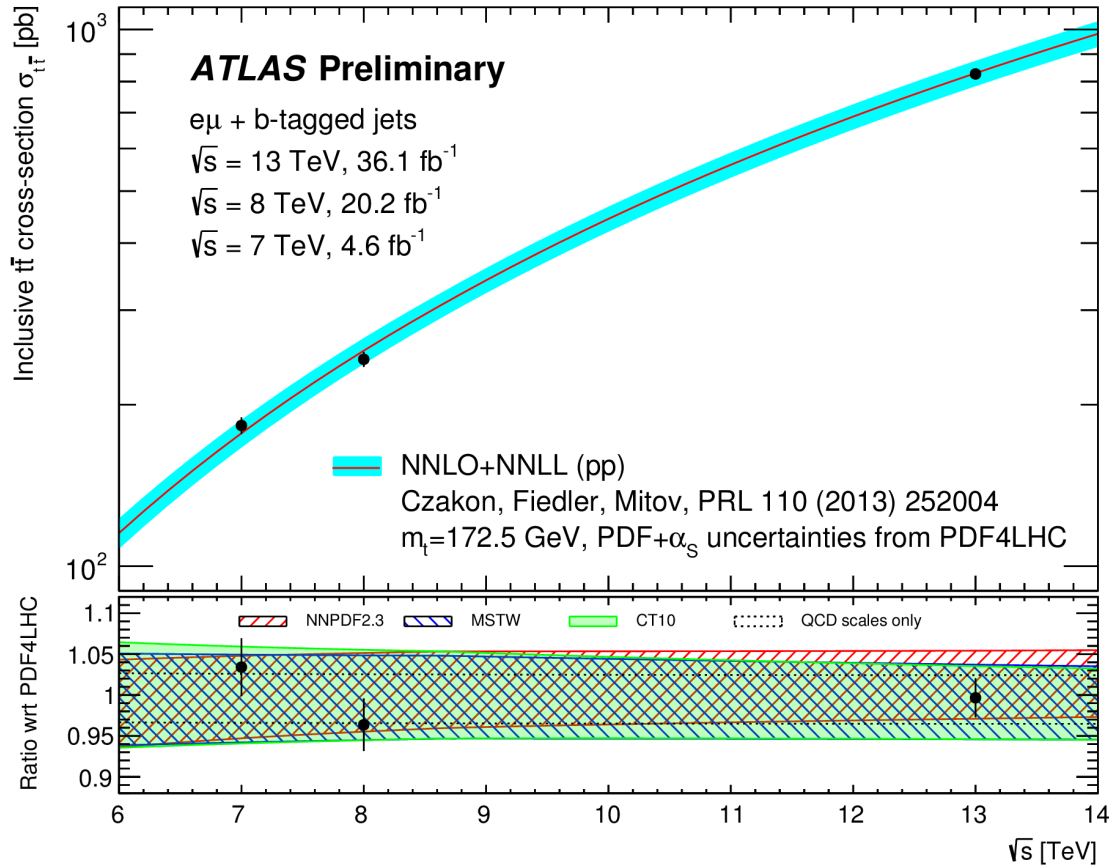


Total cross-section result

$$\sigma(t\bar{t}) = 826.4 \pm 3.6 \text{ (stat)} \pm 11.5 \text{ (syst)} \pm 1.9 \text{ (beam)}$$

2.4% precision

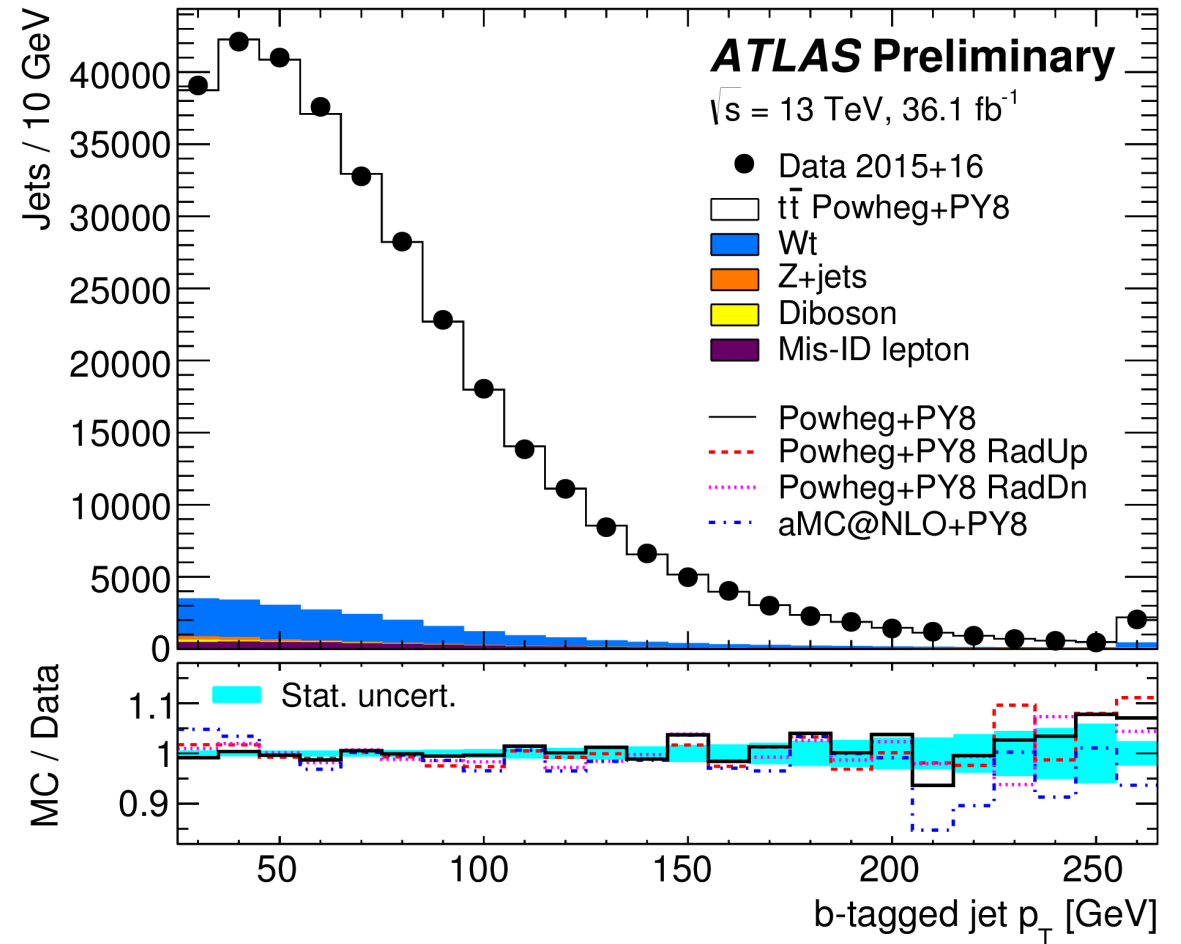
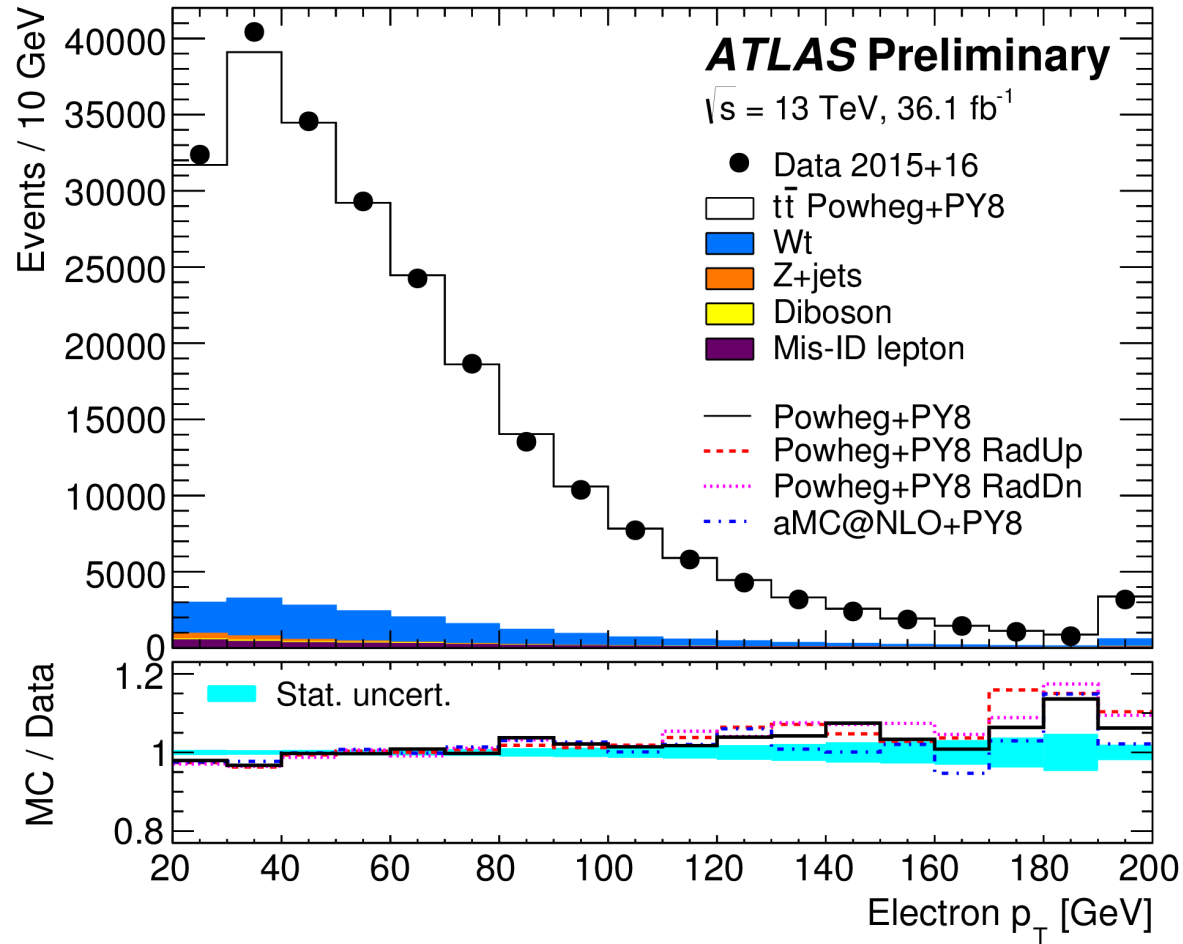
Precision of theory prediction @ NNLO: 5.5%



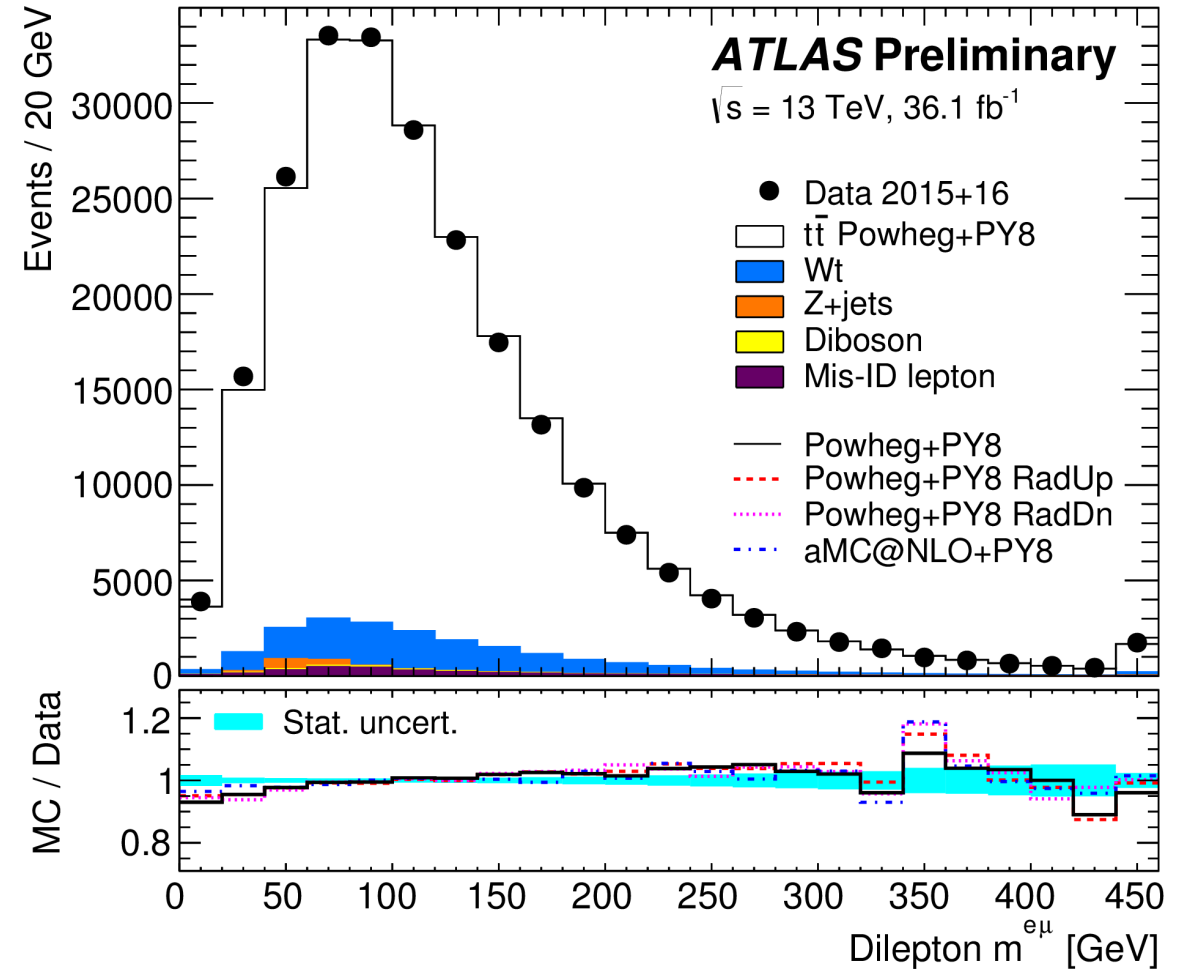
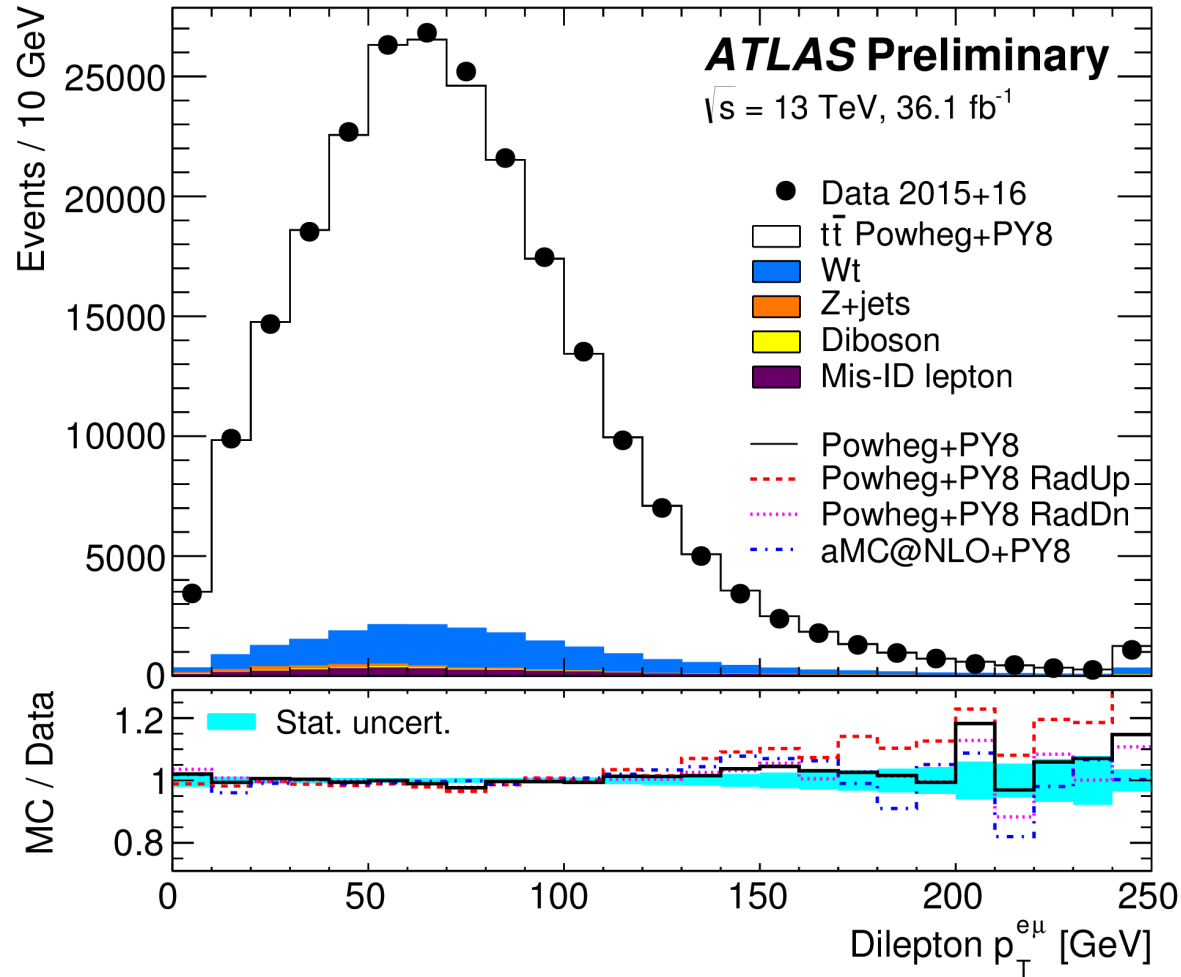
Extract the pole mass from the dependence of $\sigma(t\bar{t})$ on m_t :

$$m_t^{\text{pole}} = 173.1^{+2.0}_{-2.1} \text{ GeV}$$

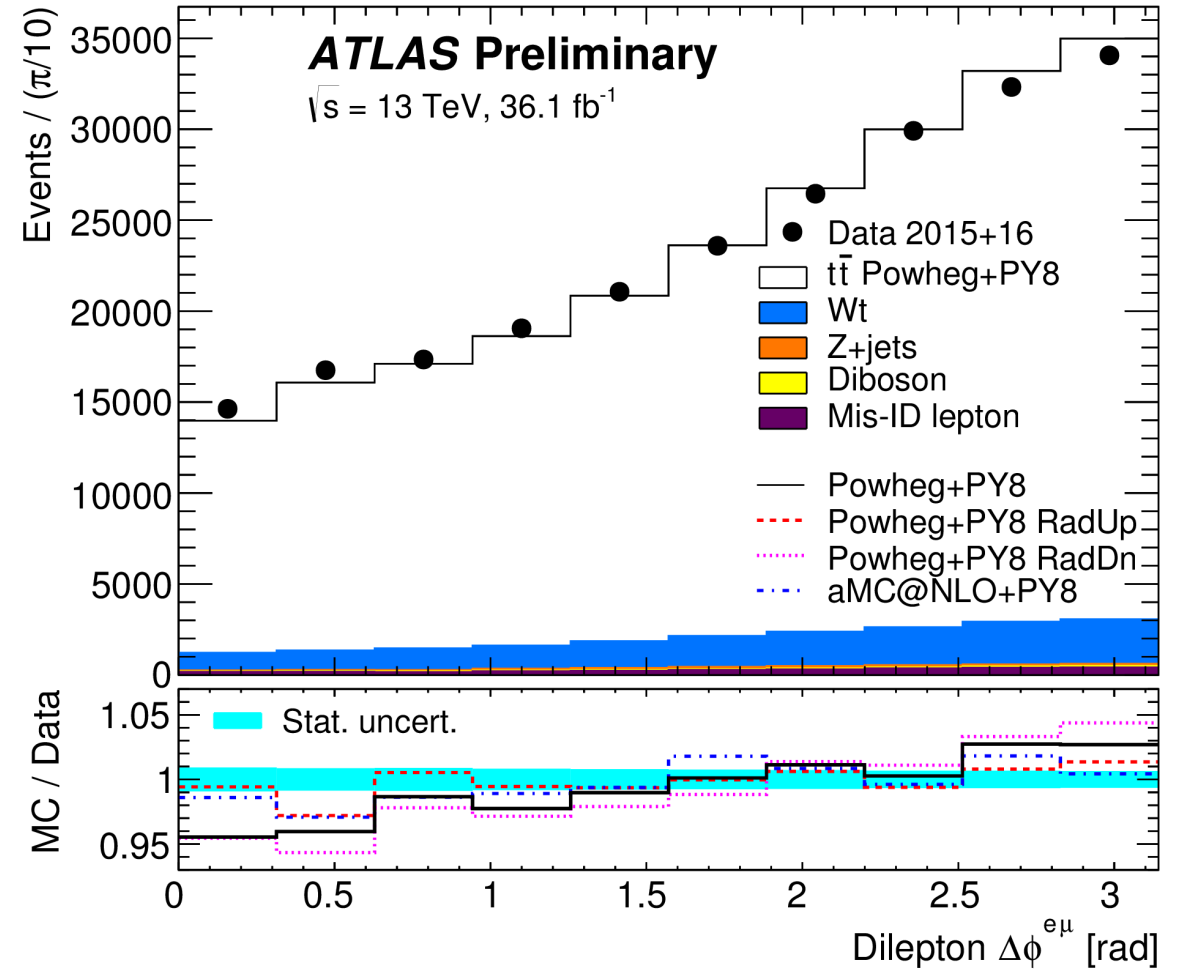
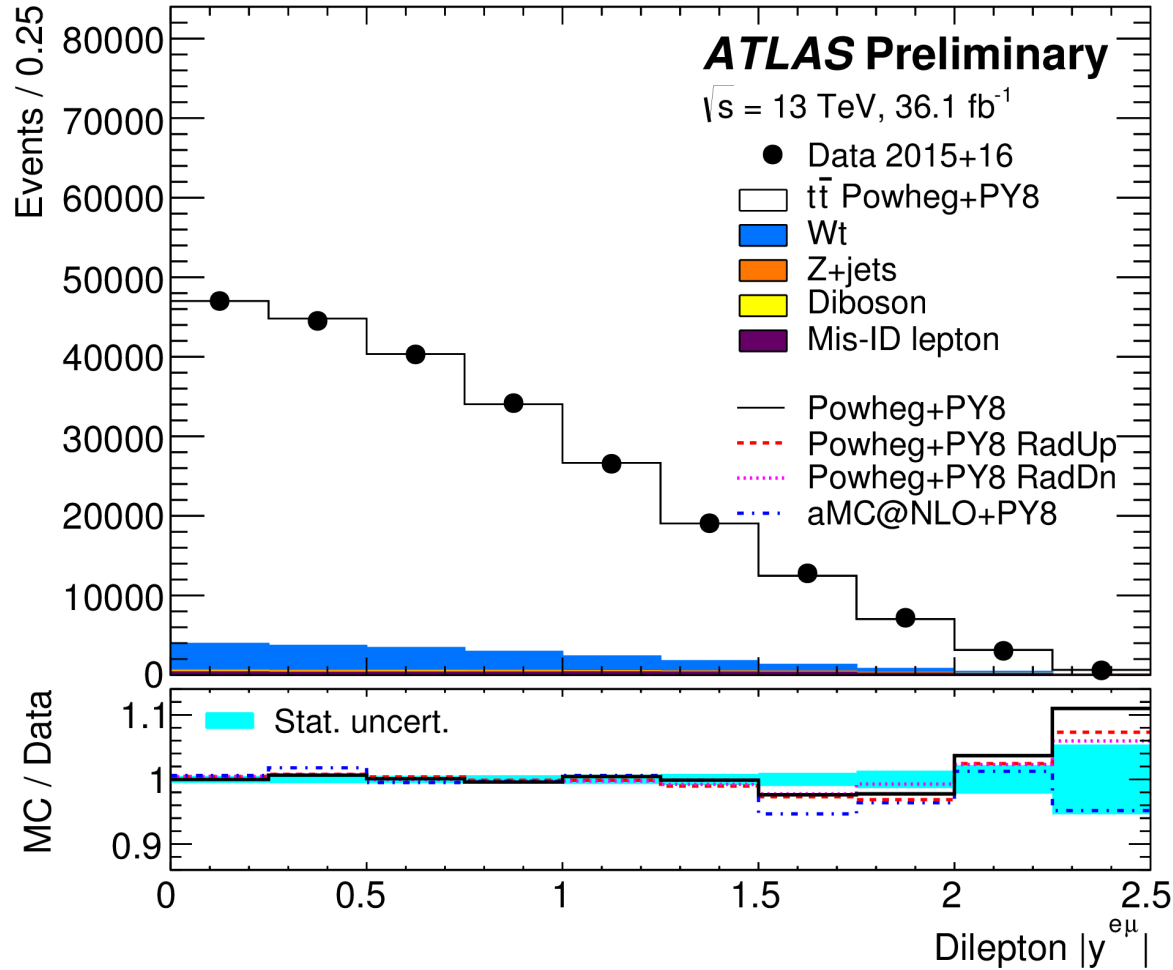
p_T spectra



Dilepton quantities



Angular distributions

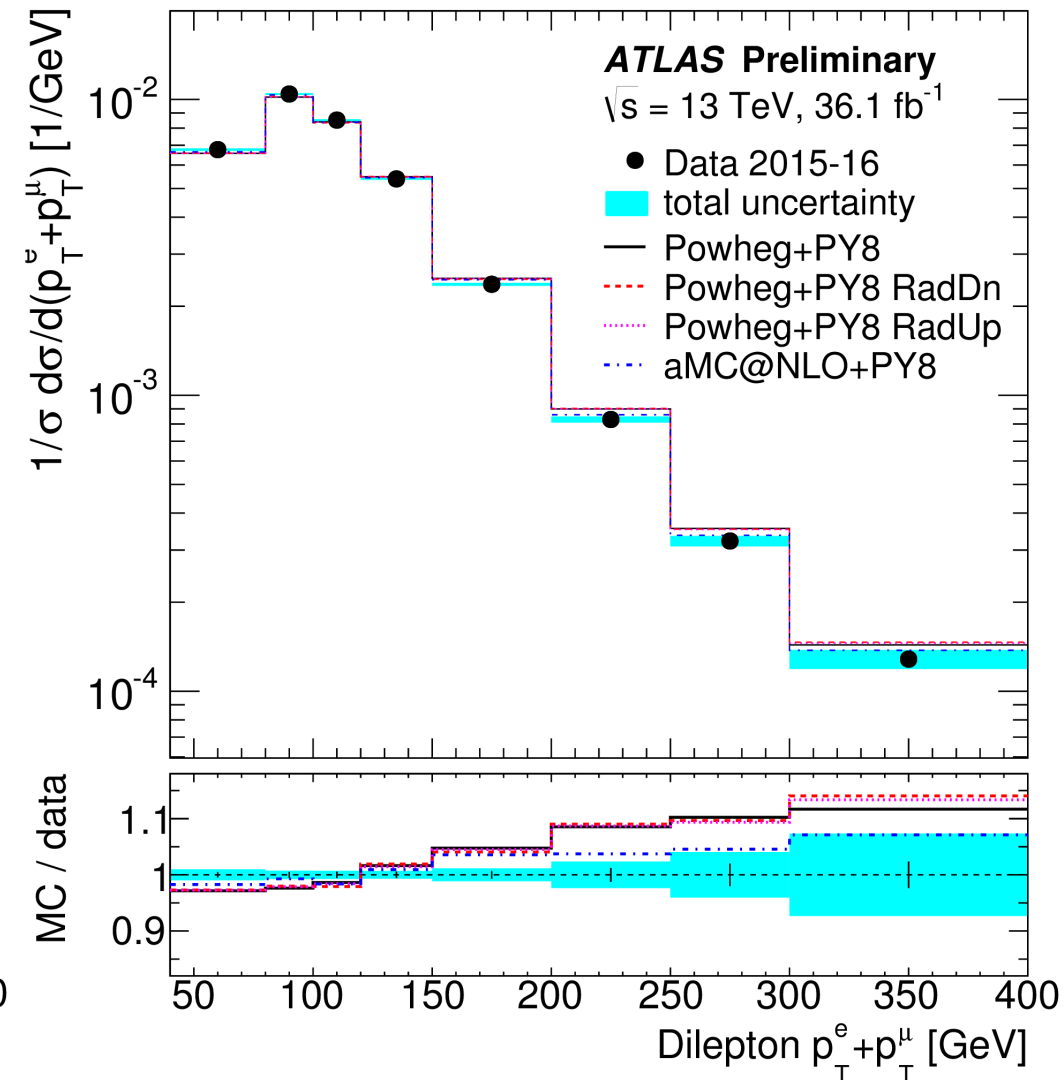
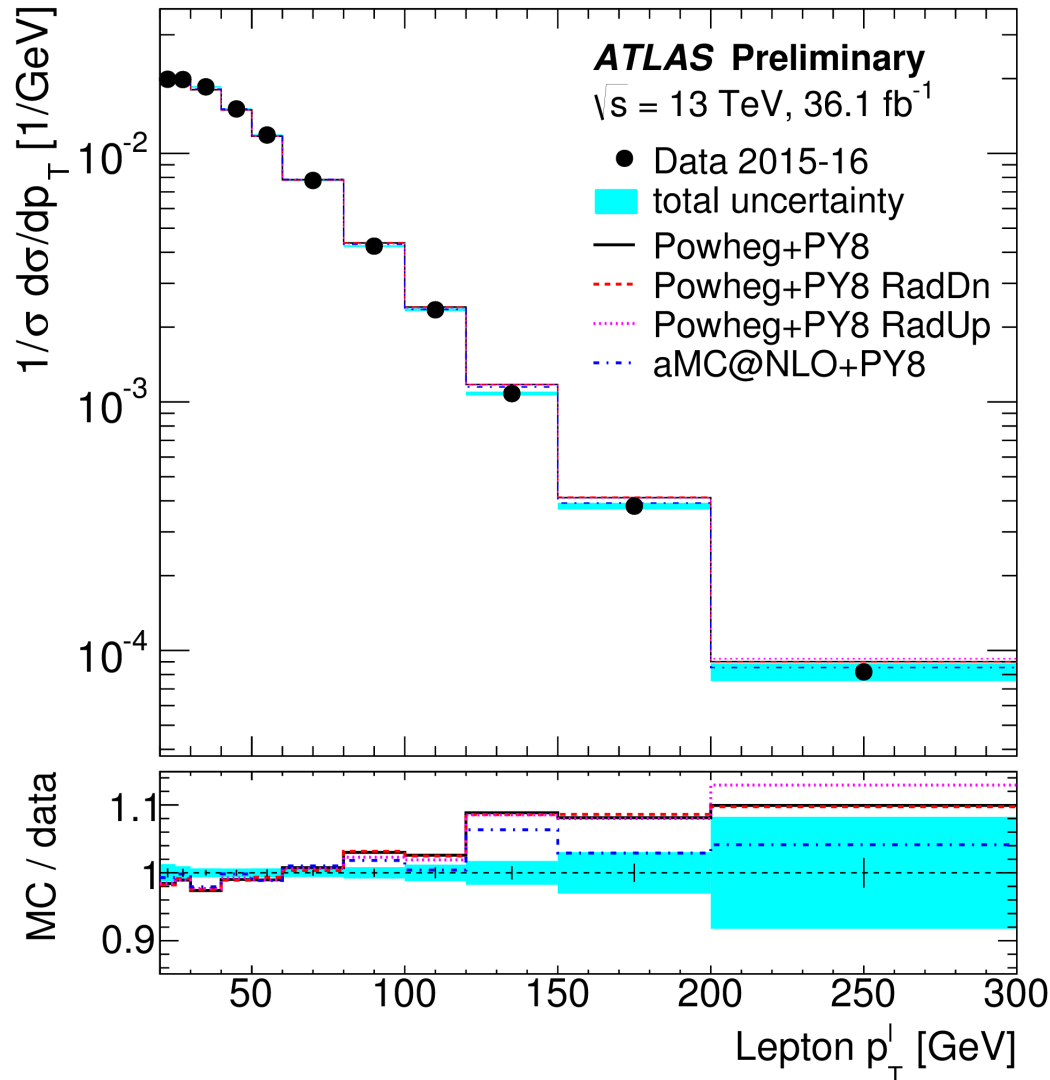


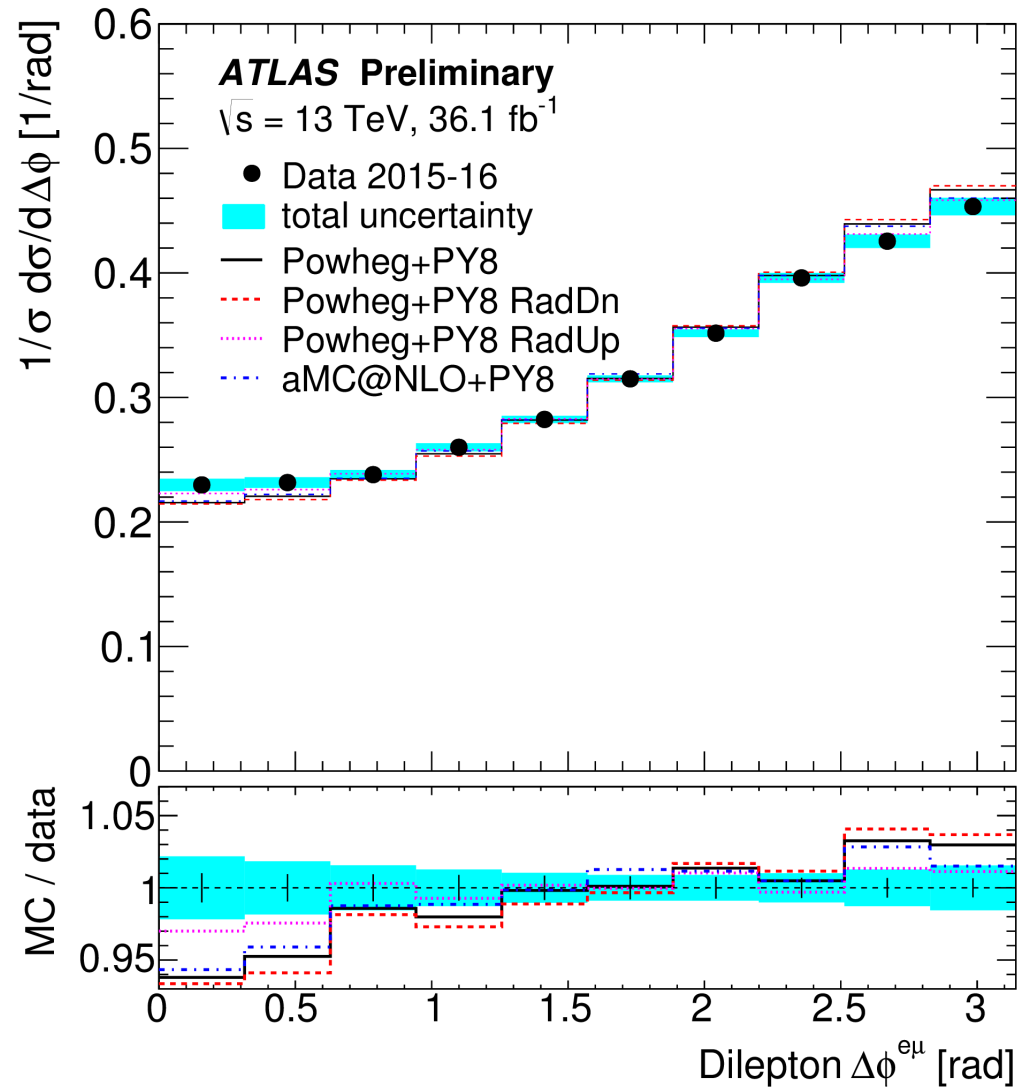
Discrepancy between MC prediction and data
(more on this later).

Differential cross sections

Apply the tagging equations bin-by-bin in a distribution.

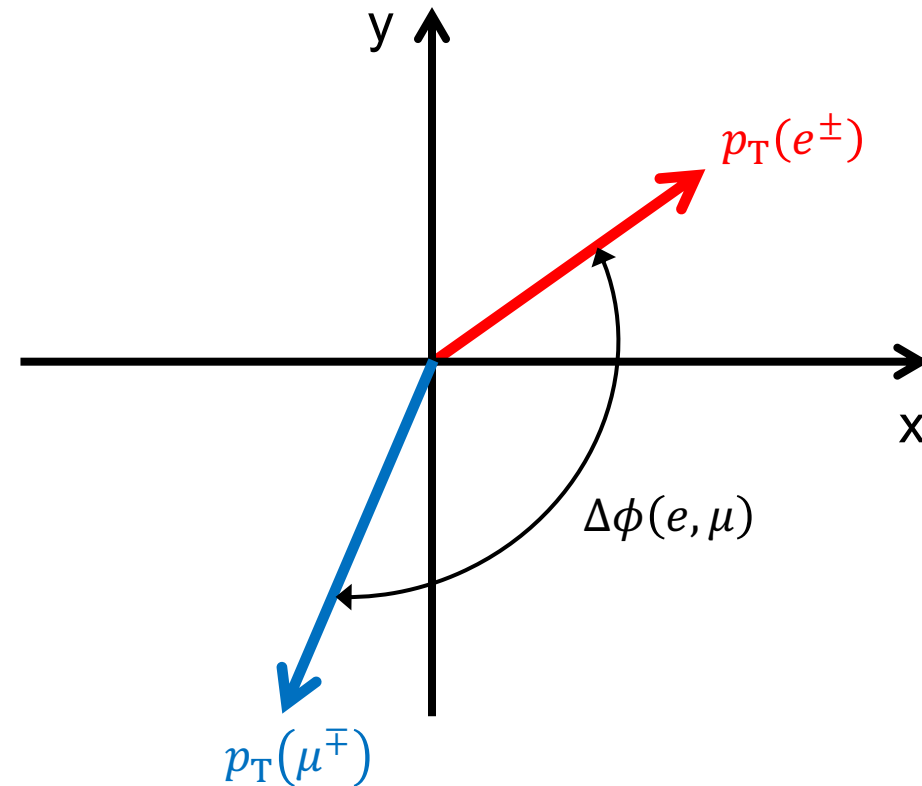
Data are softer than predictions by MC generators.



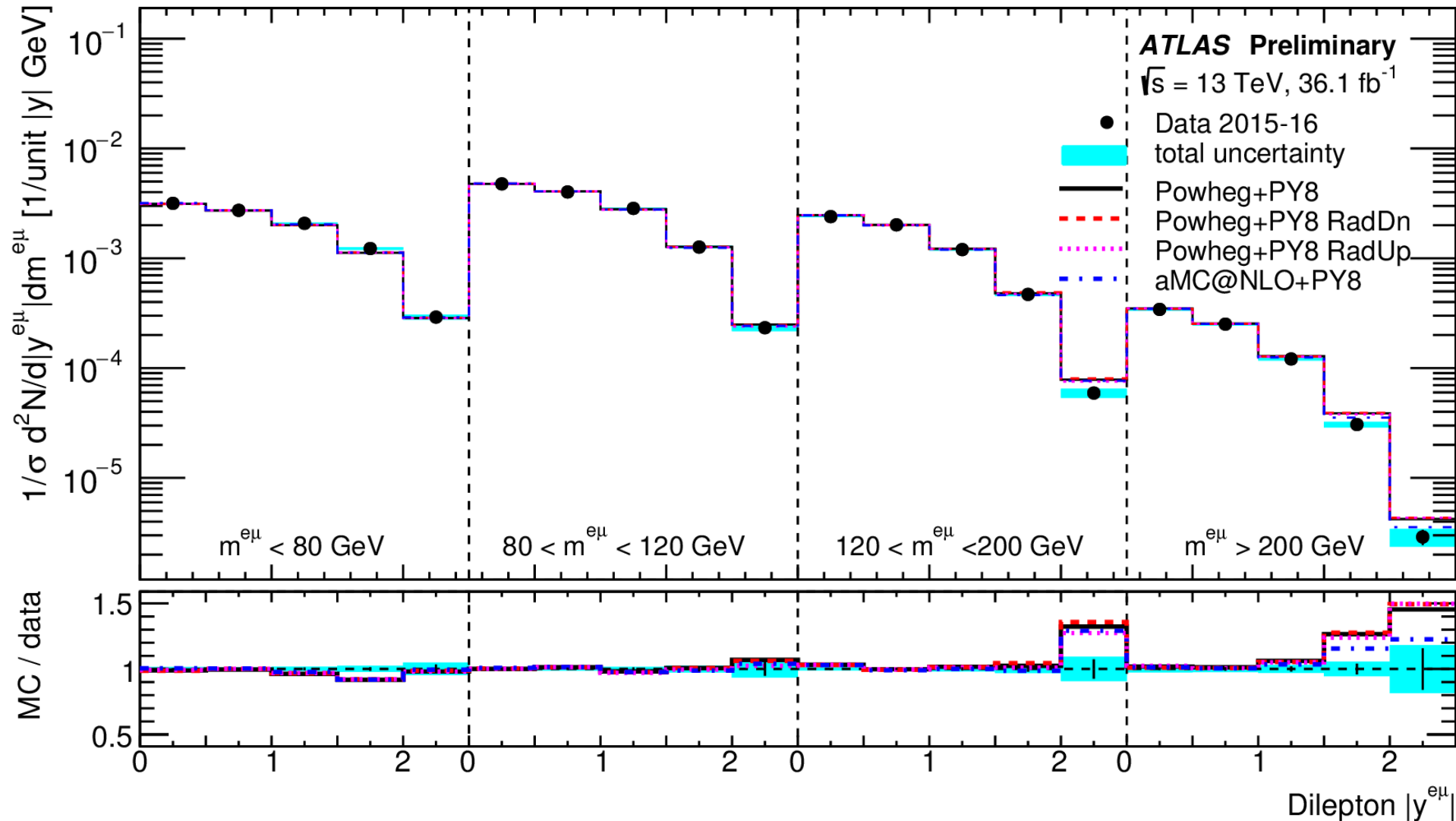


Difference in the azimuthal angle ϕ
between electron and muon

Transverse plane:



Double differential cross-sections



Some discrepancies for higher $m(e\mu)$ and $|y^{e\mu}|$.

χ^2 values

Generator N_{dof}	p_{T}^{ℓ} 10	$ \eta^{\ell} $ 8	$p_{\text{T}}^{e\mu}$ 8	$m^{e\mu}$ 11	$ y^{e\mu} $ 8	$\Delta\phi^{e\mu}$ 9	$p_{\text{T}}^e + p_{\text{T}}^{\mu}$ 7	$E^e + E^{\mu}$ 9
POWHEG + PY8	43.7	19.5	8.6	44.3	11.4	14.4	32.5	18.4
POWHEG + PY6 CT10	36.1	7.9	9.3	33.0	16.2	16.2	21.9	30.5
POWHEG + HW7	34.8	15.9	11.5	62.7	9.4	17.3	23.0	14.7
POWHEG + PY8 p_{T} rew.	20.2	14.7	2.3	38.3	8.4	12.7	9.4	14.0
POWHEG + PY8 RadDn	40.0	24.2	6.1	44.3	9.2	16.3	29.0	20.1
POWHEG + PY8 RadUp	33.0	16.3	21.9	35.3	12.3	6.4	26.7	16.5
POWHEG + PY8 $\mu_{\text{F,R}} \times 2$	46.5	21.6	6.2	42.6	8.5	16.5	28.9	17.1
POWHEG + PY8 $\mu_{\text{F,R}} \times 0.5$	39.8	17.3	11.4	38.0	10.7	10.9	27.6	14.2
POWHEG + PY8 PDF4LHC15	43.4	14.6	7.4	39.0	6.2	13.5	28.0	15.9
POWHEG + PY8 CT14	44.1	9.3	7.6	37.0	8.2	13.5	28.5	18.2
POWHEG + PY8 MMHT	41.2	17.7	6.9	39.0	6.3	13.2	26.3	14.3
AMC@NLO + PY8	26.2	25.7	11.4	19.7	16.7	13.2	12.5	14.0
AMC@NLO + PY8 CT10	24.9	11.7	10.6	16.9	10.0	13.4	12.0	19.0
AMC@NLO + PY8 HERA2	17.1	96.6	6.9	26.0	68.5	12.5	6.1	38.4

χ^2 probabilities

POWHEG + PY8	$4 \cdot 10^{-6}$	0.012	0.37	$6 \cdot 10^{-6}$	0.18	0.11	$3 \cdot 10^{-5}$	0.030
POWHEG + PY6 CT10	$8 \cdot 10^{-5}$	0.45	0.32	$5 \cdot 10^{-4}$	0.039	0.062	$3 \cdot 10^{-3}$	$4 \cdot 10^{-4}$
POWHEG + HW7	$1 \cdot 10^{-4}$	0.043	0.18	$3 \cdot 10^{-9}$	0.31	0.045	$2 \cdot 10^{-3}$	0.098
POWHEG + PY8 p_{T} rew.	0.028	0.065	0.97	$7 \cdot 10^{-5}$	0.39	0.18	0.23	0.12
POWHEG + PY8 RadDn	$2 \cdot 10^{-5}$	$2 \cdot 10^{-3}$	0.64	$6 \cdot 10^{-6}$	0.32	0.060	$1 \cdot 10^{-4}$	0.017
POWHEG + PY8 RadUp	$3 \cdot 10^{-4}$	0.038	$5 \cdot 10^{-3}$	$2 \cdot 10^{-4}$	0.14	0.70	$4 \cdot 10^{-4}$	0.057
POWHEG + PY8 $\mu_{\text{F,R}} \times 2$	$1 \cdot 10^{-6}$	$6 \cdot 10^{-3}$	0.62	$1 \cdot 10^{-5}$	0.39	0.056	$1 \cdot 10^{-4}$	0.048
POWHEG + PY8 $\mu_{\text{F,R}} \times 0.5$	$2 \cdot 10^{-5}$	0.027	0.18	$8 \cdot 10^{-5}$	0.22	0.28	$3 \cdot 10^{-4}$	0.12
POWHEG + PY8 PDF4LHC15	$4 \cdot 10^{-6}$	0.067	0.49	$5 \cdot 10^{-5}$	0.62	0.14	$2 \cdot 10^{-4}$	0.068
POWHEG + PY8 CT14	$3 \cdot 10^{-6}$	0.32	0.47	$1 \cdot 10^{-4}$	0.42	0.14	$2 \cdot 10^{-4}$	0.033
POWHEG + PY8 MMHT	$1 \cdot 10^{-5}$	0.024	0.55	$5 \cdot 10^{-5}$	0.62	0.15	$5 \cdot 10^{-4}$	0.11
AMC@NLO + PY8	$3 \cdot 10^{-3}$	$1 \cdot 10^{-3}$	0.18	0.049	0.034	0.15	0.086	0.12
AMC@NLO + PY8 CT10	$5 \cdot 10^{-3}$	0.16	0.23	0.11	0.27	0.15	0.10	0.025
AMC@NLO + PY8 HERA2	0.073	0	0.54	$6 \cdot 10^{-3}$	0	0.19	0.53	$1 \cdot 10^{-5}$

$\sigma(t\bar{t})$ in the lepton+jets channel

New for
TOP2019

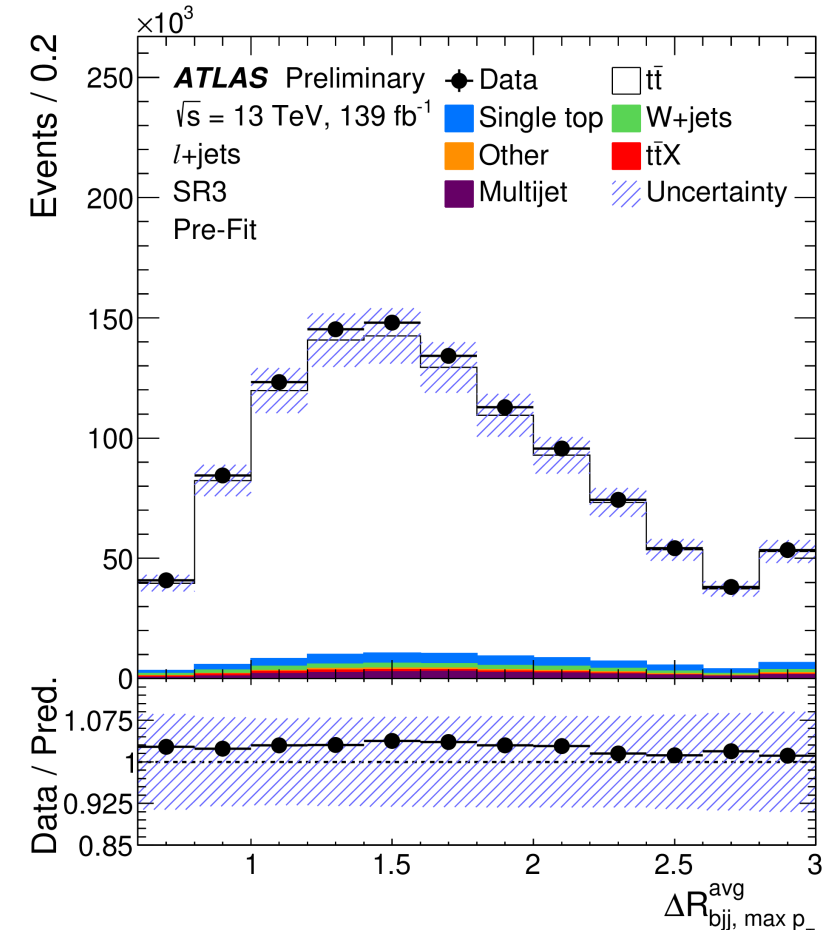
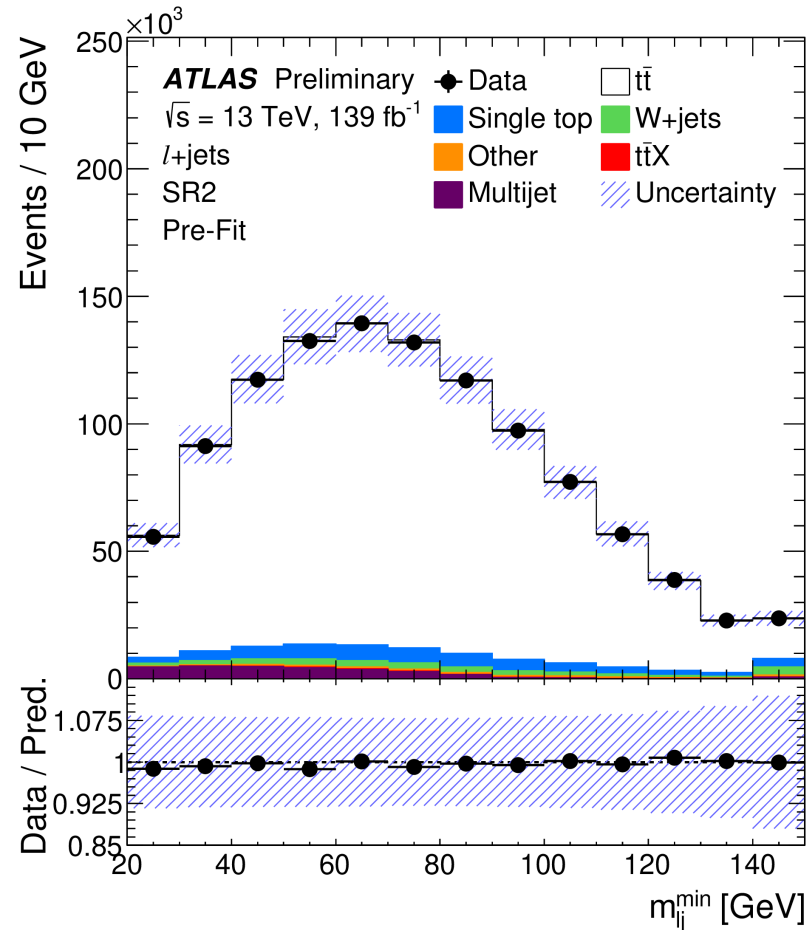
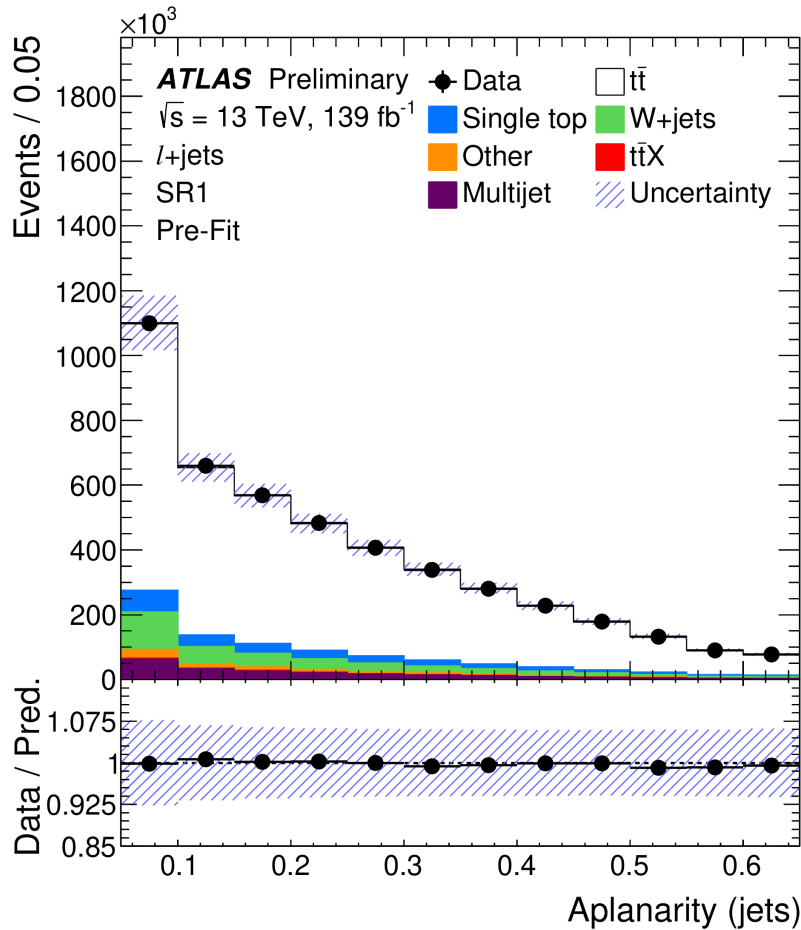
Use kinematic variables in 3 channels

ATLAS-CONF-2019-044

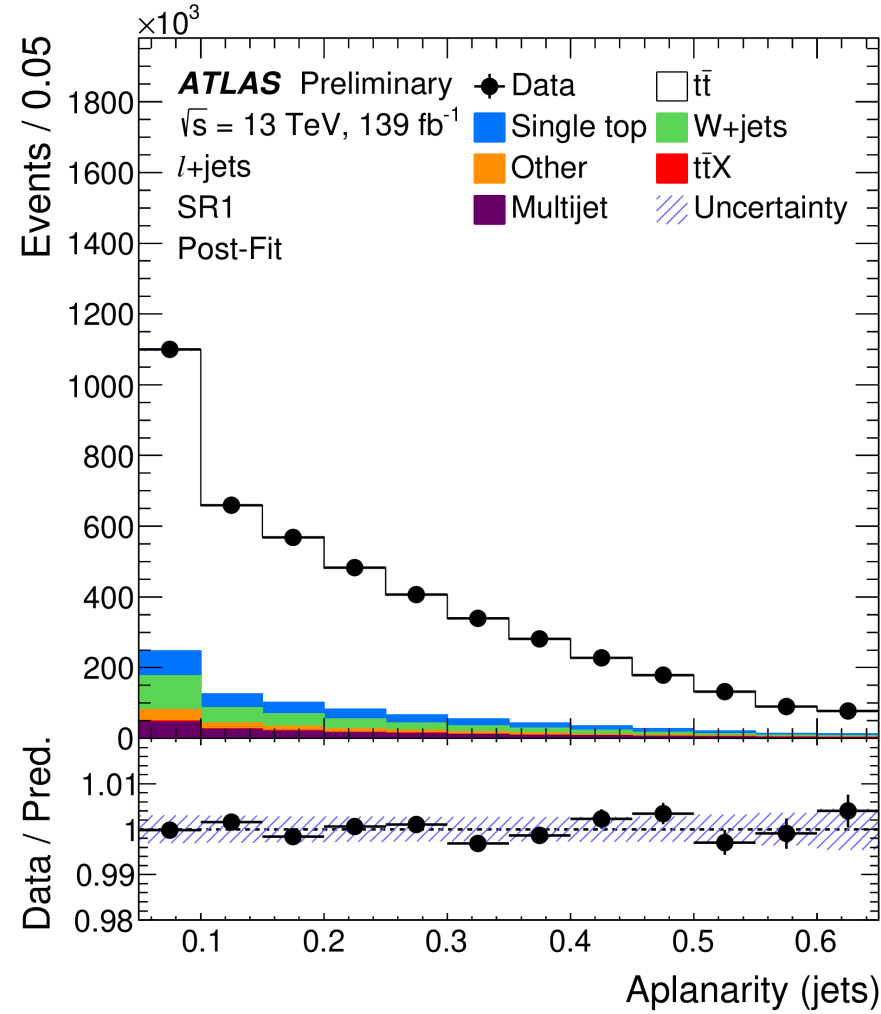
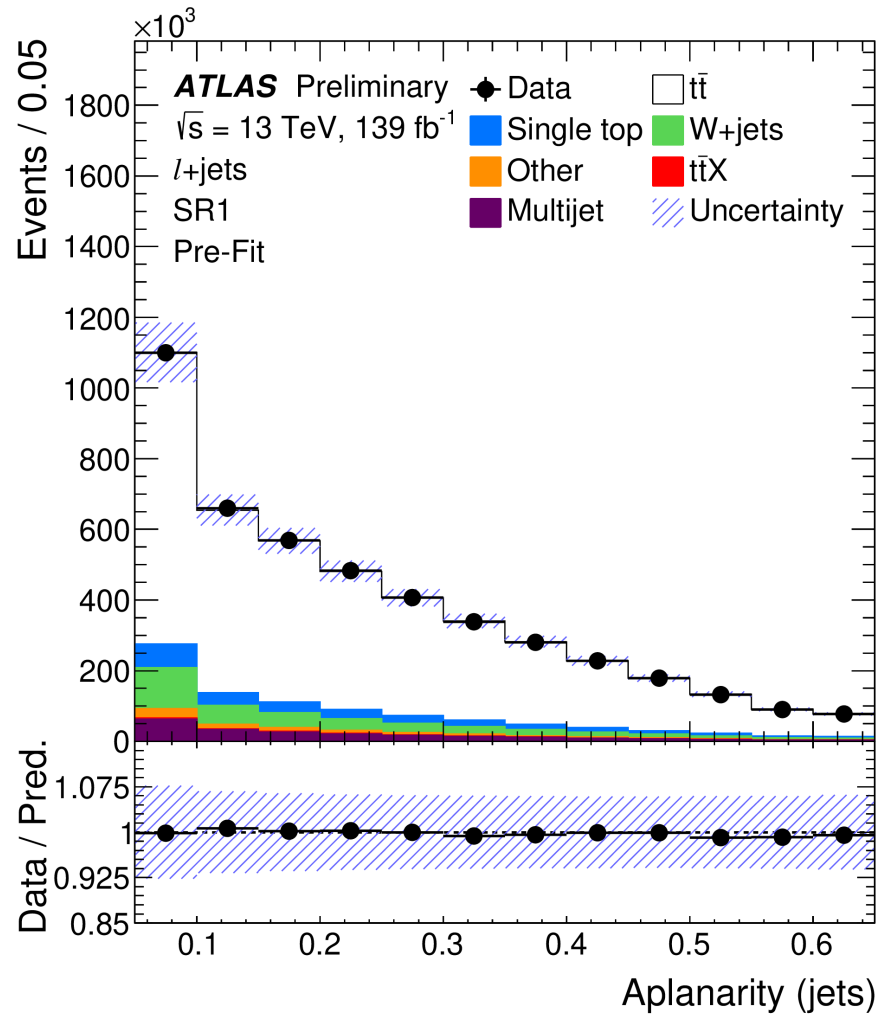
≥ 4 jets and = 1 b-tag

= 4 jets and = 2 b-tags

≥ 5 jets and = 2 b-tags



Uncertainties are reduced as a result of the fit.



$\sigma(t\bar{t})$ result

$$\sigma(t\bar{t}) = 830.4 \pm 0.4 \text{ (stat.) } {}^{+38.2}_{-37.0} \text{ (syst.)}$$

4.6% precision

Theory prediction:

$$\sigma(t\bar{t}) = 832 {}^{+20}_{-29} \text{ (scale)} \pm 35 \text{ (PDF} + \alpha_s)$$

Dominating uncertainties are due to modelling of the $t\bar{t}$ process by event generators.

Category	$\frac{\Delta\sigma_{\text{fid}}}{\sigma_{\text{fid}}}$ [%]		$\frac{\Delta\sigma_{\text{inc}}}{\sigma_{\text{inc}}}$ [%]	
Signal modelling				
$t\bar{t}$ shower/hadronisation	+2.1	-1.9	+2.7	-2.7
$t\bar{t}$ scale variations	+2.0	-1.8	+2.5	-2.6
Background modelling				
MC background modelling	+1.8	-1.7	+1.6	-1.8
Multijet background	+0.5	-0.6	+0.6	-0.7
Detector modelling				
Jet reconstruction	+2.4	-2.3	+2.5	-2.3
Luminosity	+1.8	-1.7	+1.8	-1.6
Flavour tagging	+1.4	-1.4	+1.5	-1.4
E_T^{miss} + pile-up	+0.3	-0.2	+0.5	-0.5
Muon reconstruction	+0.4	-0.6	+0.4	-0.5
Electron reconstruction	+0.4	-0.2	+0.2	-0.4
Simulation stat. uncertainty	+0.7	-0.6	+0.9	-0.9
Total systematic uncertainty	+4.1	-3.9	+4.6	-4.5
Data stat. uncertainty	+0.05	-0.05	+0.05	-0.05
Total uncertainty	+4.1	-3.9	+4.6	-4.5

Charge asymmetry in $t\bar{t}$ production

- Top-quarks are produced slightly more forward than top-antiquarks.
→ central-forward asymmetry
- Only the $q\bar{q}$ initial state contributes.
- Quantum interference effect involving NLO amplitudes, in particular ISR and FSR for $q\bar{q} \rightarrow t\bar{t}g$.
- Observable:

$$A_c = \frac{N(\Delta|y|>0) - N(\Delta|y|<0)}{N(\Delta|y|>0) + N(\Delta|y|<0)}$$

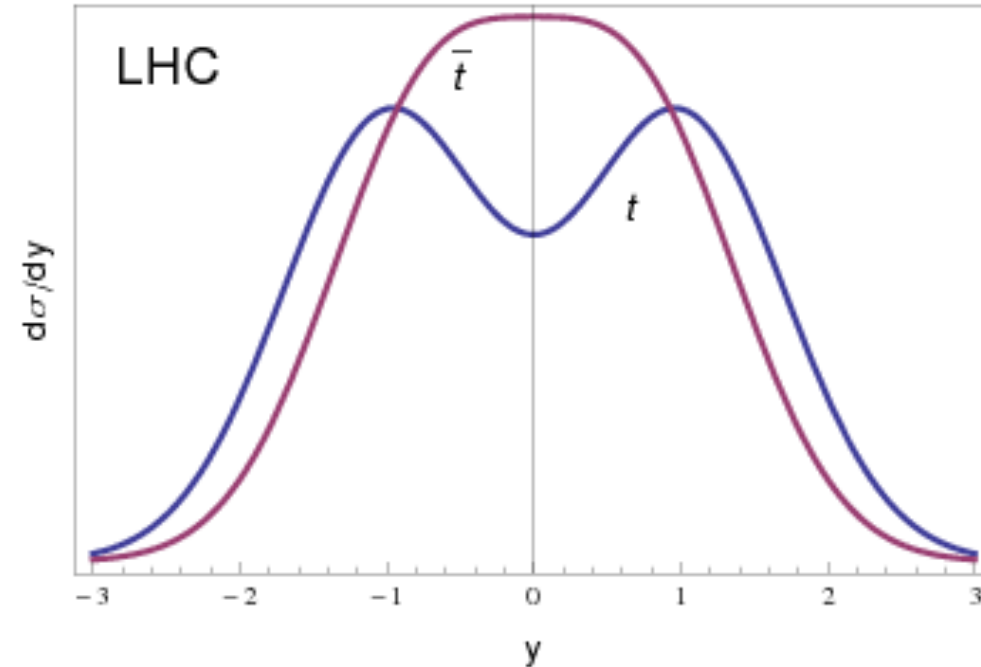
with $\Delta|y| = |y_t| - |y_{\bar{t}}|$

- SM Prediction at QCD NLO + EWK NLO precision:

@ 7 TeV: $A_c = 0.0123 \pm 0.0005$

@ 8 TeV: $A_c = 0.0111 \pm 0.0004$

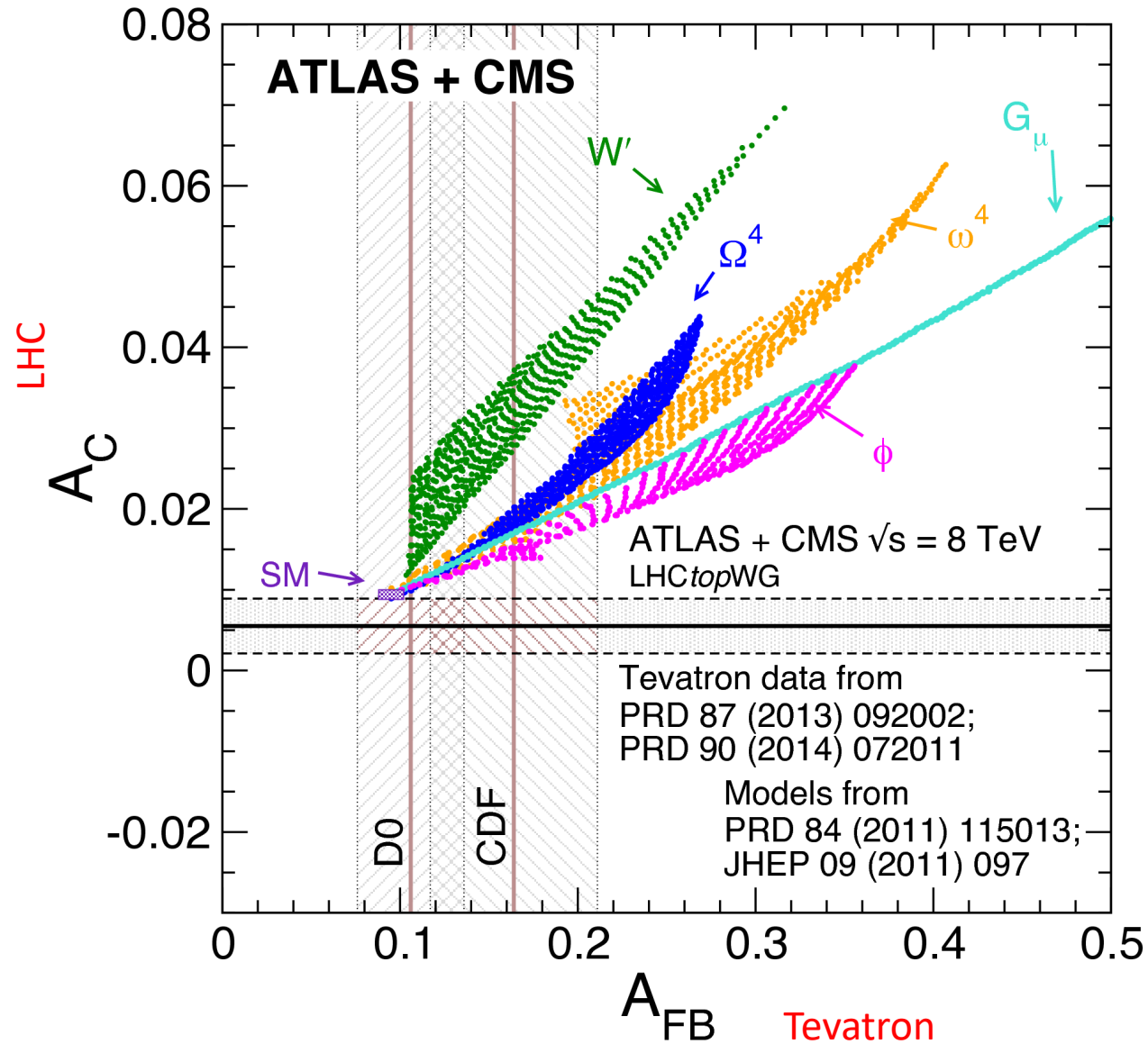
@ 13 TeV: $A_c = 0.0 \pm 0.000$



(Effect strongly exaggerated for illustration)

- SM effect is quite small, but
- Sensitive to new physics contributions
- Tevatron observed large forward-backward asymmetries ($p\bar{p}$ initial state), but tensions have eased in the meanwhile.

Impact on BSM physics

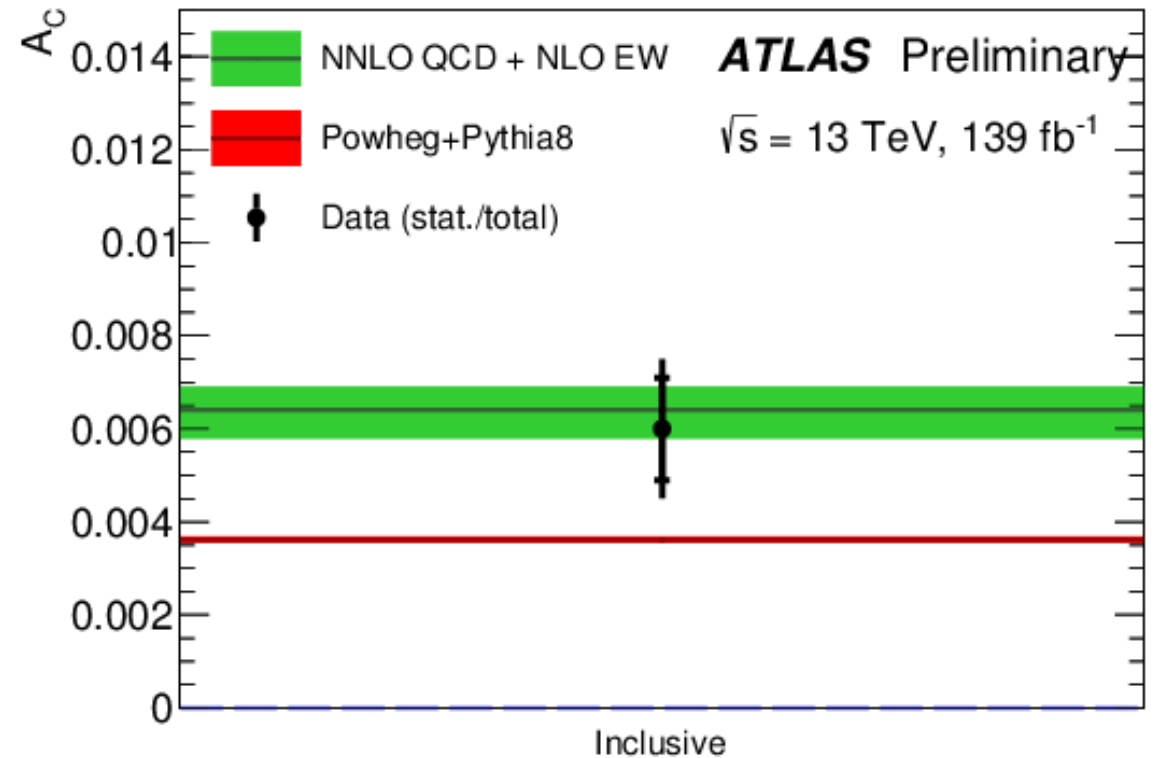
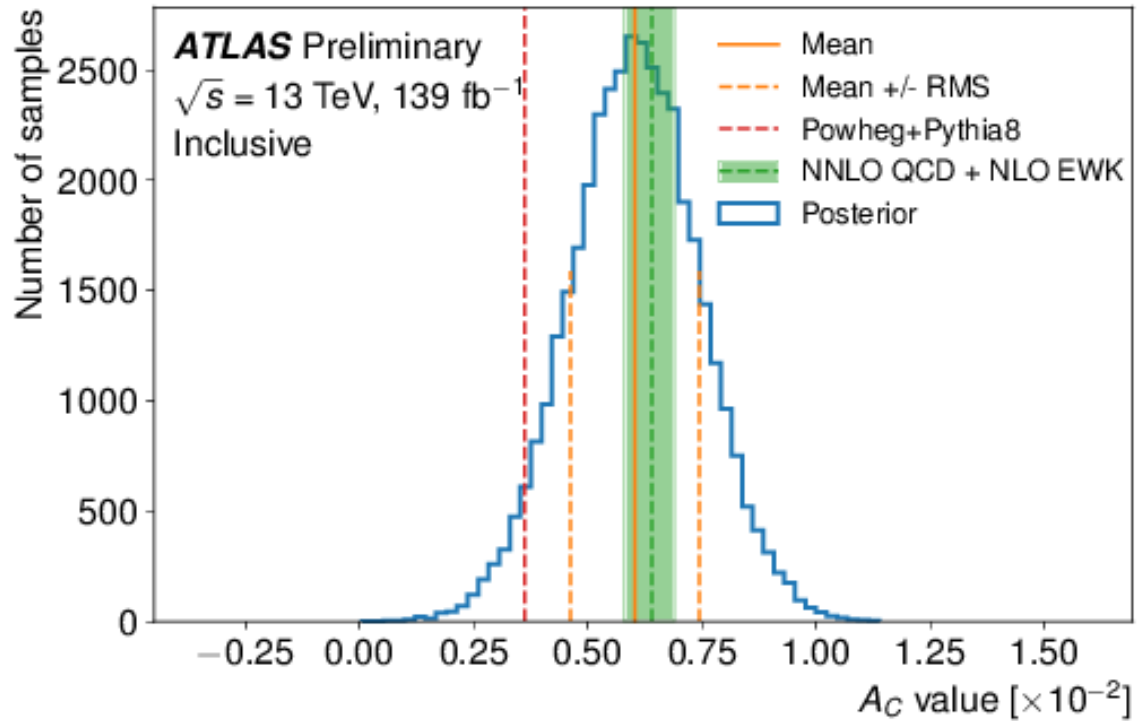


Tested models:

- W' boson
- Heavy axi-gluon G_μ
- Scalar isodoublet ϕ
- Colour triplet scalar ω^4
- Colour sextet scalar Ω^4

Charge asymmetry: results

- Use fully Bayesian unfolding (FBU)
- Integrate out nuisance parameters of systematic uncertainties in the likelihood function

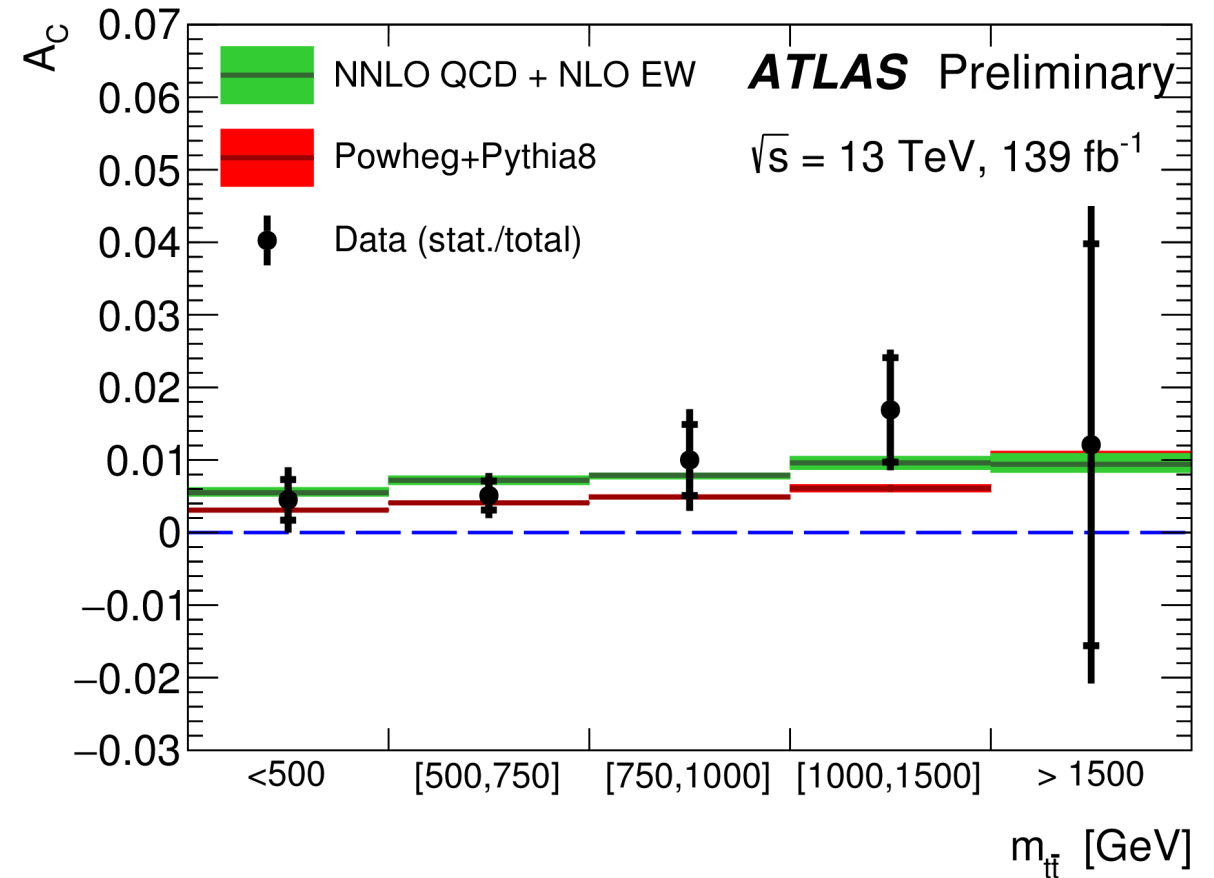
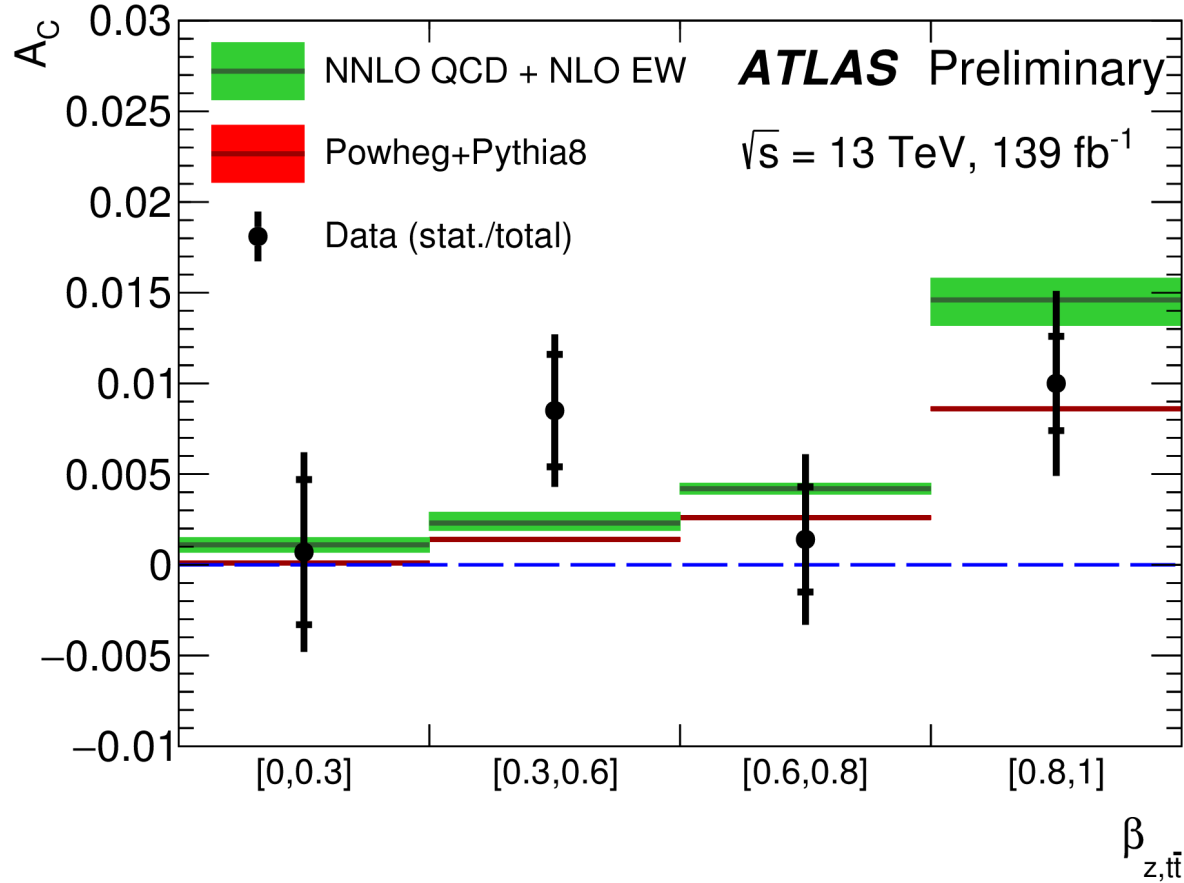


Differential results

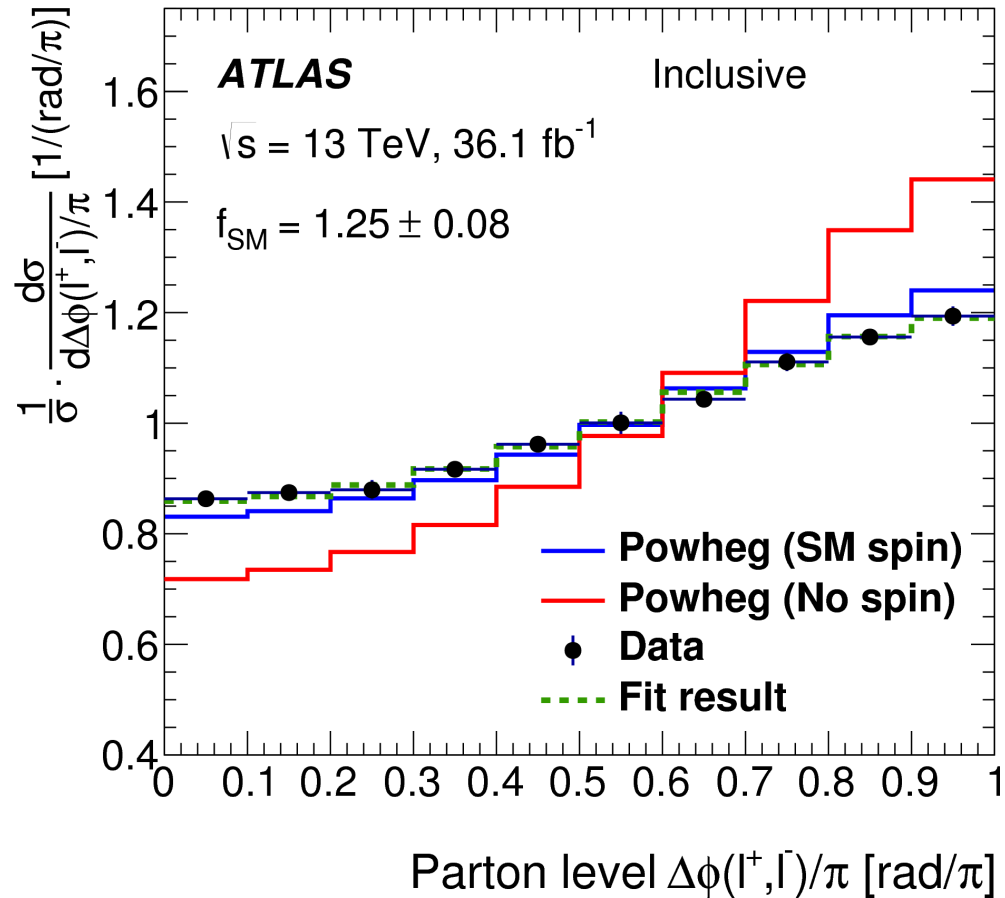
Longitudinal boost of the $t\bar{t}$ system along the z axis = $\beta_z(t\bar{t})$

$m(t\bar{t})$

[ATLAS-CONF-2019-026](#)



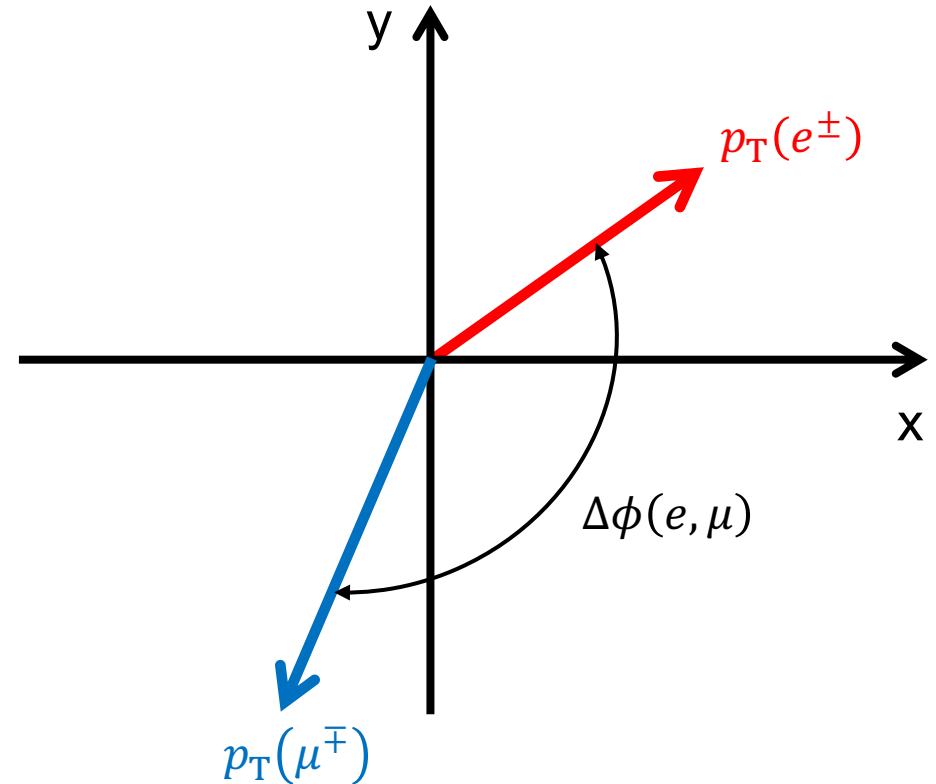
Spin correlations between top-quark and top-antiquark



„No spin“ hypothesis is clearly rejected.

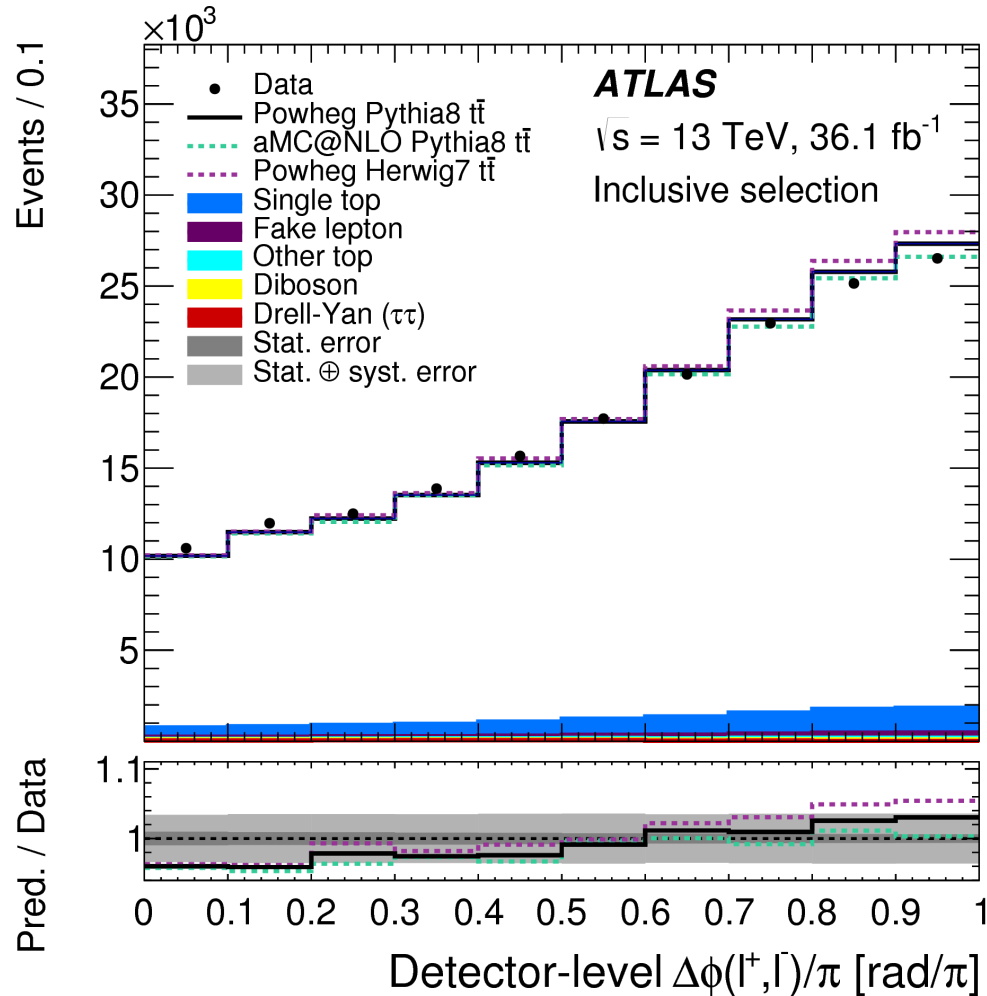
Difference in the azimuthal angle ϕ between electron and muon

Transverse plane:



Normalised differential cross-section

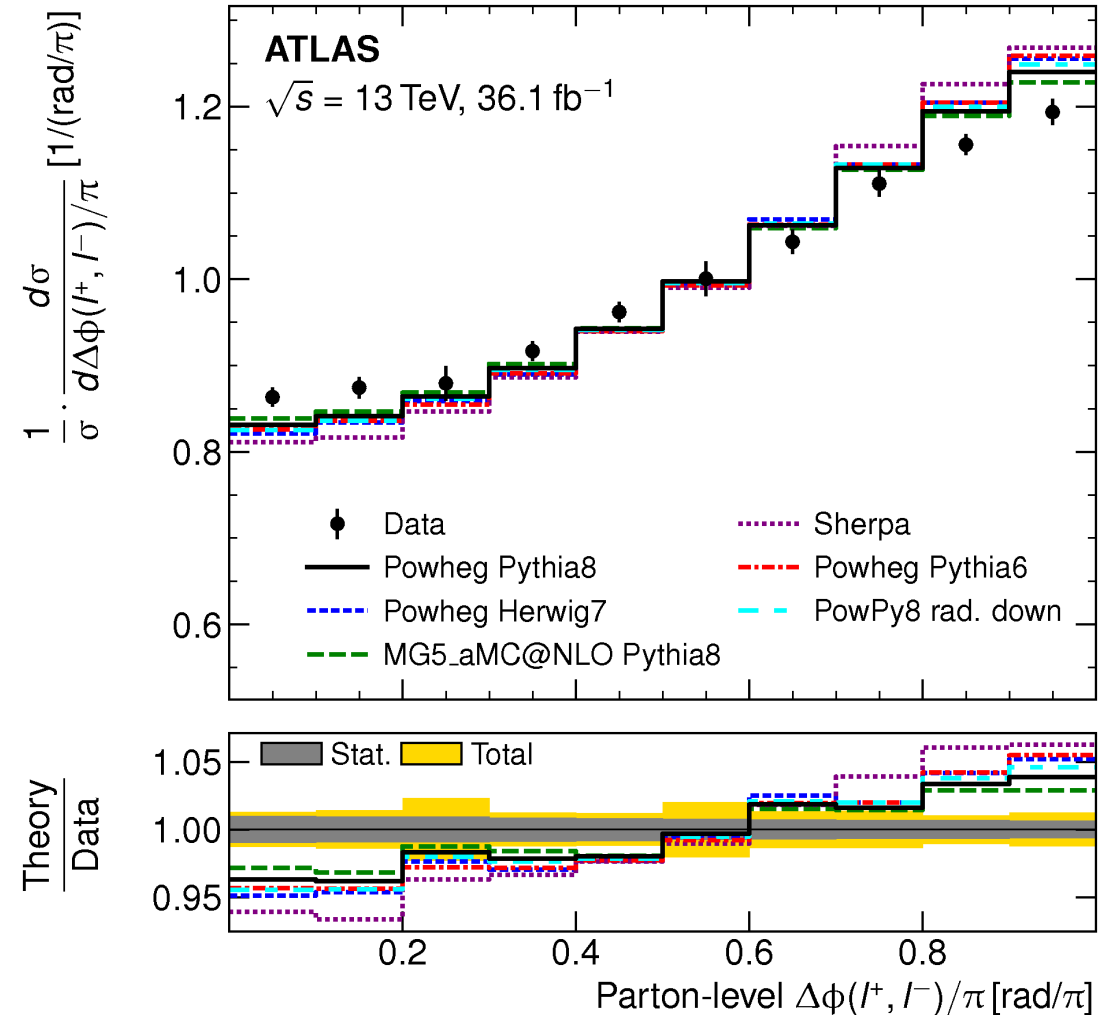
Detector-level (reconstructed) distribution



Uncertainties are too large to test the predictions.

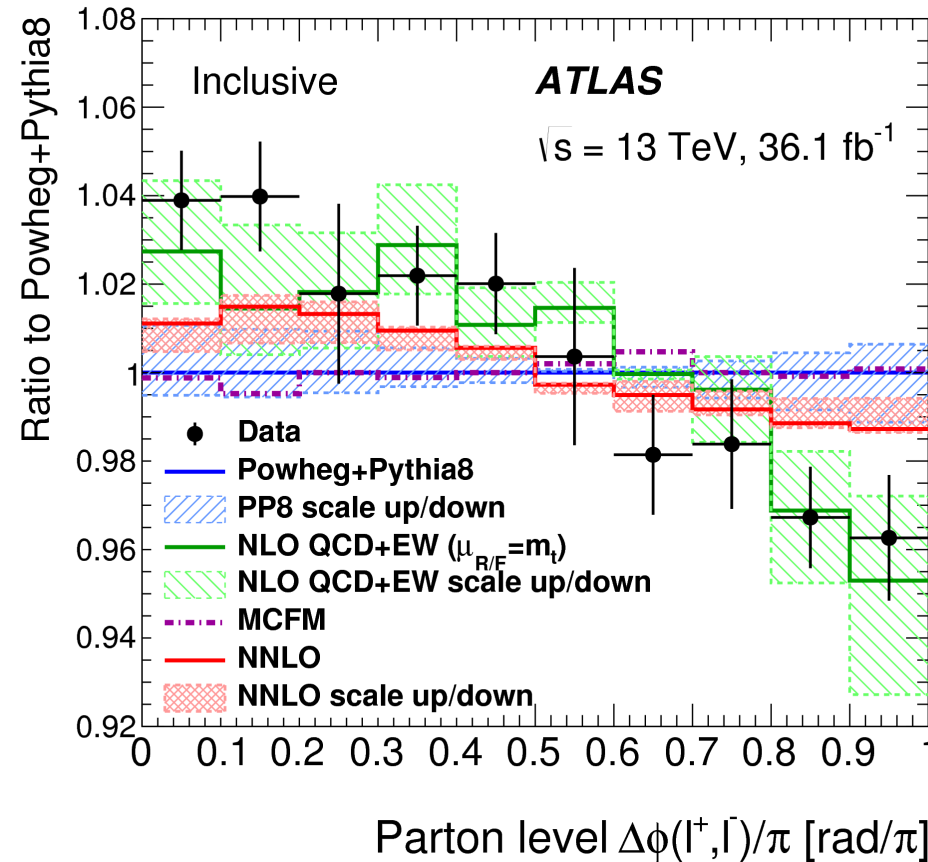
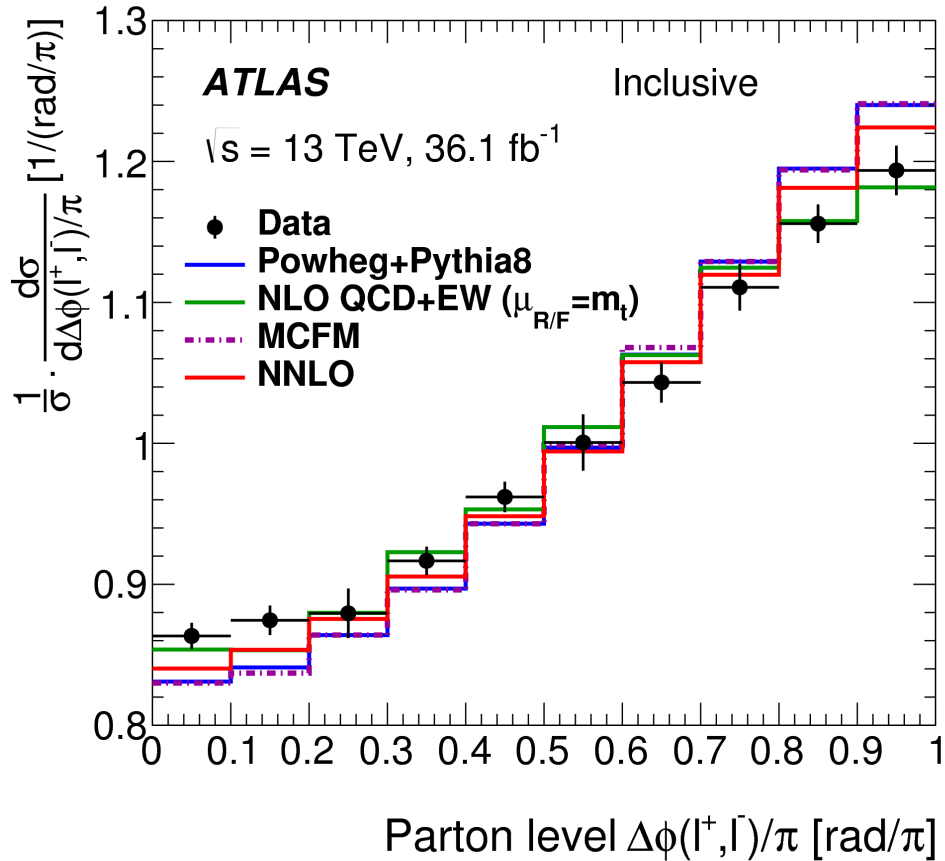
Wolfgang Wagner, Challenging the Standard Modell ...

Normalised differential cross-section



Uncertainties shrink to the level of 1%.

Comparison to fixed-order calculations



Powheg+Pythia8 and NLO fixed-order (MCFM) calculations do not describe the data.

NNLO result is closer to the data, but still no good description.

NLO calculation by Werner Bernreuther and Zongguo Si describes data well!

Main difference of B+S compared to MCFM and Powheg+Pythia: direct perturbative expansion of $\frac{1}{\sigma} \frac{d\sigma}{d\Delta\phi}$

Other differences: choice of renormalisation and factorisation scales, electroweak corrections and PDFs.

Latest cross-checks

Fresh from Top2019: Talk by Alexander Mitov

Did expansion of normalized differential cross-section

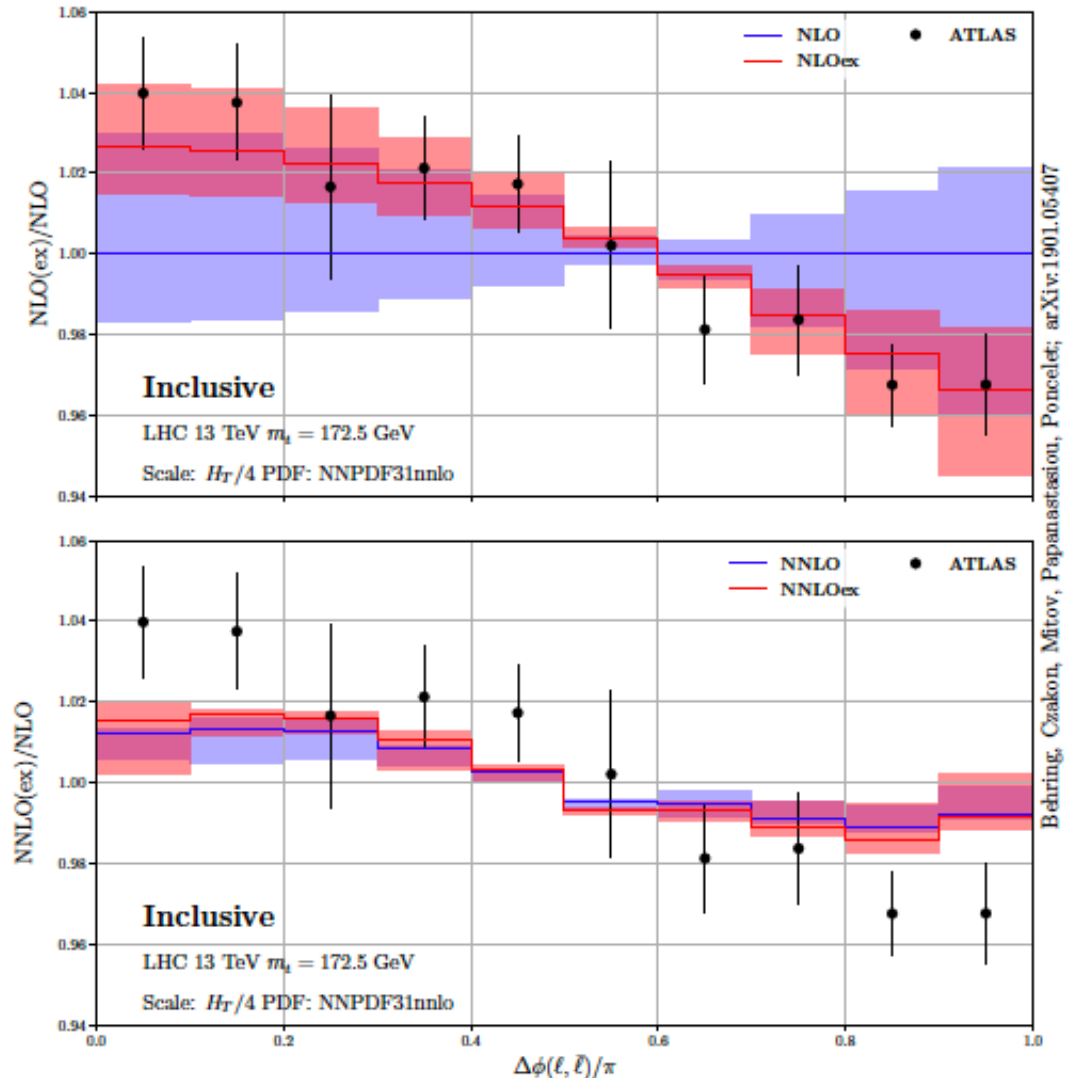
$$R^{\text{NNLO,exp}} = R^0 + \alpha_S R^1 + \alpha_S^2 R^2,$$

$$R^0 = \frac{1}{\sigma^0} \frac{d\sigma^0}{dX},$$

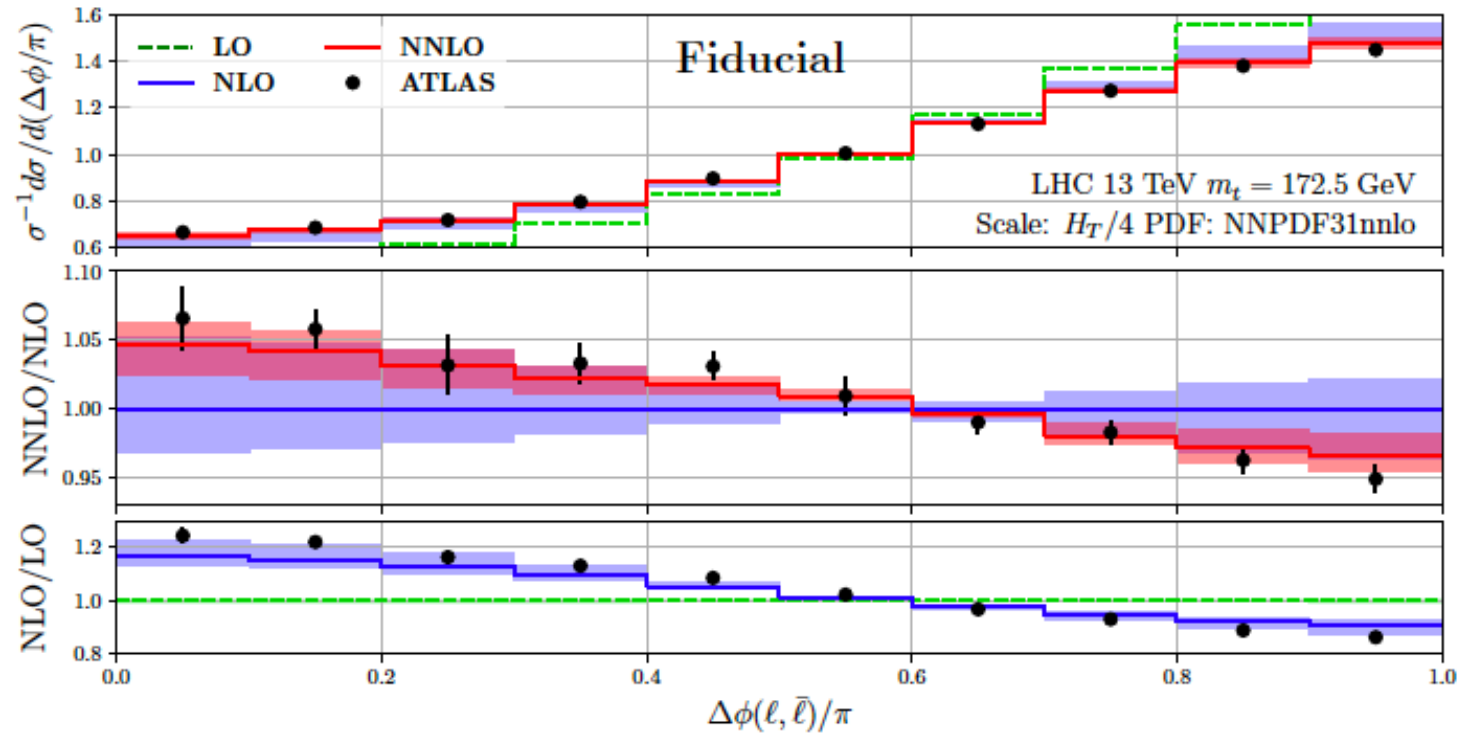
$$R^1 = \frac{1}{\sigma^0} \frac{d\sigma^1}{dX} - \frac{\sigma^1}{\sigma^0} \frac{1}{\sigma^0} \frac{d\sigma^0}{dX},$$

$$R^2 = \frac{1}{\sigma^0} \frac{d\sigma^2}{dX} - \frac{\sigma^1}{\sigma^0} \frac{1}{\sigma^0} \frac{d\sigma^1}{dX} + \left(\left(\frac{\sigma^1}{\sigma^0} \right)^2 - \frac{\sigma^2}{\sigma^0} \right) \frac{1}{\sigma^0} \frac{d\sigma^0}{dX}$$

- Confirms that expansion of $\frac{1}{\sigma} \frac{d\sigma}{d\Delta\phi}$ describes the data at NLO!
- But no effect at NNLO!



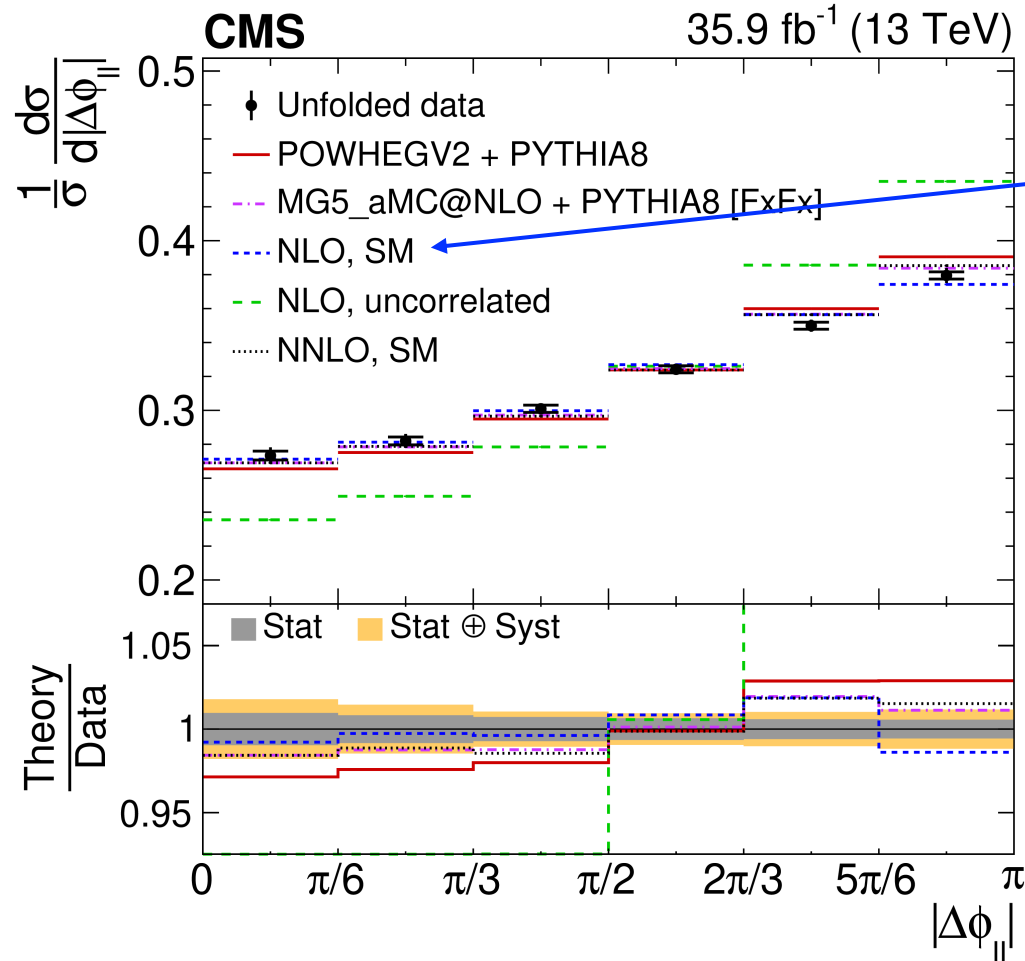
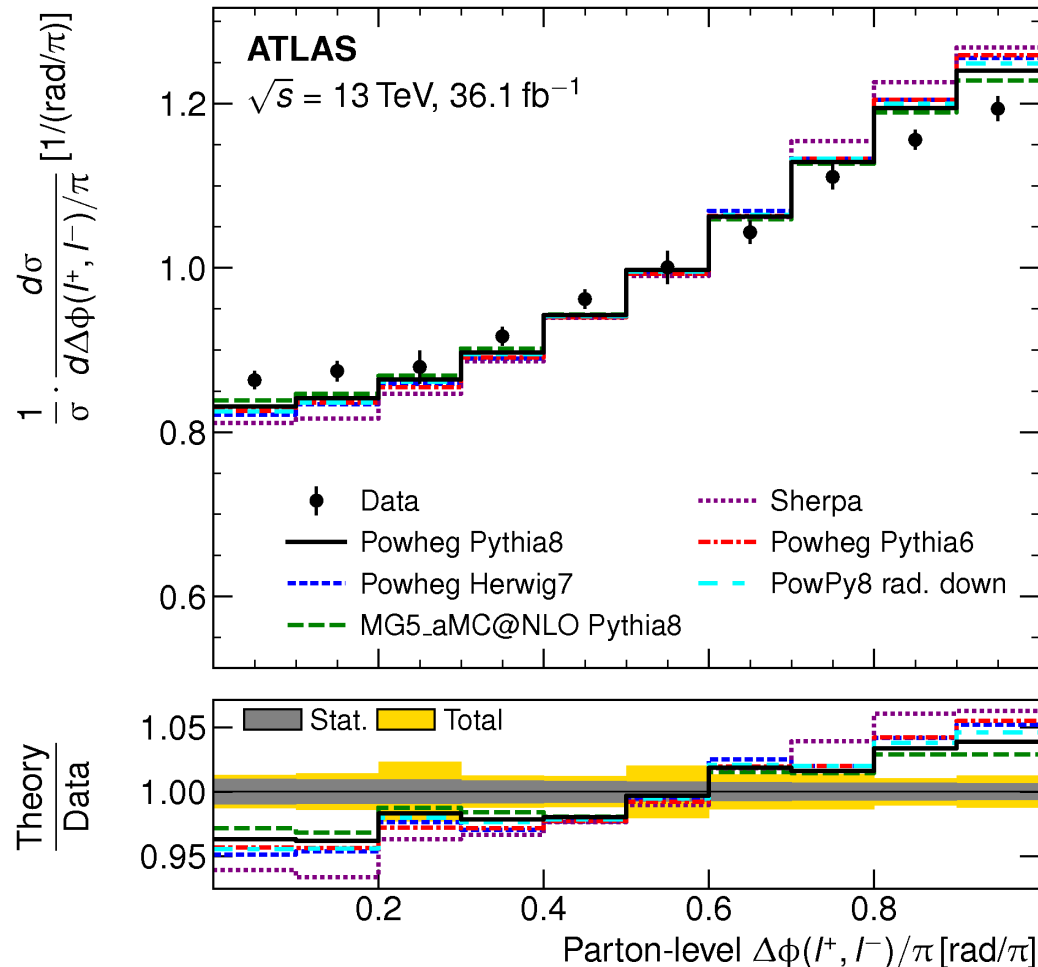
At the fiducial level NNLO describes the data well.



Behring, Czakon, Mitov, Papanastasiou, Poncelet arXiv:1901.05407

Points to the Monte-Carlo-based acceptance corrections as the cause of the difference.

Comparison ATLAS and CMS



Bernreuther + Si

The MG5_aMC@NLO+Pythia8 [FxFx] setup of CMS agrees with the data within the 1 s.d. band.

- In $\Delta\phi(e, \mu)$ both experiments observe a slope with respect to the Powheg prediction.
- In ATLAS the slope is slightly larger $(1.03 - 0.97)/\pi$ versus $(1.025 - 0.975)/\pi$.

Summary and Conclusions

- The top-quark plays an important role in the SM, mainly through loop corrections.
- The LHC is a copious source of top quarks. Run 2 provides us with millions of reconstructed top-quark events.
- The SM is challenged by direct and indirect searches, as well as by precision measurements.

